Institute of Genetics and Animal Biotechnology
of the Polish Academy of Sciences
Department of Genomics and Biodiversity

Doctoral Thesis

Effect of a diet enriched with omega-6 and omega-3 fatty acids on the pig liver transcriptome

Agnieszka Szostak

Ph.D. thesis under the supervision of:

Prof. dr hab. Mariusz Pierzchała
Institute of Genetics and Animal Biotechnology
Polish Academy of Sciences, Poland

Dr Marinus F.W. te Pas
Wageningen University and Research Centre
The Netherlands

Jastrzębiec, 2020

Acknowledgments

The author would like to express her gratitude to Dr. hab Mariusz Pierzchała, Dr. Marinus Te Pas, and Prof. Dr. hab Chandra Shekhar Pareek for their critical reading and insights. This work was supported by grants from BIOFOOD – innovative, functional products of animal origin no. POIG.01.01.02-014-090/09 co-financed by the European Union from the European Regional Development Fund within the Innovative Economy Operational Programme 2007 – 2013, and by the National Science Centre, Poland (grant no. 2014/13/N/NZ9/00906).

Table of content

Acknowledgments....3
Abstract....8
Streszczenie....10
1. Introduction....12
1.1. Dissertation‘s research hypothesis....12
1.2. Review of the literature related to the doctoral dissertation....13
1.2.1. Biochemistry and functions of polyunsaturated fatty acids (PUFAs)....13
1.2.2. Omega-3 and omega-6 fatty acids as vital components of a diet....20
1.2.3. Supplementation of human and animal diet with PUFAs....24
1.2.4. Pig as a model in biomedical research....25
1.2.5. Nutrigenomics – innovative methods in PUFAs studies....25
2. Dissertations’ research objectives and goals....28
3. Materials and methods....30
3.1. Feeding experiment including Polish Landrace purebred and Polish Landrace x Duroc crossbred....30
3.1.1. Study design in the feeding experiment....30
3.1.2. Laboratory procedures in the feeding experiment....35
3.1.3. Statistical analysis on fatty acids phenotypic data....35
3.2. NGS based RNA-Seq experiment including Polish Landrace purebred (MiSeq Illumina platform) and Polish Landrace x Duroc crossbred (HiSeq Illumina platform) pigs. 37
3.2.1. Study design....37
3.2.2. Samples preparation in the NGS based RNA-Seq experiment....38
3.2.3. Laboratory procedures in the NGS based RNA-Seq approach....38
3.2.4. Bioinformatic analysis of RNA-Seq data of porcine liver transcriptome....48
3.2.5. Validation of gene expression analysis results by Quantitative RT-PCR....51
3.2.6. Statistical analysis....60
4. Results....61
4.1. Feeding experiment including Polish Landrace purebred and Polish Landrace x Duroc crossbred pigs....61
4.1.1. Linseed and rapeseed oil supplementation reduces the hepatic omega-6/omega-3 ratio....61

4.2. NGS based RNA-Seq experiment of porcine liver representing Polish Landrace purebred and Polish Landrace x Duroc crossbred pigs 67
4.2.1. Preprocessing and post-processing of porcine liver RNA-Seq data representing Polish Landrace purebred and Polish Landrace x Duroc crossbred pigs 67
4.2.2. DEGs analysis of porcine liver by comparing the standard (control) diet versus experimental nutritional PUFAs diets within Polish Landrace purebred pigs (MiSeq RNA-Seq data) using CLC Genomics workbench 68
4.2.3. DEGs analysis of porcine liver by comparing the standard (control) diet *versus* experimental nutritional PUFAs diets within Polish Landrace x Duroc crossbred pigs (HiSeq RNA-Seq data) using CLC Genomics workbench 77
4.2.4. DEGs analysis of porcine liver by comparing the Polish Landrace purebred pigs (MiSeq RNA-Seq data) and Polish Landrace x Duroc crossbred pigs (HiSeq RNA-Seq data) after experimental feeding with standard (control) diet using CLC Genomics workbench 86
4.2.5. DEGs analysis of porcine liver by comparing the Polish Landrace purebred pigs (MiSeq RNA-Seq data) and Polish Landrace x Duroc crossbred pigs (HiSeq RNA-Seq data) after experimental feeding with the supplementary healthy diet enriched with omega-6 and omega-3 fatty acids (PUFAs) diet using the CLC Genomics workbench .. 99
4.2.6. Overall comparisons of identified up- and down-regulated genes (Third filtering) 121
4.3. Visualization of identified upregulated and downregulated DEGs in investigated purebred and crossbred pigs 141
4.3.1. Visualization of identified upregulated and downregulated DEGs in Volcano plot and in Heatmap 141
4.4. Biological gene networks and pathways analysis of DEGs using Cytoscape ClueGO 146
4.4.1. Identification of biological gene networks and pathways analysis by comparing the standard (control) diet *versus* supplementary healthy diet enriched with omega-6 and omega-3 fatty acids (PUFAs) in liver transcriptome Polish Landrace purebred pigs (First comparison). 146
4.4.2. Identification of biological gene networks and pathways analysis by comparing the standard (control) diet *versus* supplementary healthy diet enriched with omega-6 and omega-3 fatty acids (PUFAs) in the liver transcriptome of Polish Landrace x Duroc crossbred pigs 151

4.4.3. Identification of biological gene networks and pathways analysis by comparing the Polish Landrace purebred *versus* Polish Landrace x Duroc crossbred pigs liver transcriptome after experimental feeding with standard (control) diet 156
4.4.4. Identification of biological gene networks and pathways analysis by comparing the Polish Landrace purebred *versus* Polish Landrace x Duroc crossbred pigs liver transcriptome after experimental feeding with the diet enriched with omega-6 and omega-3 fatty acids (PUFAs) 161
4.5. Validation of RNA-Seq data by quantitative real-time PCR 166
5. Discussion 168
5.1. Discussion on feeding experiment 169
5.2. Discussion on NGS experiment 170
6. Conclusions 180
7. References 181

Abstract

Thesis title: Effect of a diet enriched with omega-6 and omega-3 fatty acids on the pig liver transcriptome

Background: Omega-6 and omega-3 polyunsaturated fatty acids (PUFAs) have been recognized as molecules regulating a variety of functions in a cell. They serve as a source of energy, are a vital component of cell membranes, and act as signaling molecules, which can regulate gene expression. Discussion over the impact of omega-6 and omega-3 PUFAs on potential health outcomes has been settled, however their way of action on the whole transcriptome level is still not definitively resolved. The aim of the study was to investigate the effect of dietary omega-6 and omega-3 fatty acids on liver transcriptome activity in pigs by examination of the alterations in hepatic gene expression, as well as metabolic pathways associated with pig genotype.

Experimental design and Methods: The feeding experiment was performed on Polish Landrace (PL) purebred (n=99) and Polish Landrace x Duroc (PL x Duroc) crossbred (n=102) female pigs. The animals were fed with omega-6 and omega-3 PUFAs enriched (three tested mixtures) and a standard (control) diet. The hepatic profiles of fatty acids were analyzed by gas chromatography (GC-FID). The next-generation sequencing (NGS) based transcriptome sequencing (RNA-Seq) experiment was performed on 22 pigs using MiSeq Illumina platform (commercial service: Genomed, Poland) for PL (n=12), and HiSeq Illumina platform (commercial service: Centrum Badan DNA, Poland) for PL x Duroc (n=10). RNA-Seq reads were mapped onto the pig reference genome *Sus scrofa* v.11.1. Four differentially expressed genes (DEGs) comparisons analysis between diets (n=2) and genotypes (n=2) were performed to identify the upregulated and downregulated DEGs using CLC Genomics Workbench v. 6.0. The biological interactions between gene networks and metabolic pathways of DEGs were carried out using ClueGO v 2.2.0 Cytoscape v. 3.1.0 software. The DEGs results were confirmed and validated on the larger group of animals, PL n=30 and PL x Duroc n=20, using quantitative real-time PCR (qRT-PCR).

Results: Feeding experiment study showed that among three tested diets, PUFAs enriched diet in the content of 2% of linseed oil and 1% of rapeseed oil in fodder mixture effectively changed hepatic fatty acid profile and decreased omega-6/omega-3 ratio in the liver for both

PL (from 32.73 to 4.25; $p<0.001$) and PL x Duroc (from 14.42 to 4.74; $p<0.01$). The study shows that the changed fatty acids profiles in liver affected gene expression at large scale transcriptomic level for both investigated purebred and crossbred pigs. By comparing the upregulated and downregulated DEGs in all four comparisons, several diet-specific and breed-specific hepatic gene expression networks and metabolic pathways were identified using the ClueGO plugin. Validation of RNA-Seq experiment performed using qRT-PCR showed similar changes in expression levels, indicating that the RNA-Seq data were reliable.

Conclusions: Endogenous omega-3 fatty acids affected physiological pathways associated mainly with processes involved in decreased cellular lipid accumulation (triglycerides content as lipid droplets): 1) elevated fatty acid oxidation, 2) enhanced cholesterol transport outside the hepatocytes, 3) decreased autophagy (lipophagy). Affected pathways support the antisteatotic function of endogenous omega-3 fatty acids in the liver. We found indications that omega-3 fatty acids can probably act against lipid accumulation in the liver through the improvement of the hepatic fatty acids profile. The manner of conversion showed that PUFAs enriched diet hint mainly on the omega-3 pathway. Our results confirm the essential role of omega-6 and omega-3 fatty acids in homeostasis through markedly improved fatty acids profile (decreased omega-6/omega-3 ratio in the liver) and in a consequence regulation of expression of many genes involved in lipid metabolism, signal transduction and pathways related to the inflammatory response.

Keywords: fatty acids, omega-3, omega-6, PUFAs, pig, liver, NGS, RNA-Seq, transcriptome, gene expression

Streszczenie

Tytuł pracy: Wpływ diety wzbogaconej w kwasy tłuszczowe omega-6 i omega-3 na transkryptom wątroby świni.

Wstęp: Wielonienasycone kwasy tłuszczowe (WNKT) omega-6 i omega-3 zostały uznane za cząsteczki regulujące istotne funkcje w komórce. Służą jako źródło energii, stanowią podstawowy składnik błon komórkowych, czy też pełnią rolę cząsteczek sygnałowych, które mogą wpływać na regulację ekspresji genów. Dyskusja nad potencjalną zdrowotną funkcją WNKT z rodziny omega-6 i omega-3 toczy się od wielu lat, niemniej jednak kwestia sposobu działania na poziomie całego transkryptomu została niewyjaśniona. Celem niniejszej pracy było prześledzenie zmian w transkryptomie wątroby świni będących efektem diety wzbogaconej w WNKT omega-6 i omega-3 poprzez analizę różnic poziomu ekspresji genów w wątrobie oraz ścieżek metabolicznych powiązanych z dwoma genotypami świń.

Schemat doświadczenia i Metody: Doświadczenie żywieniowe zostało przeprowadzone na loszkach świń rasy Polska Biała Zwisłoucha (PBZ, n=99) i mieszańców międzyrasowych PBZ i Duroc (PBZ x Duroc, n=102). Zwierzętom podawano paszę wzbogaconą w WNKT omega-6 i omega-3 (początkowo testowano trzy diety) bądź paszę standardową (kontrola). Profile kwasów tłuszczowych w wątrobie przeanalizowano za pomocą chromatografii gazowej (GC-FID). Sekwencjonowanie nowej generacji (NGS) metodą sekwencjonowania transkryptomu (RNA-Seq) wykonano dla 22 osobników za pomocą urządzenia MiSeq Illumina (usługa komercyjna: Genomed, Polska) dla PBZ (n=12) oraz na platformie HiSeq Illumina (usługa komercyjna: Centrum Badan DNA, Polska) dla PBZ x Duroc (n=10). Odczyty RNA-Seq zmapowano do referencyjnego genomu świni *Sus scrofa* v.11.1. Za pomocą programu CLC Genomics Workbench v. 6.0. wykonano cztery analizy porównawcze między rodzajem diety (n=2) i genotypem świń (n=2), aby zidentyfikować geny ulegające istotnie zmienionej ekspresji (DEGs; ang. differentially expressed genes) regulowane w górę (ang. upregulated genes) lub w dół (ang. downregulated genes). Przy użyciu programów ClueGO v. 2.2.0 i Cytoscape v. 3.1.0 wyznaczono biologiczne interakcje pomiędzy sieciami genów i ścieżkami metabolicznymi na podstawie zidentyfikowanych DEGs. Uzyskane wyniki RNA-Seq potwierdzono i zwalidowano na większej grupie zwierząt, PBZ n=30 i PBZ

x Duroc n=20, za pomocą ilościowej łańcuchowej reakcji polimerazy w czasie rzeczywistym (qRT-PCR, ang. quantitative real-time polymerase chain reaction).

Wyniki: Doświadczenie żywieniowe wykazało, że spośród trzech testowanych pasz, pasza wzbogacona w WNKT w ilości 2% oleju lnianego i 1% oleju rzepakowego skutecznie zmieniła profil kwasów tłuszczowych w wątrobie zmniejszając proporcję kwasów omega-6/omega-3 zarówno dla PBZ (z 32.73 do 4.25; $p<0.001$) jak i PBZ x Duroc (z 14.42 do 4.74; $p<0.01$). Badanie pokazało, że zmienione profile kwasów tłuszczowych w wątrobie wpłynęły na ekspresję genów na poziomie transkryptomu zarówno dla czystej rasy jak i mieszańców międzyrasowych. Poprzez porównanie DEGs regulowanych w górę i w dół przy użyciu programu ClueGO podczas wszystkich czterech analiz porównawczych, zidentyfikowano sieci genów i ścieżki metaboliczne specyficzne dla diety i genotypu. Walidacja eksperymentu RNA-Seq wykonana za pomocą metody qRT-PCR pokazała podobne zmiany w poziomie ekspresji, wskazując na miarodajność przedstawionych danych RNA-Seq.

Wnioski: Endogenne kwasy tłuszczowe omega-3 wpłynęły na ścieżki fizjologiczne zaangażowane głównie w procesy związane ze zmniejszoną akumulacją lipidów w komórce (trójglicerydów zawartych w postaci kropli lipidowych): 1) zwiększenie oksydacji kwasów tłuszczowych, 2) nasilenie transportu cholesterolu na zewnątrz hepatocytów, 3) zmniejszenie aktywności autofagii (lipofagii). Zmienione ścieżki podtrzymują antystłuszczeniową funkcję kwasów tłuszczowych omega-3 w wątrobie. Badania wskazują, że endogenne kwasy tłuszczowe omega-3 przeciwdziałają nadmiernej akumulacji lipidów w wątrobie poprzez preferencyjną konwersję na ścieżce kwasów omega-3, poprawiając znacznie profil kwasów tłuszczowych. Podsumowując, wyniki niniejszej pracy potwierdzają istotną rolę kwasów tłuszczowych omega-6 i omega-3 w homeostazie organizmu poprzez znacząco zmieniony profil kwasów tłuszczowych (zmniejszona proporcja kwasów omega-6/omega-3 w wątrobie), a w następstwie regulację ekspresji wielu genów zaangażowanych w metabolizm lipidów, przekaźnictwo sygnałowe oraz ścieżek związanych z odpowiedzią zapalną.

Słowa kluczowe: kwasy tłuszczowe, omega-3, omega-6, WNKT, świnia, wątroba, NGS, RNA-Seq, transkryptom, ekspresja genów

1. Introduction

Poly-unsaturated fatty acids (PUFAs) comprise a group of lipids essential for all organisms. Omega-6 and omega-3 fatty acids are two families representing the PUFAs group. They have been recognized as molecules regulating a variety of functions in the cell, serving as a source of energy, being a vital component of the cell membranes and acting as signaling molecules, which regulate different processes, including gene expression. Despite being essential for maintaining homeostasis in animal organisms, lack of enzymes responsible for endogenous synthesis of the omega-6 and omega-3 fatty acids by mammals necessitates their constant dietary intake, hence they are referenced as essential fatty acids (EFA) (**Simopoulos, 2001; El-Badry et al., 2007)**. The omega-6 linoleic acid (LA) and omega-3 α-linolenic acid (ALA) are critically essential fatty acids, since they are exclusively delivered from a diet as their only source. They are at the beginning of conversion pathways for long-chain omega-6 and omega-3 PUFAs as their precursors. Long-chain PUFAs (LC-PUFAs) are supplied most of all with a diet or can be metabolized from dietary precursors LA and ALA, but the efficiency of conversion by mammals is very low. Nowadays, many studies are focused on measurement of systemic changes of gene expression caused by natural compounds of a diet at various levels (transcriptomic, proteomic and metabolomic) to unravel the biological processes and multidirectional mechanisms of their action. Although the debate over the impact of omega-6 and omega-3 PUFAs on potential health outcomes has been settled, it is still not definitively clear, what is the manner of action as health-promoting molecules both in disease and physiological conditions at the whole transcriptomic level.

1.1. Dissertation‘s research hypothesis

1. Nutritional properties of the dietary omega-3 and omega-6 PUFAs control hepatic gene expression regulation through series of physiological, biochemical and metabolic mechanisms.

2. Based on the literature studies, we considered omega-3 and omega-6 PUFAs as a potential supplementary healthy diet with high efficiency of metabolic action and the effects of dietary supplementation of PUFAs were successfully performed using animal models. In this dissertation, pig as a proven animal model for digestive system health study was utilized.

3. Nutrigenomics studies involving comprehensive transcriptome investigations on standard (control) and health-ptomoting (PUFAs) diets in pig animal model will provide new insights on mammalian gut health, hepatoprotective mechanism and present novel research findings such as: identification of potential candidate genes, metabolic pathways based on gene networks interactions.

1.2. Review of the literature related to the doctoral dissertation.

1.2.1. Biochemistry and functions of polyunsaturated fatty acids (PUFAs)

1.2.1.1. Fatty acids classification and conversion pathways

Different types of fatty acids can be distinguished on the basis of the presence and the number of double bonds in their carboxylic chain into three main classes. Saturated fatty acids (SFAs) do not contain double bonds in their chemical structure. Unsaturated fatty acids contain at least one double bond and are referenced as monounsaturated fatty acids (MUFAs) when only one double bond exists, or PUFAs with more double bonds. Most of the animals or mammalian organisms convert SFAs to MUFAs, while direct conversion of MUFAs to PUFAs requires specific desaturase enzyme adding more double bonds into fatty acids chain, the process which does not occur naturally in animals. Polyunsaturated fatty acids have to be delivered exogenously with a diet, especially EFA, which belong to omega-6 and omega-3 fatty acids series of PUFAs group.

The difference between omega-6 and omega-3 PUFAs refers to the position of the first double bond, located on the third (for omega-3) or sixth (for omega-6) carbon of carboxylic chain counting from the methyl group of the molecule. (**FIGURE 1** – positioning of double bonds in omega-6 and omega-3 fatty acids). Additional classification concerns the length of the carboxylic chain and distinguishes fatty acids on short-, medium-, and long-chain fatty acids, which further influence the manner in which they are transported through the cell and are metabolized. Short-chain fatty acids contain from 2 to 6 carbon atoms, medium-chain fatty acids from 6 to 18, and long-chain fatty acids have more than 18 carbon atoms in the carboxylic chain.

The omega-6 linoleic acid (LA; C18:2n6) and omega-3 α-linolenic acid (ALA; C18:3n3) are the precursors for the synthesis of LC-PUFAs **(Simopoulos, 2016).** The most common LC-PUFAs are arachidonic acid (AA; C20:4n6) derived from LA, and eicosapentaenoic acid (EPA; C20:5n3), further elongated to docosapentaenoic acid (DPA; C22:5n3), which are formed by elongation of ALA. Docosapentaenoic acid is further desaturated to docosahexaenoic acid (DHA; C22:6n3). Desaturation and elongation for LA and ALA are localized in the endoplasmic reticulum (ER) except for the final step, which is translocation to peroxisomes for partial beta-oxidation. LA and ALA conversion pathways are presented in **FIGURE 2.**

Two desaturase enzymes are involved in the conversion of LA and ALA into their longer chain derivatives LC-PUFAs and are the key and rate-limiting enzymes for this conversion (see FIGURE 2) – delta-6 and delta-5 desaturase encoded by the FADS1 and FADS2 genes, respectively. The same desaturase and elongase enzymes act on omega-6 and omega-3 fatty acids pathways causing competition between the two series, but the higher affinity of desaturases and elongases have been observed for the omega-3 pathway.

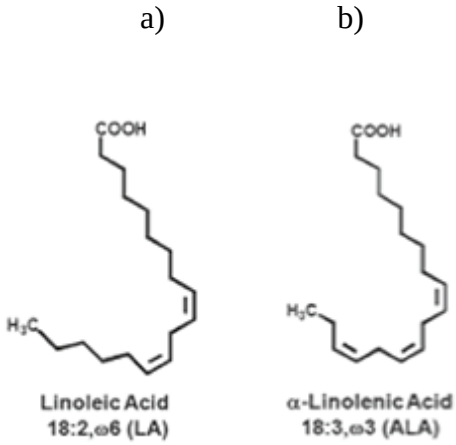

Figure 1. Biochemical structure of a) omega-6 linoleic acid (LA) and b) omega-3 α-linolenic acid (ALA) and location of double bonds in carboxylic chains (http://lpi.oregonstate.edu/book/export/html/50).

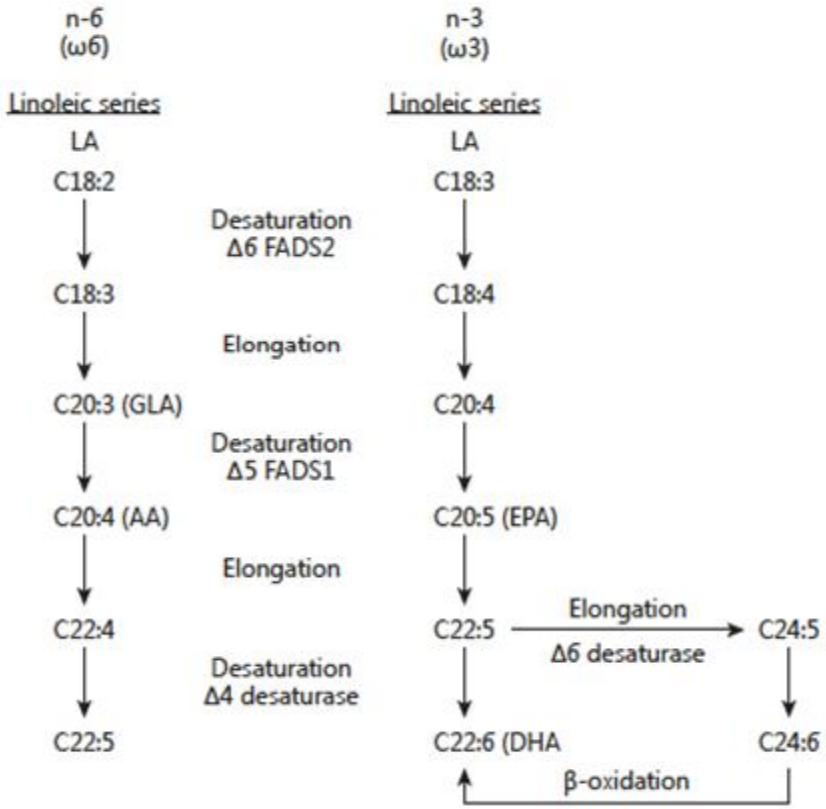

Figure 2. Linoleic acid and α-linolenic acid conversion pathways (**Simopoulos, 2016**).

PUFAs role as a cell membrane component: Omega-6 AA and omega-3 EPA and DHA fatty acids play a vital role in the cell membrane function and fluidity as molecules incorporated into phospholipids of the lipid bilayer structure. Membrane DHA level in the brain, where DHA is primarily abundant, affects the diffusion of membrane lipids, receptors and the rate of protein-protein interactions (**Guixà-González et al., 2016**). The ratio of saturated to unsaturated fatty acids in membrane phospholipids influence the membrane fluidity and further affect the activity of embedded enzymes (**Storch and Schachter, 1984**). The proteins anchored in the structure of lipid bilayer as receptors, transporters or enzymes are affected by alterations in membrane composition. Different kinds of fatty acids embedded in cell membranes affect their fluidity and permeability, influence the action of transmembrane proteins and decide on the signal transduction effectiveness and efficiency. Membrane fluidity is releted to the number of cis-double bonds in the carboxylic chain of fatty acids influencing its three-dimensional structure. Both presence and localization of double bonds in the fatty acyl chain affects the properties of cell membranes. The more

curved and kinked carbon chain is, the more space it takes in the cell membrane increasing its fluidity.

Moreover, omega-3 fatty acids displace cholesterol from the membrane (**Turk and Chapkin, 2013**) increasing the fluidity of the phospholipid bilayer (**Storch and Schachter, 1984**). Dietary PUFAs influence lipid raft domains stability in plasma membranes. The lipid rafts are particularly abundant in the composition of plasma membranes being their major domain (**Turk and Chapkin, 2013**). They are modulated by dietary fats, including both cholesterol and fatty acids, especially omega-3 DHA (**Turk and Chapkin, 2013**). Omega-3 DHA is incorporated into membranes with particularly high affinity. Lipidomic remodeling of membranes induced by supplementation of omega-3 DHA influencing compositional and biophysical properties of membranes have been recently reported in many studies using new lipidomic approaches (**Shaikh 2012; Williams et al., 2012; Lamaziere at al., 2013; Balogun et al., 2013; Levental et al., 2016; Levental et al., 2017; Levental et al., 2020**).

PUFAs function in cell signaling: Nutrients are one of the signals from the extracellular environment, that are able to control gene expression and enzymes synthesis (**Wymann and Schneiter, 2008**). Lipids including fatty acids and their secondary derivatives – eicosanoids, act as signaling molecules, that control cellular processes like metabolism, cell migration and proliferation (**Wymann and Schneiter, 2008**). Polyunsaturated fatty acids are considered one of the factors markedly influencing the immune response and regulating homeostatic processes by eicosanoids and cytokines production from their precursors – PUFAs (**Norris and, Dennis 2014; Dennis and Norris, 2015**). Eicosanoids, the group of molecules including prostaglandins, prostacyclins, thromboxanes and leukotrienes, act as local hormones, which stimulate inflammation, blood flow to organs, ion transport through membranes and signal transduction. Eicosanoids derivatives of omega-6 and omega-3 fatty acids elicit opposite properties. Products synthesized from omega-6 AA such as prostaglandin E2 and leukotriene B4 have a stronger prothrombotic and inflammatory effect than corresponding eicosanoids derived from omega-3 EPA, which are prostaglandin E3 and leukotriene B5 (**Patterson et al., 2012; Simopoulos, 2016; Molfino et al., 2017**) (**Figure 3**). Omega-6 AA derived from LA is usually the primary precursor of eicosanoids.

The release of fatty acids from the cellular membrane causes a cascade of reactions. Phospholipase A2 enzyme release AA and other PUFAs from phospholipids of the cellular membrane stored in an esterified form and after oxidation, free AA and other PUFAs are

converted to eicosanoids by one of three subsequent pathways – the action of cyclooxygenase (COX), lipoxygenase or cytochrome P450 enzymes (**Norris and Dennis, 2012**). EPA and DHA omega-3 family exert anti-inflammatory and cardioprotective effect based on the inhibition of AA metabolism (through competition between omega-3 and omega-6 metabolic pathways) mainly by COX1 but also COX2 (**Norris and Dennis, 2012**). The inhibition of COX1 and COX2 pathways are different for omega-3 and omega-6 affecting eicosanoids production. Omega-3 EPA decreases AA-derived COX metabolites. Thus, indirectly, EPA cause inhibition of the COX pathway changing the production of the eicosanoids. Omega-3 fatty acids supplementation support a temporal production of anti-inflammatory and pro-resolution eicosanoids **(Norris and Dennis, 2012**).

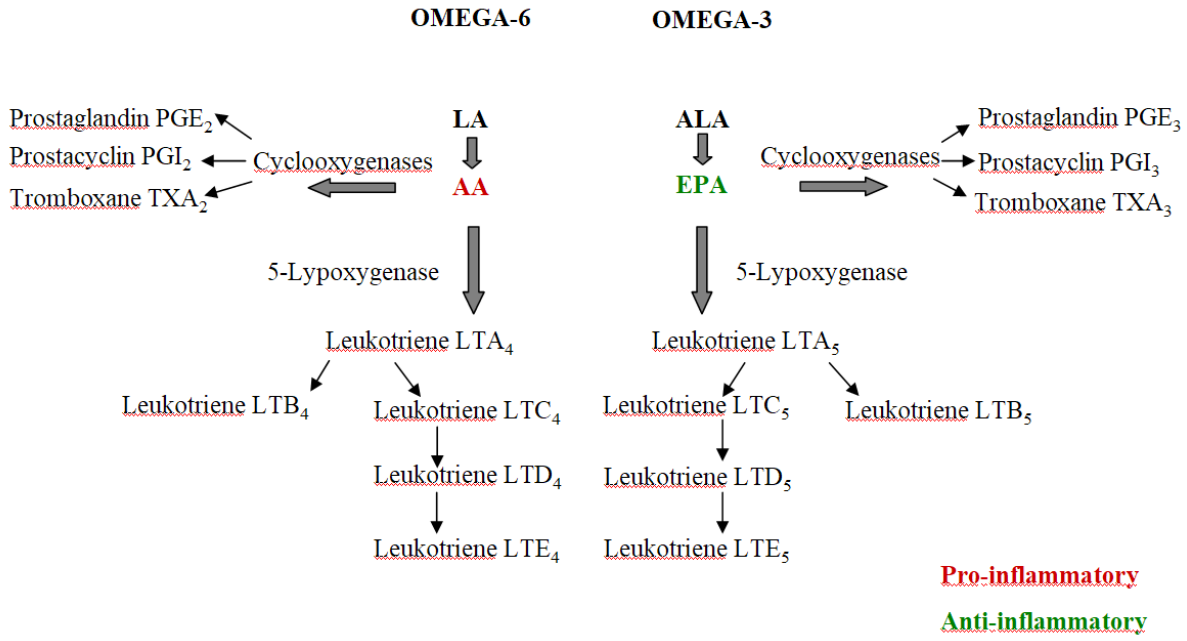

Figure 3. Eicosanoids synthesis from omega-6 and omega-3 fatty acids.

PUFAs action in a gene transcription process: Dietary PUFAs control hepatic gene transcription through regulation of the activity of transcription factors and their nuclear abundance. The mechanism of gene expression regulation can be achieved through direct binding to the transcription factor as a ligand or by the indirect mechanism by protein phosphorylation, ubiquitination or proteolytic cleavage acting on transcription factors function (**Sessler and Ntambi, 1998; Jump et al., 2013**). The main transcription factors induced by PUFAs in the liver and responsible for fatty acids homeostasis are peroxisome proliferator-activated receptor (PPARα), sterol regulatory element-binding protein (SREBPC1), liver X receptor α (LXRα), farnesoid X receptor (FXR), retinoid X receptor

(RXR) and HNF4 (α and γ) (**Chamouton and Latruffe, 2012; Jump et al., 2013; Oppi-Williams et al., 2013; Jiao et al., 2015; Lu 2016; Preidis et al., 2017**). Polyunsaturated fatty acids act as natural ligands for PPARα, LXR, and HNF4 and modulate the expression of their target genes (**Jump et al., 2013).**

The peroxisome proliferator-activated receptor is a major transcription factor activated by nutrients and crucial for lipid homeostasis. Its expression is specific to the liver, wherein hepatocytes induction of PPAR signaling pathway is involved in fatty acid β-oxidation (**Gormaz et al., 2010**). Polyunsaturated fatty acids bind with a high affinity to the ligand-binding domain of PPARα (**Murakami et al., 1999**), which creates heterodimer with RXR and bind to the promoter of the target gene in cis-regulatory elements (**Ijpenberg et al., 1997; Jump et al., 2013**). PPARα can be activated both by dietary and endogenous fatty acids and their derivatives produced upon food restriction during hepatic lipogenesis (**Chakravarthy et al., 2005**). PPARα participates in hepatic lipid metabolism – fatty acids uptake through membranes, fatty acids activation, intracellular fatty acid trafficking, fatty acid oxidation and ketogenesis, triglyceride storage, and lipolysis. Omega-6 and omega-3 fatty acids stimulate the hepatic lipid metabolism by PPARα pathway and interactions with its target genes. Induction of PPARα by PUFAs increases fatty acids β-oxidation, which further decreases the availability of fatty acids for storage as triglycerides (**Clarke, 2004**). Each enzymatic step within the fatty acid oxidation process is controlled by PPARα. This transcription factor induces expression of genes responsible for fatty acids import into the mitochondria (CPT1, CPT2, SLC25A20, SLC22A5) and the major enzymes involved in the β-oxidation pathway such as acyl-CoA dehydrogenases (ACAD), DCI, DECR and ACOX1, which is the rate-limiting enzyme in peroxisomal fatty acid β-oxidation (**Rakhshandehroo et al., 2010**). PPARα induces fatty acids oxidation and additionally regulates hepatic lipogenesis by targeting genes such as FADS2, MOD1, LPIN2, SCD1, which is an indirect mechanism of *de novo* fatty acid synthesis (**Rakhshandehroo et al., 2010**).

Liver X receptor α is the crucial regulator of lipid transport and metabolism (**Jump et al., 2013**), mainly responsible for fatty acid synthesis due to the activation of transcription of lipogenic genes (**Afman and Muller 2012**). Fatty acids are positive regulators of LXRα. However, this transcription factor induces expression of CYP7A1, which is the rate-limiting enzyme in the conversion of cholesterol into bile salts, like that LXRα mediates fatty acid and cholesterol metabolism (**Tobin et al., 2000; Heckmann et al., 2017**). The liver X receptor is

involved in the induction of SREBP-1c, which is also involved in *de novo* lipogenesis and its enhanced expression hints on short and medium long-chain fatty acid synthesis (**El-Badry et al., 2007**). The HNF4 ligand-binding domains for PUFAs exist. In particular, LA is preferentially bonded to this transcription factor, but the changes in transcriptional activity of HNF4 are not statistically significant and the role of PUFAs in HNF4 regulation is still not definitely clear (**Jump et al., 2013**). Among other transcription factors, which are indirectly affected by PUFAs are SREBP-1c involved in lipid metabolism, ChREBP responsible for carbohydrate metabolism and NF-κB related to inflammation (**Jump et al., 2013**). Their nuclear abundance is suppressed by PUFAs without binding to the protein (**Jump et al., 2013**).

The SREBP family contains SREBP-1a, SREBP-1c and SREBP-2 transcription factor subtypes expressed in the liver. SREBP-1a and SREBP-1c are responsible for gene transcription, which synthesize fatty acids and triglycerides, while SREBP-2 controls expression of genes involved in cholesterol synthesis and uptake (**Clarke, 2001; Jump et al., 2013**). SREBP-1c is predominantly expressed in the liver and stimulates *de novo* synthesis and transport of fatty acids (e.g., fatty acid synthase FASN) in hepatocytes and synthesis of cholesterol (**Jump et al., 2013**). PUFAs suppress the abundance of SREBP-1c in the liver and expression of its target genes responsible for *de novo* lipogenesis (**Clarke, 2001**) (SCD1), fatty acids desaturation (FADS1 and FADS2) and elongation (ELOVL5, ELOVL6) (**Jump et al., 2013**). Dietary PUFAs suppress further desaturation and elongation of LC-PUFAs and synthesis of SFAs and MUFAs in the liver (Jump et al., 2013). SFAs and MUFAs unlike PUFAs had no effect on SREBP-1c nuclear abundance (**Clarke, 2001**).

The ChREBP create heterodimer with MLX and is the transcription factor, which is involved in pathways responsible for glucose transport in the liver (GLUT2), glycolysis (L-PK), synthesis of MUFAs (SCD1, ELOVL6) and *de novo* lipogenesis (ACC, FASN) similarly to SREBP-1c. The nuclear abundance of heterodimers in the liver and their target gene expression (e.g., L-PK) are suppressed by PUFAs and induced by glucose (**Jump et al., 2013**). The NF-κB regulates the transcription of many genes involved in inflammation such as COX2, cytokines (e.g., TNFα), adhesion molecules (ICAM1 and VCAM1). Omega-6 PUFAs act as pro-inflammatory molecules, while omega-3 PUFAs have anti-inflammatory properties, hence they act differently on NF-κB nuclear abundance (**Jump et al., 2013**).

1.2.2. Omega-3 and omega-6 fatty acids as vital components of a diet

Natural sources of omega-6 and omega-3 fatty acids: The most intensively studied omega-3 fatty acids - EPA and DHA are particularly abundant in fish oil, that is why they are called marine fatty acids. They are particularly efficiently metabolized in fish organisms from ALA, which can be found in algae and use as a dietary source of omega-3 ALA for marine fish. The precursor of EPA and DHA – ALA, is found in high amounts also in oils from plants seeds such as linseed (flax) (*Linum usitatissimum*), rapeseed (canola) (*Brassica napus*), chia (*Salva hispanica*), perilla (*Perilla frutescens*), walnuts (*Juglans regia*) or soybean (*Glycine max*). Additionally omega-3 ALA can be found in small amounts in animal fat. The omega-6 arachidonic acid (AA) is common in animal products, such as meat, dairy products and eggs **(Simopoulos, 2016)**, while the appropriate precursor of AA, which is LA, can be found mainly in plants oils such as rapeseed, hemp (*Cannabis sativa*), poppy (*Papaver somniferum*), sesame (*Sesamum indicum)* and safflower (*Carthamus tinctorius*), sunflower (*Helianthus annuus)*, corn (*Zea mays*), soybean (*Glycine max*). In recent years many reports concern the beneficial effect of PUFAs on human health. The influence of LC-PUFAs like EPA, DHA and AA is often primarily reported concerning human health, neglecting the influence or their precursors – LA and ALA.

Fatty acids absorption in digestive tract and turnover cycle: The fundamental property of fatty acids is a hydrophobic nature making them soluble in organic solvents but insoluble in water, which further influence their digestion, absorption and metabolism (**Ramírez et al., 2001; Kerr et al., 2015**). The absorption of fatty acids highly depends on the length of the carboxylic chain and the number of double bonds. Long-chain PUFAs are less efficiently absorbed than short-chain fatty acids. Long-chain PUFAs derived from a diet can be stored in esterified forms as triglycerides in organelles called lipid droplets or in phospholipids as a component of cell membranes. Absorption of dietary PUFA largely depends on the form of their esterification (**Ramírez et al., 2001; Kerr et al., 2015**). Short-chain fatty acids, with length less than 6 carbons in the carboxylic chain can be very easily absorbed. They are solubilized in the aqueous phase in the intestinal tract, absorbed passively via enterocytes, then transported by albumin to the liver through the portal vein. On the contrary, medium and long-chain fatty acids require specific carrier proteins for transport throughout the cells such as fatty acids transporters protein (CD36) and fatty acids binding protein (FABP).

The general mechanism of LC-PUFAs digestion engages enzymes releasing a nonesterified form of fatty acids – free fatty acids from esterified fatty acids as a dietary triglycerides or phospholipids, which depends on the activity of lipase in the stomach producing free fatty acids and diacylglycerol (DG). Pancreatic lipase in the intestine reduce DG to 2-mono-glycerides and free fatty acids. Triglycerides containing LC-PUFAs are also hydrolyzed by cholesterol ester hydrolase. Pancreatic phospholipase A2 hydrolyzes dietary phospholipids to 1-lysophospholipids and free fatty acids. Subsequently free fatty acids and 2-mono-glycerides are mixed with bile salts into micelles formed with phospholipids, which helps with transport through the water layer as apolar lipids and goes to the microvillus membrane, where enterocytes can finally absorbed them. Then lipids are used to create chylomicrons (lipids such as triglycerides, phospholipids but also cholesterol and apoproteins). Chylomicrons are secreted to the lymph, bloodstream, and peripheral tissues. Lipoproteins lipases cleave chylomicrons losing triglycerides and giving chylomicrons remnants, which exchange components with other plasma lipoproteins. Eventually, they are transported to the liver, where they are further metabolized (**Ramírez et al., 2001; Kerr et al., 2015**).

The liver is a metabolic organ primarily responding to diet, and one of the essential sites where lipid metabolism takes place. It is responsible for lipid homeostasis and the place for their excessive deposition. This organ actively metabolizes fatty acids as a source of energy, regulates the uptake and synthesis of lipids, and secretion of lipoproteins, and regulates the availability of fatty acids for peripheral tissues by the production of very-low-density lipoprotein (VLDL) (**Nguyen et al., 2008**). Fatty acids, triglycerides, and cholesterol are synthesized mainly in the liver, but these processes are species-dependent, and in some organisms the adipose tissue takes over these functions (**Bergen and Mersmann 2005**). Dietary PUFAs affect the synthesis of triglycerides in the liver (**Vallim and Salter 2010**) and influence the fatty acids oxidation process in hepatic mitochondria and peroxisomes. The process of lipogenesis takes place mainly in the liver and is moderated by dietary PUFAs by changing the expression of critical genes involved in the fatty acids synthesis, such as coding for enzymes acetyl-CoA carboxylase (ACC) or FASN **(Guillevic et al., 2009**). The liver plays a fundamental role in lipid metabolism and recent studies on the role of dietary compounds modifing hepatic gene expression in animal models are of great interest **(Osada, 2013; Gabás-Rivera et al., 2013; Nojima et al., 2013; Luo et al., 2016; Siersbæk et al., 2017).**

Fatty acids derived from a diet are one of the sources for the turnover of free fatty acids in the liver. Additionally, free fatty acids can be synthesized during *de novo* lipogenesis from glucose, which takes place mainly in the liver, or can circulate in the plasma as a pool of nonesterified free fatty acids. Excessive fatty acids are stored in reesterified form accumulated as a new triglycerides or embedded in cell membranes as phospholipids. Both triglycerides and phospholipids are synthesized in the smooth endoplasmic reticulum. Triglycerides accumulated in the liver or adipose tissue are released as free fatty acids when it is necessary by the process of lipolysis (hydrolyzed by lipases) or lipophagy (autophagy of lipid droplets) as have been shown in many studies (**Dong and Czaja, 2011; Singh and Cuervo, 2012; Liu and Czaja, 2013; Carmona-Gutierrez et al., 2015**). The lipolysis of triglycerides in adipose tissue provides free fatty acids into plasma and are consequently transported to the liver. Other sources of free fatty acids come from the lipolysis of peripheral lipoproteins (chylomicrons, VLDL). The uptake of fatty acids by hepatocytes (medium- and long-chain fatty acids) is mediated by fatty acids binding proteins like FABP and fatty acid transporters such as CD36. After absorption *via* hepatocytes, PUFAs can be utilized during the fatty acids oxidation process in hepatic mitochondria and peroxisomes. During this catabolic process, fatty acids are utilized and serves as a source of ATP for energy production, which is one of the primary function of fatty acids. Triglycerides are secreted in the form of VLDL into the plasma. When in plasma excess circulating VLDL occur, they are re-estrified into triglycerides in cytoplasmic organelles called lipid droplets (LD) (**Debeer et al., 1982; Alves-Bezerra and Cohen, 2017**). The efficiency of fatty acids absorption can be affected by different factors. Omega-3 LC-PUFAs absorption depends on the sex, due to different metabolism and they are better absorbed by women than men **(Decsi and Kennedy, 2011; Lohner et al., 2013; Howe et al., 2014; De Groot et al, 2019**). Additionally, a higher proportion of omega-3 was reported to be deposited in the tissues of female rats compared with male rats (**Ghasemifard et al., 2015**). Female rats synthesize LC-PUFAs DHA from short-chain precursor ALA more efficiently than male rats, perhaps due to differences in expression of delta-5- and delta-6- desaturases in the liver (**Extier et al., 2010; Kitson et al., 2012**).

Balanced omega-6 to omega-3 ratio in organisms' homeostasis: Today's Western diet is characterized by omega-3 fatty acids deficiency together with excessive omega-6 fatty acids intake. In the World Health Organizations' (WHO) recommendations, one of the crucial parts of the healthy diet is a balanced omega-6/omega-3 fatty acids ratio, which is 4:1.

Evolutionary findings show, that the ideal ratio of both PUFAs families should be even lower, close to 1:1. Nevertheless, today's Western diet has changed markedly, with an unhealthy increase of omega-6/omega-3 ratio estimated to 20:1 (**Simopoulos, 2001; Simopoulos, 2016**). The high imbalanced ratio of omega-6/omega-3 fatty acids caused by Western diet has been linked to many disorders such as obesity, type II diabetes, cardiovascular disease (CVD) or metabolic syndrome, which occurs in advance of the full symptoms of diabetes and CVD. Omega-3 PUFAs have beneficial effects on the cardiovascular system, decreasing the risk of coronary heart disease (**Bowen et al. 2016**) or atherosclerosis (**Matsumoto et al., 2008**). Recently, the high omega-6/omega-3 ratio has been reported as a link between neurodegenerative disease like schizophrenia (**Amminger et al. 2015; Pawełczyk et al., 2015; Guixà-González et al., 2016**) as well as a cause of liver disorders like nonalcoholic fatty liver disease (NAFLD), nonalcoholic steatohepatitis (NASH) until a liver cancer (**Jump et al., 2018; Perdomo et al, 2019; Liebig et al., 2019**)

Dietary PUFAs are implicated in human health and disease. It is generally known that a higher intake of PUFAs *vs.* SFAs exerts health-promoting benefits. However, one should note that among the PUFAs group, omega-6 and omega-3 fatty acids exert the opposite effect in regard to inflammatory processes. Omega-6 fatty acids are considered to be pro-inflammatory induction molecules, contrary to omega-3 fatty acids, which serves as a source of anti-inflammatory derivatives. Therefore, for a healthy diet important is not just a simple amount of these fatty acids, but the maintenance of the proper balance between omega-6 and omega-3 fatty acids, which is essential for health and metabolic disease prevention **(El-Badry et al. 2007; Simopoulos 2016)**.

Type II diabetes is one of the metabolic disorders caused by an imbalanced dietary intake of omega-6/omega-3 ratio. Nowadays, it is one of the most occurring disorders in Western countries, arising from 108 million people suffering in 1980 to 422 million in 2014 (https://www.who.int/news-room/fact-sheets/detail/diabetes). Type II diabetes is associated with insulin resistance, impaired insulin signaling, β-cell dysfunction and abnormal glucose levels. Additionally, during type II diabetes occur sub-clinical inflammation, increased oxidative stress, and altered lipid metabolism, which can be therapeutically targeted by dietery intake of omega-6 and omega-3 fatty acids. One of the recommendations of WHO to prevent or delay the onset of diabetes is healthy diet including balanced omega-6/omega-3 fatty acids intake.

The risk of obesity rise with the increased ratio of omega-6/omega-3, moreover the occurrence of obesity is associated with raised omega-6 fatty acids in red blood cells membranes. Development of obesity is promoted by eicosanoid metabolites from omega-6 AA and may be counteracted by increased intake of omega-3 EPA and DHA (**Simopoulos, 2016**).

The potential for therapeutic application of omega-3 fatty acids is also promising for NAFLD prophylaxis (**Li and Chen, 2012**). Nonalcoholic fatty liver disease occurs predominantly in Western countries and is characterized by increased inflammation and abnormal lipid accumulation in the liver, where it is stored mainly as triglycerides (**Bechmann et al., 2012**). It is considered as an obesity-related disorder, and its prevalence is also connected to type II diabetes. Excessive deposition of lipids leads to liver steatosis with its progression from steatosis to steatohepatitis, cirrhosis, and even hepatocellular carcinoma. The composition of hepatic fatty acids influences on the liver damage degree – an increased ratio of SFAs to unsaturated fatty acids (UFAs) in the liver may mediate the development of NAFLD and its progression to NASH. The increased presence of circulating or deposited SFAs in the liver is associated with increased production of pro-inflammatory cytokines and oxidative stress (**Gentile and Pagliassotti, 2008**).

1.2.3. Supplementation of human and animal diet with PUFAs

The limitations connected to experiments performed on human cohort studies make it difficult and imprecise to evaluate the real impact of dietary components on gene expression changes (**Afman and Müller, 2012**). Evaluation of subtle changes caused by nutrition in humans is extremely difficult due to the lack of precise measurements of intake of experimental ingredients, individual differences of human susceptibility to genetic diseases, and individual medical history (**Afman and Müller, 2012**). Human nutrigenomic studies are still challenging because of difficulties in tissue sampling taking into account only easily accessible, such as blood. In contrast, biopsies from organs such as the liver, pancreas, muscles and visceral adipose tissue from healthy volunteers are problematic to collect due to ethical reasons (**Afman and Müller, 2012**). The limitations of research in humans necessitate the replacement by using animals in controlled experiments. Animal models enable precise and accurate measurements of direct diet effects. New technologies being used in nutrigenomic research on animal models develop and improve nutrition studies and our

understanding of the effect of dietary components on gene expression modulation (**Afman and Müller, 2012**).

1.2.4. Pig as a model in biomedical research

Pig is considered to be a suitable animal model for nutrigenomic and metabolic research (**Litten-Brown et al., 2010; Koopmans et al., 2011; Koopmans and Schuurman, 2015**). Similarities in anatomy and physiology with humans, particularly the gastrointestinal tract, similar body size and body morphology as well as shared metabolic and digestive features with humans are reasons for choosing this large farm animals for nutritional studies. The availability of porcine fully annotated genome as well as high sequence homology and similar chromosomal structure to the human genome, compared to other domestic animal species (**Lunney 2007**) determine them as a particularly suitable choice for the transcriptomic studies. Processes revealed in the pig transcriptome are more likely to be similar to those in humans. Pigs have been widely used in biomedical research over the past dozen years (**Bendixen et al., 2010; Gutierrez et al., 2015**). Pig models for the early stage of metabolic syndrome and diabetes are validated and now effectively used in research searching for biomarkers of early onset of metabolic syndrome (**Neeb et al., 2010; Te Pas et al., 2013; Newell-Fugate et al., 2014; Zhang and Lerman, 2016; Eirin et al., 2017; Te Pas et al., 2018**).

1.2.5. Nutrigenomics – innovative methods in PUFAs studies

The advent of new technologies in genomics, transcriptomics, proteomics, and metabolomics in the last 15 years in elucidating diet-genome interactions enabled a more comprehensive understanding of subtle genomic changes caused by bioactive molecules and their health outcomes. The development of sequencing methods opened a new area of research referenced as nutrigenomics. Nutrigenomics is defined as a science elucidating the role of bioactive components of a diet on gene expression, and it is different from nutrigenetics, which study the influence of individual genetic variation on the dietary response (**Ferguson, 2009; Fenech et al., 2011; Ordovas et al., 2018**). Nutrigenomics is a multidisciplinary science, which involves studies of the effects of dietary compounds on different genomic level including genome stability (chromosomal or molecular damage of DNA), epigenetic changes (DNA methylation and histone acetylation), RNA and micro RNA expression

(transcriptomics), protein expression (proteomics), and metabolite differences (metabolomics) (**Fenech et al., 2011**).

The beginning of broad transcriptomic research has become possible along with sequencing for the first time the entire DNA of the human genome in the 1990s within the Human Genome Project (**Fenech et al., 2011**). Development of the NGS as a powerful genetic analysis tool facilitated discovering the modulatory effect of different factors on a wide genome expression scale, this cause that NGS is rapidly gaining popularity in recent years. Changes in transcription under environmental factors such as nutrients, especially the influence of omega-3 fatty acids on the whole genome, requires comprehensive bioinformatic analysis. Data analysis and interpretation are still challenging. The application of transcriptomic technologies in nutrigenomic research of lipids is still limited. However, it is becoming clear that different intake and composition of dietary fatty acids have a significant impact on the regulation of homeostatic control mechanism and cellular adaptation by modulation of gene transcription (**Afman and Müller, 2012**).

Nutrigenomic research tools such as transcriptomics are useful for screening of large sets of genes under the influence of diet components, which can upregulate or downregulate gene expression. Many of the nutrigenomic studies were focused on nutrition imbalanced disorders (**Mead et al. 2007; German et al. 2011; Rana et al. 2016**), including omega-3 effects interventions (**Depner et al, 2013; Gladine et al. 2014; Manousopoulou et al. 2019**). Recently, transcriptomic tools are being used for investigation the omega-6 and omega-3 fatty acids influence on gene expression in particular tissues (**Szostak et al., 2016; Ogłuszka et al., 2017; Vitali et al., 2018; Zhang et al., 2019; Xue et al. 2020**). Further technological advances in lipidomic research will be helpful in the evaluation of the omega-3 fatty acids impact on metabolic changes and understanding of their effect on health **(Yang and Han, 2016; Zárate et al. 2017).**

Lipidomics enable identification and expression level of lipids in different tissues. Full lipid profiles can be obtained through newly developed techniques, including MALDI-TOF. Together with other omics technologies, lipidomics provides a wide screen of the molecular signatures of tissues. Transcriptomics using techniques such as NGS evaluates the activity of the genes metabolizing lipids. However, the molecular changes and profiles of the lipids cannot be evaluated with NGS. The combination of transcriptomics and lipidomics highlights the genome activity and physiological activity for lipid metabolism. One of the examples of

the lipidomic approach employed to omega-3 research is the investigation of the effects of omega-3 fatty acids on hepatic phospholipids composition and lipogenesis in rats after fish oil supplementation (**Lamaziere et al., 2013**). Lipidomics is still in its infancy. Still, more in-depth studies are necessary to elucidate the impact of omega-3 fatty acids.

2. Dissertations' research objectives and goals

1) The primary aim of the present work was the investigation of the effect of dietary omega-6 and omega-3 PUFAs on hepatic gene expression in a pig model, and to investigate and identify the physiological and molecular processes associated with upregulated and downregulated genes at whole hepatic transcriptomic level in most popular in Poland purebred pigs (PL) as well as crossbred pigs (PL x Duroc). The genome-wide mRNA expression in the liver was assessed using the RNA-Seq approach of the NGS method. The porcine hepatic transcriptomes changed by omega-6 and omega-3 PUFAs dietary supplements feeding were compared to outcomes of standard diets.

2) The second aim of the research was to examine the differences in gene expression alterations associated with the genetic back ground by comparison of purebred and crossbred pig breeds. We used PL purebred and crossbred PL x Duroc because Duroc differs in the quality and quantity of lipid content in the carcass. Purebred Duroc was not available at the commercial farm, so we had to rely on crossbred animals.

Based on the above mentioned targeted aims, this dissertation was carried out to achieve the following research objective tasks:

1. To analyze and construct the phenotypic data based on the hepatic profiles of fatty acids using gas chromatography (GC-FID)
2. To generate the hepatic gene expression RNA-Seq (FASTq) data of PL purebred and the PL x Duroc crossbred and submit to the short read archive (SRA) NCBI resource database.
3. To align and map the RNA-Seq reads of hepatic gene expression data of PL purebred and the PL x Duroc crossbred to the *Sus scrofa* reference genome.
4. To identify the differentially expressed gene-transcripts (DEGs-transcripts) within PL purebred by comparing the standard (control) diet *versus* supplementary diet enriched with omega-6 and omega-3 fatty acids (PUFAs) on the liver transcriptome.
5. To identify the DEGs-transcripts within PL x Duroc crossbred by comparing the standard (control) diet *versus* supplementary diet enriched with omega-6 and omega-3 fatty acids (PUFAs) on the liver transcriptome.
6. To identify the DEGs-transcripts in pigs fed with standard (control) diet by comparing between the PL purebred *versus* PL x Duroc crossbred liver transcriptome.

7. To identify the DEGs-transcripts in pigs fed with omega-6 and omega-3 fatty acids (PUFAs) supplementary diet by comparing between the PL purebred *versus* PL x Duroc crossbred liver transcriptome.
8. To identify hepatic gene expression networks and metabolic pathways within PL purebred by comparing the standard (control) diet *versus* supplementary diet enriched with omega-6 and omega-3 fatty acids (PUFAs) on the liver transcriptome.
9. To identify hepatic gene expression networks and metabolic pathways within PL x Duroc crossbred by comparing the standard (control) diet *versus* supplementary diet enriched with omega-6 and omega-3 fatty acids (PUFAs) on the liver transcriptome.
10. To identify hepatic gene expression networks and metabolic pathways in pigs fed with standard (control) diet by comparing between the PL purebred *versus* PLxDuroc crossbred liver transcriptome.
11. To identify hepatic gene expression networks and metabolic pathways in pigs fed with omega-6 and omega-3 fatty acids (PUFAs) supplementary diet by comparing between the PL purebred *versus* PLxDuroc crossbred liver transcriptome.
12. To validate the RNA-Seq experiment using qRT-PCR.

3. Materials and methods

3.1. Feeding experiment including Polish Landrace purebred and Polish Landrace x Duroc crossbred

The feeding experiment was carried out in two pig breeds: *viz.*, purebred PL (n=99) and PL x Duroc (n=102) crossbreed female pigs to investigate the effect of omega-6 and omega-3 PUFAs supplementation on the hepatic fatty acids profile.

3.1.1. Study design in the feeding experiment

The feeding experiment was conducted on three commercial farms in Poland localized in Sierpc, Chojnice, and Sosnowiec. Both purebred and crossbred pigs were distributed on each of the farms, and animals from the same litter were allocated into separate diet groups. The animals were housed under standard conditions, in small groups up to 6 individuals *per* pen, with fodder and water *ad libitum*. The animals within each of the purebred and crossbred pigs were divided into four dietary groups within each breed – three experimental groups containing PUFAs enriched diet, and one control group containing standard diet (**TABLE 1)**.

The experimental diets were comprised of the standard diet enriched with PUFAs using linseed and/or rapeseed oil in the following percentages in the fodder: rapeseed oil 2% (R group), rapeseed oil 2% and linseed oil 1% (RL group), rapeseed oil 1% and linseed oil 2% (LR group). The control diets (C) included a standard diet adjusted to pigs' age and development stage. The diets raw components are listed in a **TABLE 2** and **FIGURE 4.**

The linseed and rapeseed oils used in the study were a source of LA – omega-6 fatty acids family, and ALA – omega-3 family. Each diet was isoenergetic and protein balanced (**TABLE 1)**. The metabolizable energy (ME) values were 12.8 MJ/kg, 13.29 MJ/kg, 13.51 MJ/kg, and 13.51 MJ/kg for C, R, RL, LR feeding groups, respectively. The crude protein percentage were 15.66% for C diet, 15.65% R, 15.65% RL, and 15.65% LR diet. The total fat percentage was 1.78% for C diet, 3.74% R, 4.72% RL, and 4.72% LR. The pig feed formulation was prepared by the manufacturer (Inntaler Polska Sp. zoo.).

Table 1. The composition of the diets. Percentage of ingredients in mass of fodder mixtures.

Ingredients (%)	C1; C2	R1; R2	RL1; RL2	LR1; LR2
Rapeseed meal	6	7	7.2	7.2
Soybean meal	9	9	9.2	9.2
Wheat	54	51	49.6	49.6
Barley	28.5	28.5	28.5	28.5
Linseed oil	**-**	**-**	**1**	**2**
Rapeseed oil	**-**	**2**	**2**	**1**
Other*	2.5	2.5	2.5	2.5
Total	**100**	**100**	**100**	**100**
Composition (%)				
Crude protein	15.66	15.65	15.65	15.65
Crude fibre	4.12	4.16	4.16	4.16
Crude fat	1.78	3.74	4.72	4.72
Ash	2.87	2.88	2.88	2.88
Starch	45.91	44.18	43.37	43.37
Energy (MJ/kg DM)				
ME	12.86	13.29	13.51	13.51

1 – PL groups; 2 – PL x Duroc groups; C – control diet (standard diet without supplementation); R – standard diet plus 2% of rapeseed oil; RL – standard diet plus 2% of rapeseed oil + 1% of linseed oil; LR – standard diet plus 1% of rapeseed oil + 2% of linseed oil; *vitamins, minerals and additives used in standard commercial fodder mixtures by the producer; ME – metabolizable energy; MJ/kg DM – energy per kilogram of dry matter.

Table 2. Major chemical components of the diets as the percentage in feed mixture mass, and metabolizable energy (ME) values:

[#]dry matter, C – control diet, R – rapeseed oil 2% , RL – rapeseed oil 2% and linseed oil 1%, LR – rapeseed oil 1% and linseed oil 2%.

Composition	C	R	RL	LR
Crude protein (%)	15.66	15.65	15.65	15.65
Crude fat (%)	1.78	3.74	4.72	4.72
Starch (%)	45.91	44.18	43.37	43.37
Sugar (%)	3.62	3.6	3.59	3.59
Ash (%)	2.87	2.88	2.88	2.88
Crude fiber (%)	4.12	4.16	4.16	4.16
ME (MJ/kg DM[#])	12.86	13.29	13.51	13.51

[#]dry matter, C – control diet, R – rapeseed oil 2% , RL – rapeseed oil 2% and linseed oil 1%, LR – rapeseed oil 1% and linseed oil 2%.

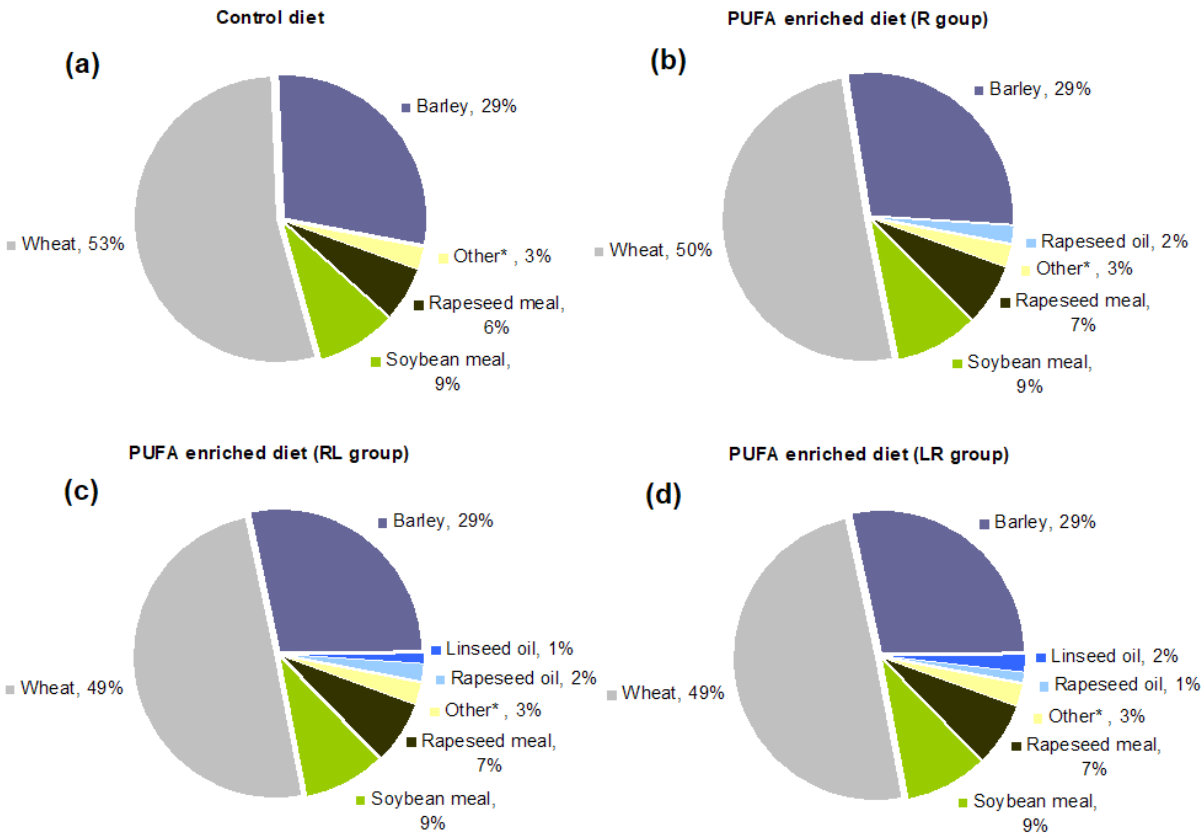

Figure 4. Percentages of raw components in the PUFAs enriched and control diets. a) – control diet, b) – rapeseed oil 2% , c) – rapeseed oil 2% and linseed oil 1%, d) – rapeseed oil 1% and linseed oil 2%. *vitamins, minerals and feed additives.

The scheme of the feeding experiment is presented in **FIGURE 5.** Before the feeding experiment, all pigs were fed with the standard diet. The feeding experiment began when animals reached 2 months of age and 60 kg of weight. The experimental and control diets were administered for 4 months in parallel groups within each of the farms. At the study, endpoint pigs weighed 110 kg in the age of 6 months. They were sacrificed by electrical stunning and exsanguination according to the industry standards. Tissue collection included liver samples cut out from the right lobe and samples were immediately frozen in liquid nitrogen. The slaughter procedure was carried out with the required permits, according to Minister of Agriculture and Rural Development dated April 2, 2004. Storage (-80ºC) and laboratory procedures were held in the Institute of Genetics and Animal Biotechnology of the Polish Academy of Sciences in Jastrzębiec.

The frozen liver samples were processed for total lipids (n=201) or total RNA extraction (n=22). The lipids were analyzed using gas chromatography in order to examine the fatty acid profiles. Total RNA was analyzed using NGS in order to examine the transcriptomic profiles and real-time PCR (n=50) for standard validation of NGS results (**TABLE 4**).

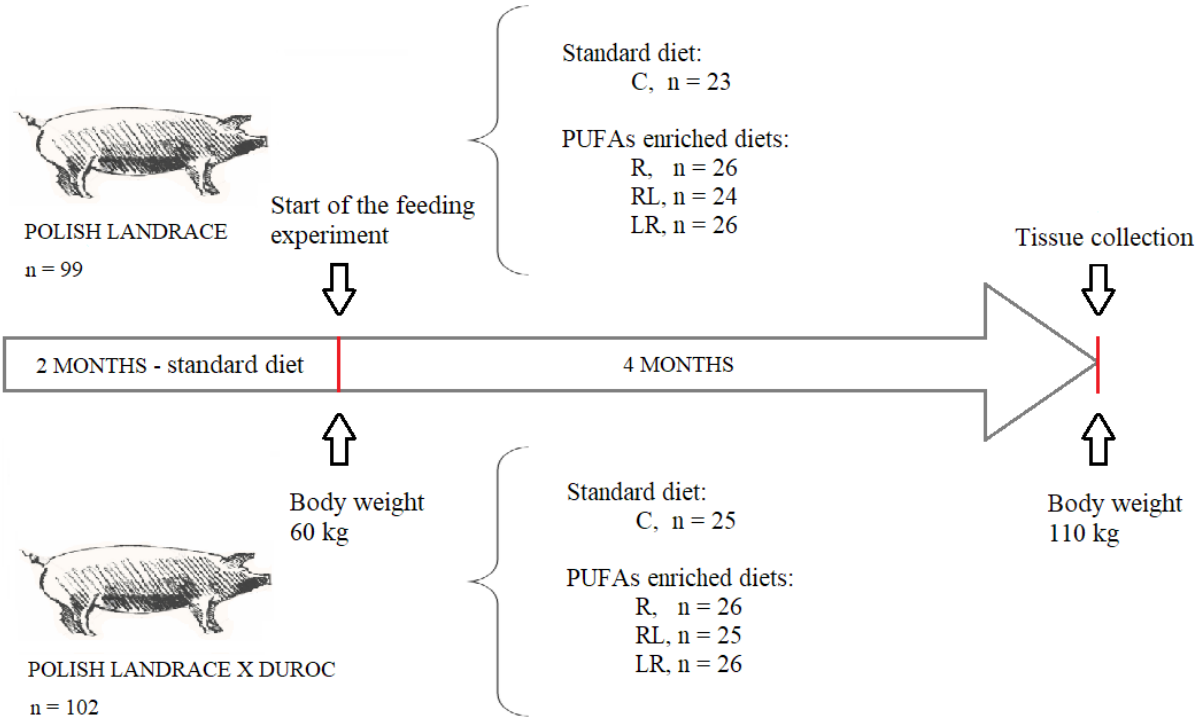

Figure 5. The scheme of the feeding experiment. C – control diet; R – standard diet plus 2% of rapeseed oil; RL – standard diet plus 2% of rapeseed oil + 1% of linseed oil; LR – standard diet plus 1% of rapeseed oil + 2% of linseed oil.

Table 3. Sample size (n) used in different analysis and distribution of animals in the feeding experiment.

Analysis	Sample size (n)							
	PL				PL x Duroc			
	C1	R1	RL1	LR1	C2	R2	RL2	LR2
Fatty acids profile	23	26	24	26	25	26	25	26

1 – PL groups; 2 – PL x Duroc groups; C – control diet (standard diet without supplementation); R – standard diet plus 2% of rapeseed oil; RL – standard diet plus 2% of rapeseed oil + 1% of linseed oil; LR – standard diet plus 1% of rapeseed oil + 2% of linseed oil

Table 4. Number of individuals used in each analysis.

Animals	Dietary groups		Fatty acids profiling (n)	RNA-Seq (n)	qRT-PCR (n)
Polish Landrace (n=99)	Standard diet	C	23	6	15
	PUFA enriched diets	R	26	–	–
		RL	24	–	–
		LR	26	6	15
Polish Landrace x Duroc (n=102)	Standard diet	C	25	5	8
	PUFA enriched diets	R	26	–	–
		RL	25	–	–
		LR	26	5	12

C – control diet, R – rapeseed oil 2% , RL – rapeseed oil 2% and linseed oil 1%, LR – rapeseed oil 1% and linseed oil 2%.

3.1.2. Laboratory procedures in the feeding experiment

The hepatic fatty acids profiles were analyzed by GC-FID.

3.1.2.1. Lipid extraction

Total lipids were extracted from the liver (n = 201) using the method described by **Folch et al. (1957)**. Briefly, 1 gram of tissue was homogenized in chloroform-methanol (2:1 v/v) mixture. Agilent 7890 Series GC system with FID detector (Agilent Technologies, Santa Clara, CA, USA) was used to separate fatty acid methyl esters (FAME), and to identify the relative concentrations of individual fatty acids.

3.1.2.2. Gas chromatography

Gas chromatography was performed on capillary column Hewlett-Packard-88 (60 m x 0.25 mm x 0.20 μm) (Agilent, J&W GC Columns, Agilent J&W, Santa Clara USA) using helium as a carrier gas, with a flow rate of 50 mL/min. The injector and detector were maintained at 260°C, and the temperature of column oven was as follows – 140°C for 5 min increasing at the rate of 4°C/min to 190°C and then to 215°C at a rate of 0.8°C/min (**Poławska et al. 2013**). Various fatty acids percentage were calculated in relation to a methyl ester as a calibrator (Supelco 37 Component FAME mix, 47885-U – 10 mg/ml in methylene chloride, Sigma-Aldrich Co.). The analytical standard was expressed in 1g/100g of FAME. The modifications implemented in the method were described previously in **Poławska et al. 2013.**

3.1.3. Statistical analysis on fatty acids phenotypic data

Data were evaluated for four PL purebred, and four PL x Duroc crossbred feeding groups. The equality of variances was tested using Levene's statistics. Shapiro Wilk and Kołmogorow-Smirnow statistics were used for normality testing. The lack of variances homogeneity and normal distribution did not allow for ANOVA testing. Data, including various fatty acids content measured in individual samples were summarized and presented as mean and standard deviation (SD). The statistical differences between the fatty acids mean percentage were assessed using the Kruskal-Wallis test. Significance was based on a Dunn's multiple comparison test for post-hoc analysis. Statistical significance was considered at

$p<0.05$, $p<0.01$ and $p<0.001$. One star was used to indicate $p<0.05$, two stars for $p<0.01$ and three stars for $p<0.001$. Calculations were carried out using IBM SPSS statistics within PS IMAGO PRO 5.1. package (IBM Corporation, Chicago, IL, USA), GraphPad Prism software and Microsoft Excel.

3.2. NGS based RNA-Seq experiment including Polish Landrace purebred (MiSeq Illumina platform) and Polish Landrace x Duroc crossbred (HiSeq Illumina platform) pigs.

3.2.1. Study design

In the NGS based RNA-Seq experiment, two different independent NGS Illumina platforms were utilized to sequence the porcine liver transcriptome (RNA-Seq). The RNA-Seq experiment for the purebred PL (n=12) was performed using the MiSeq Illumina platform (commercial service: Genomed: http://www.genomed.pl/) and for the crossbred PL x Duroc (n=10) using HiSeq Illumina platform (commercial service: CB DNA: https://www.cbdna.pl/).

Two dietary groups, control diet, and PUFAs enriched diet were investigated in the NGS based RNA-Seq experiment. Initially, three different PUFAs diets were verified in the feeding experiment (**SECTION 3.1**). The PUFAs enriched dietary group, which effectively affected omega-6/omega-3 ratio in the liver of both pig breeds was selected for RNA-Seq. The selected PUFAs diet (LR, referred further as PUFAs enriched diet) was enriched both with LA and ALA including 660 mg of LA in 100 g of fodder and 64 mg ALA in 100 g of fodder, whereas the control diet contained 268 mg of LA and 25 mg of ALA in 100g of fodder. Both control and PUFAs enriched diets were isoenergetic, with ME=12.86 MJ/kg and ME=13.51 MJ/kg of dry matter, respectively, and isoproteic with crude protein percentages rate 15.66% and 15.65%, appropriately. Total fat content was 1.78% for the control diet and 4.72% for the PUFAs enriched diet.

The comparison of gene expression profiles was performed for the control and PUFAs enriched dietary groups within as well as between each breed – C1, C2 and LR1, LR2 (**TABLE 5).** The selection of liver samples (n=22) for NGS was based on fatty acid profiles in order to compare hepatic transcriptomes characterized by low (control groups) with high (PUFAs enriched diet groups) omega-6/omega-3 fatty acids ratio in both purebred and crossbred pigs. Therefore, samples that revealed the extreme ratio of omega-6/omega-3 fatty acids within dietary groups were chosen for RNA-Seq analysis. The threshold value of < 7 for low and > 7 for high omega-6/omega-3 fatty acids ratio was used in this study. Finally, the number of liver samples used in the NGS experiment was 6 *per* group for PL purebred

using MiSeq Illumina platform, and 5 *per* group for PL x Duroc crossbred using HiSeq Illumina platform (**TABLE 5**).

Table 5. Distribution of animals in the NGS experiment (MiSeq and HiSeq Illumina platforms).

Analysis	Sample size							
	PL (MiSeq)				PL x Duroc (HiSeq)			
	C1	R1	RL1	LR1	C2	R2	RL2	LR2
RNA-Seq	6	–	–	6	5	–	–	5
qRT-PCR	15	–	–	15	8	–	–	12

3.2.2. Samples preparation in the NGS based RNA-Seq experiment

The frozen liver samples were processed for total RNA isolations (n=22: **TABLE 5**). Total RNA was analyzed using NGS based RNA-Seq method in order to examine the transcriptomic gene expression profiles and qRT-PCR for standard validation of NGS results.

3.2.3. Laboratory procedures in the NGS based RNA-Seq approach

The laboratory procedures for both purebred and crossbred hepatic transcriptome sequencing experiments are described as below in two sub-sections.

3.2.3.1. Laboratory procedures of NGS based RNA-Seq experiment for Polish Landrace purebred pigs using the MiSeq Illumina platform

RNA extraction: Initially, total RNA was extracted from 20 mg of liver samples (n=12) of **PL purebred pigs** using RNeasy Lipid Tissue Mini Kit (Qiagen, Hilden, Germany) following the manufacturer's instructions. The concentration and purity of RNA were measured using NanoDrop spectrophotometer (Thermo Scientific, USA). RNA integrity number (RIN) was assessed by Bioanalyzer 2100 and RNA 6000 Nano kit (Agilent Technologies, Inc., Santa Clara, CA, USA). The high-quality extracts (RIN≥5.) were used for cDNA libraries synthesis.

cDNA libraries preparation (MiSeq)*:* The construction of cDNA libraries was performed using Illumina TruSeq RNA Sample Prep Kit v2 (Illumina, San Diego CA, USA). The detailed laboratory procedures of cDNA library preparation are described in the next section. Briefly, 1µg of total RNA was used as an input for poly(A) selection for the enrichment of mRNA. The purified extracts of mRNA were pooled together within each, high or low omega-6/omega-3 ratio group, and an equal amount of mRNA was used to ensure the most robust transcriptome. The synthesis of libraries for each breed-experimental group combination was prepared in duplicate (technical replicates) – two for control groups (high omega-6/omega-3 ratio) and two for experimental groups (low omega-6/omega-3 ratio). The cDNA libraries were loaded onto the flow cell channels of the Illumina platform.

Liver transcriptome sequencing (RNA-Seq) using the MiSeq Illumina NGS platform: The transcriptome profiling was performed on Illumina MiSeq using the standard Illumina sequencing approach for RNA-Seq and according to the manufacturer's recommendations. Experiments were performed using paired-end sequencing reads and selected length of reads was 151 bps.

3.2.3.2. Laboratory procedures of NGS based RNA-Seq experiment for Polish Landrace x Duroc crossbred pigs using the HiSeq Illumina platform

RNA extraction*:* Initially, total RNA was extracted from 20 mg of liver samples (n=10) **PL x Duroc crossbred pigs** using RNeasy Lipid Tissue Mini Kit (Qiagen, Hilden, Germany) following the manufacturer's instructions. The concentration and purity of RNA were measured using NanoDrop spectrophotometer (Thermo Scientific, USA). RNA integrity number was assessed by Bioanalyzer 2100 and RNA 6000 Nano kit (Agilent Technologies, Inc., Santa Clara, CA, USA). The high-quality extracts (RIN≥7.3) were used for cDNA libraries synthesis.

cDNA libraries preparation (Protocol for both MiSeq and HiSeq platform):

For both Illumina platform NGS sequencing, the total RNA from each dietary group (n=5 for PL and n=6 for PL x Duroc) were pooled together. An example of the pooling of total RNA samples in PL x Duroc crossbred pigs is presented below in **TABLE 6**.

Table 6. Pooling of the total RNA samples of Polish Landrace x Duroc crossbred pigs (HiSeq experiment).

Sample ID	Concentration (ng/µl)	RIN	Pool	Dietary groups
51 W	72	8.1	**I**	**H**
88 W	72	8.1		**H**
45 W	70	8.1		**H**
55 W	70	7.5		**H**
65 W	500	7.3		**H**
Sample ID	**Concentration (ng/µl)**	**RIN**	**Pool**	**Dietary groups**
49 W	70	7.6	**II**	**L**
48 W	69	7.8		**L**
64 W	66	7.3		**L**
68 W	66	7.8		**L**
32 W	72	8.1		**L**

RIN – RNA integrity number; H – high omega-6/omega-3 ratio (control group); L – low omega-6/omega-3 ratio (PUFAs enriched diet group).

Table 7. Pooling of the total RNA samples of Polish Landrace purebred pigs (MiSeq experiment).

Sample ID	Concentration (ng/µl)	RIN	Pool	Dietary groups
63 W	124	7.7	**I**	**H**
159 W	152	7.7		**H**
95 W	143	6.7		**H**
23 W	241	7.2		**H**
142 W	157	5.0		**H**
109 W	127	7.5		**H**
Sample ID	**Concentration (ng/µl)**	**RIN**	**Pool**	**Dietary groups**
128 W	291	7.2	**II**	**L**
28 W	264	8.4		**L**
77 W	157	6.9		**L**
106 W	215	6.8		**L**
117 W	153	7.9		**L**
134 W	247	8.0		**L**

RIN – RNA integrity number; H – high omega-6/omega-3 ratio (control group); L – low omega-6/omega-3 ratio (PUFAs enriched diet group).

Fragmentation procedures: The RNA fragmentation was performed using the 0.4 µg total RNA from each pool of dietary groups using the TruSeq RNA sample preparation kit. Firstly, by thawing the TruSeq RNA sample preparation kit (Elution, Prime, Fragment mix, Bead Binding Buffer, Bead Washing Buffer, Elution Buffer, and Temperate RNA purification beads) at room temperature, and preheat the thermal cycler lid to 100°C. After thawing, the selection and fragmentation were performed by diluting total RNA with distilled water into a final volume of 50 µl in a 96-well 0,3 ml PCR plate (RNA bead plate, RBP), followed by adding of 50 µl RNA purification beads. Beads were gently mixed by vortexing and sealed the plate with adhesive seal to perform the denaturation of mRNA at the temperature of 65°C for 5 min and 4°C. Transferred the samples to the bench when the temperature reaches 4°C and incubate 5 min at room temperature. Transferred the plate to a magnetic stand and capture the magnetic beads for 5 minutes at room temperature or until the supernatant appears clear. Carefully aspirate and discard the supernatant without disturbing the magnetic beads, and remove the plate from the magnetic stand.

Washing procedures: The washing of the magnetic beads was performed by adding 200 µl Bead Washing Buffer and then transferring the plate to a magnetic stand and capture the magnetic beads for 5 minutes at room temperature, followed by carefully aspirate and discard the supernatant without disturbing the magnetic beads. Take any remaining washing buffer off with 10 µl pipette tip and remove the plate from the magnetic stand. The elution of mRNA was performed by adding 50 µl Elution Buffer at the temperature of 80°C for 2 min and followed by 25°C. transferred the samples to the bench when the temperature reaches 25°C.

Binding procedures*:* The binding of the magnetic beads was performed by adding 50 µl Bead Binding Buffer and move the plate to a magnetic stand and capture the magnetic beads, for 5 minutes at room temperature or until the supernatant appears clear. Carefully aspirate and discard the supernatant without disturbing the magnetic beads, and remove the plate from the magnetic stand. Repeat the binding step by adding the 200 µl Bead Washing Buffer and move the plate to a magnetic stand and capture the magnetic beads for 5 minutes at room temperature or until the supernatant appears clear. Carefully aspirate and discard the supernatant without disturbing the magnetic beads. Take any remaining washing buffer off with 10 µl pipette tip and remove the plate from the magnetic stand.

Elution procedures: Finally the Elution of Prime, Fragmentation mix mRNA was perfomed by adding 19,5 µl Elution at the temperature of 80°C for 2 min, and followed by 4°C. transferred the samples from thermal cycler when the temperature reaches 4°C. After a brief centrifuge, place the plate on a magnetic for 5 minutes at room temperature or until the supernatant appears clear, do not remove from the magnetic stand until noted. Transfer 17 µl to new 96-well 0.3 ml PCR plate for cDNA synthesis (cDNA plate, CDP) and proceed immediately to cDNA synthesis.

cDNA synthesis procedures: The first-strand cDNA synthesis was performed by using and mixing the following reagents:

Extracted mRNA: 17µl fragmented and primed mRNA in CDP plate.

Add 8 µl First Strand/SuperScript II mix (1 µl of SuperScript II and 7 µl of First Strand Master Mix). After gentle mixing, sealed the plate with adhesive seal and centrifuge briefly. Put the plate on thermocycler under following PCR program (**TABLE 8)**:

Table 8. First-strand program

Temperature	Time
25°C	10 min
42°C	50 min
70°C	15 min
4°C	∞

After transferring the samples to the bench when the temperature reaches 4°C, the second strand preparation step proceeded immediately.

The second strand cDNA synthesis was performed by adding the 25 µl Second Strand Master Mix to the prepared first-strand mix. After gentle mixing, sealed the plate with adhesive seal and centrifuge briefly. Put the plate on thermocycler under following PCR program (**TABLE 9**):

Table 9. Second strand program:

Temperature	Time
16°C	60 min
4°C	∞

Move samples to the bench when the temperature reaches 4°C and placed the plate to room temperature to proceed further to clean up procedures.

The cleanup procedures of second-strand cDNA (50 µl cDNA in CDP plate) was performed by using 80% EtOH and AMPure XP beads as follows.

Before starting clean up procedure, AMPure XP beads were mixed by vortexing before dispensing the beads. Then, after adding and mixing the 90 µl AMPure XP beads to the 50 µl cDNA in CDP plate, Incubated the CDP plate for 20 min at room temperature, and moved the plate to a magnetic stand and capture the magnetic beads, for 5 minutes at room temperature or until the supernatant appears clear. Carefully aspirated and discarded the supernatant without disturbing the magnetic beads and leave the plate on the magnetic strand until noted.

Washing procedures were performed twice by adding 200 µl EtOH without disturbing the magnetic beads, followed by incubation for the 30s at room temperature. Carefully aspirate and discard all supernatant without disturbing the magnetic beads. After taking any remaining EtOH off with 10 µl pipette tip and air dry for up to 15 min at room temperature, and remove the plate from the magnetic stand.

The resuspension procedures were performed by adding 52,5 µl resuspension buffer to CDP plate. After mixing the plate, incubated it for 2 min at room temperature. Move the plate to a magnetic stand and capture the magnetic beads for 5 minutes at room temperature or until the supernatant appears clear. Finally, transferred 50 µl supernatant to a new 96-well 0,3 ml PCR plate (Insert Modification Plate, IMP).

End repair procedures were performed using TruSeq RNA sample preparation kit box A/B (End Repair Mix, End Repair Control, IMP plate, Resuspension buffer), AMPure XP beads, 99,9% EtOH and Nuclease-Free Water (Molecular Biology Water) reagents. After thawing

the reagent, preheat the thermocycler heating block to 30°C and prepared the 80% EtOH and dilute the End Repair Control, as below (**TABLE 10**):

Table 10. Dilution of the End Repair Control:

Mix for (x) samples	For example 30 samples	(1-10 samples + each additional sample)	-
End Repair Control	3 µl	(1 µl)	(0.1µl)
Resuspension Buffer:	297 µl	(99 µl)	(9.9µl)
Total volume:	300.0 µl	(100µl)	(10µl)

End Repair procedures were performed using the starting material of 50 µl dscDNA in IMP plate and adding and mixing the 10 µl diluted End Repair Control and 40 µl End Repair Mix reagents, sealed the plate with adhesive seal and incubated it at the temperature of 30°C for 30 minutes.

After incubation, the samples were moved to the bench to start the End repair Clean-up procedures by adding and mixing the 160 µl AMPure XP beads by vortexing before dispensing the beads and incubated it for 20 minutes at room temperature. Move the plate to a magnetic stand and capture the magnetic beads for 5 minutes at room temperature or until the supernatant appears clear, then leave the plate on the magnetic strand until noted. Carefully aspirate and discard the supernatant without disturbing the magnetic beads. After that, the clean-up procedures were performed twice by adding 200 µl EtOH without disturbing the magnetic beads and incubated for the 30s at room temperature. Carefully aspirate and discard all supernatant without disturbing the magnetic beads. Take any remaining EtOH off with 10 µl pipette tip and air dry for up to 15 min at room temperature. Finally, remove the plate from the magnetic stand and add 17,5 µl Resuspension buffer and mixed the reagents well and incubate it for 2 minutes at room temperature. Move the plate to a magnetic stand and capture the magnetic beads for 5 minutes at room temperature or until the supernatant appears clear. Finally, transfer 15 µl supernatant to a new 96-well 0,3 ml PCR plate (Adapter Ligation Plate, ALP) to proceed to **3' Adenylation**.

3' Adenylation procedures were performed using TruSeq RNA sample preparation kit box A/B (A-tailing Mix, A-Tailing Control, ALP plate, Resuspension buffer) and Nuclease-Free Water (Molecular Biology Water) reagents. After thawing the reagent, preheat the thermocycler heating block to 37°C and prepare the diluted A-tailing Control, as below (**TABLE 11**):

Table 11. Dilution of the A-tailing Control:

Mix for (x) samples	For example 30 samples	(1-10 samples + each additional sample)	-
A-tailing Control	3 µl	(1 µl)	(0.1µl)
Resuspension Buffer:	297 µl	(99 µl)	(9.9µl)
Total volume:	300.0 µl	(100µl)	(10µl)

3' Adenylation procedures were performed using the starting material of 15 µl blunt-ended cDNA in ALP plate and adding and mixing the 2,5 µl diluted A-tailing Control and 12,5 µl A-tailing Mix reagents, sealed the plate with adhesive seal and incubate it at the temperature of 37°C for 30 minutes, followed by 70C for 5 minutes and when the thermal cycler temperature is 4°C, remove samples from thermal cycler and proceed immediately to **Adapter ligation.**

Adapter Ligation procedures were performed using AMPure XP beads, 99,9% EtOH, Nuclease-Free Water (Molecular Biology Water), RNA Adapter Indices and TruSeq RNA sample preparation kit, box A/B. After thawing the reagent, preheat the thermocycler heating block to 30°C and prepared the 80% EtOH and dilute the Ligase Control, as below (**TABLE 12**):

Table 12. Dilution of the Ligase Control:

Mix for (x) samples	For example 40 samples	(1-40 samples + each additional sample)	
Ligase Control	3 µl	(1 µl)	(0.025µl)
Resuspension Buffer:	297 µl	(99 µl)	(2.475µl)
Total volume:	300.0 µl	(100µl)	(2.5µl)

Adapter Ligation procedures were performed using the starting material of 30 µl 3' adenylated cDNA in ALP plate and adding and mixing the 2.5 µl diluted Ligase Control and 2.5 µl Ligase Mix and 2,5 µl RNA adapter Index reagents, sealed the plate with adhesive seal and incubated it at the temperature of 30°C for 10 minutes, followed by adding of 5 µl Stop Ligase Mix.

After incubation, the samples were moved to the bench to start the Adapter Ligation Clean up A procedures by adding and mixing the 42 µl AMPure XP beads by vortexing before dispensing the beads and incubate it for 20 minutes at room temperature. Move the plate to a magnetic stand and capture the magnetic beads for 5 minutes at room temperature or until the supernatant appears clear, then leave the plate on the magnetic strand until noted. Carefully aspirate and discard the supernatant without disturbing the magnetic beads. After that, the clean-up procedures were performed twice by adding 200 µl EtOH without disturbing the magnetic beads and incubated for the 30s at room temperature. Carefully aspirate and discard all supernatant without disturbing the magnetic beads. Take any remaining EtOH off with 10 µl pipette tip and air dry for up to 15 min at room temperature. Finally, the plate from the was removed from the magnetic stand and add 52,5 µl Resuspension buffer and mixed the reagents well and incubate it for 2 minutes at room temperature. Move the plate to a magnetic stand and capture the magnetic beads for 5 minutes at room temperature or until the supernatant appears clear. Finally, transfer 50 µl supernatant to the new 96-well 0,3ml PCR plate (Clean UP ALP Plate, CAP) to proceed to Clean up B.

Adapter Ligation **Clean up B** procedures was performed by adding and mixing the 42 µl AMPure XP beads by vortexing before dispensing the beads and incubation for 20 minutes at room temperature. Move the plate to a magnetic stand and capture the magnetic beads for 5 minutes at room temperature or until the supernatant appears clear, then leave the plate on the magnetic strand until noted. Carefully aspirate and discard the supernatant without disturbing the magnetic beads. After that, the twice clean-up procedures by adding 200µl EtOH without disturbing the magnetic beads and incubated for the 30s at room temperature. Carefully aspirate and discard all supernatant without disturbing the magnetic beads. Take any remaining EtOH off with 10 µl pipette tip and air dry for up to 15 min at room temperature. Finally, remove the plate from the magnetic stand and add 22,5 µl Resuspension buffer and mixed the reagents well and incubate it for 2 minutes at room temperature. Move the plate to a magnetic stand and capture the magnetic beads for 5 minutes at room temperature or untill

the supernatant appears clear. Finally, transfer 20 µl supernatant to the new 96-well 0,3ml PCR plate (Polymerase Chain Reaction plate 1, PCR1) to proceed to the PCR step.

The PCR procedures were performed using TruSeq kit PCR box, Qiagen Elution Buffer (EB), AMPure XP beads, 99,9% EtOH, Nuclease-Free Water (Molecular Biology Water), Resuspension buffer from TruSeq RNA sample preparation kit, box A/B reagents. After thawing the reagent, preheat the thermocycler heating block lid to 100°C and prepared the PCR mix, as below (**TABLE 13**):

Table 13. Preparation of PCR Mix:

Mix for (x) samples	(1 sample)	For example: 27samples
PCR Master Mix	(25 µl)	675 µl
PCR Primer Cocktail	(5 µl)	135 µl
Total volume:	(30 µl)	810 µl

The PCR procedures were performed using the starting material of 20 µl eluate in the PCR1 plate and adding 30 µl PCR Mix to each sample in the PCR plate. After gentle the mix, sealed the plate with adhesive seal and centrifuged it at 280g for 1 minute to perform the PCR reaction under the TruSeq library amplification program as below (**TABLE 14**):

Table 14. TruSeq library amplification program:

Temperature	**Time**	**Cycles**
98°C	30s	1
98°C	10s	13*****
60°C	30s	
72°C	30s*****	
72°C	5 min*****	1
4°C*****	∞	

After the PCR, proceed to Clean up procedures using the 50 µl AMPure XP beads and 32,5 µl Resuspension buffer as described above. Finally, transfer 30 µl supernatant to a new 96-well 0,3 ml PCR plate (Target Sample Plate 1, TSP1) to proceed to the QC step.

The QC procedures were performed using the 30 µl Qiagen EB and 1µl of prepared library sample on Agilent Bioanalyser (1000 DNA chip). After validation of libraries, proceed to KAPA quantification with samples in TSP1 plate as below (**TABLE 15**):

Table 15. Library QC of two pools:

Index	**Well**	**Sponsor and/or Project ID**	**Sample ID**	**KAPA concentration [nM]**	**Library size [bp] if QC'ed on Agilent**
ATCACG	A3	A2125	A2125_Pool1	26.99	300
ACAGTG	B3	A2125	A2125_Pool2	28.40	300

For the both MiSeq and HiSeq experiments, the paired-end sequencing reads of 151 bp were obtained.

3.2.4. Bioinformatic analysis of RNA-Seq data of porcine liver transcriptome

3.2.4.1. Preprocessing of the RNA-Seq data: After sequencing, four RNA-Seq data were obtained for each breed. The Illumina pipeline was used for image acquisition and base-calling. Raw reads were first filtered and discarded for mistaken base calling. Reads were processed by adaptor trimming and removing of low-quality bases. Very short reads (less than 20 nt) were also removed. Preprocessing of the data was performed using the Trimmomatic tool (**Bolger et al., 2014**) and included the trimming of adaptor sequences and read filtering based on Illumina Quality Score. FASTXToolkit (Version 0.0.13) was used to obtain clean reads. For checking the reliability of data, its characteristics were inspected using the FastQC tool (**Andrews 2010**). RNA-Seq data were achieved as a FASTQ file type containing raw reads with the quality score. The analyzed characteristics included presence and abundance of contaminating sequences, average read length, GC content, presence of adaptors, or overrepresented k-mers.

3.2.4.2. Post-processing normalization of the RNA-Seq data using CLC Genomics workbench: The raw RNA-Seq reads imported from Illumina were uploaded into CLC Genomics workbench v. 6.0 (CLC Bio, Aarhus, Denmark). The reference genome *Sus scrofa* v.11.1 was downloaded from pig reference genome assembly website resources (https://www.ensembl.org/Sus_scrofa/Info/Index), and RNA-Seq reads were mapped onto the reference genome. The read counts for a given gene were normalized using RPKM (reads per

kilobase of exon model per million reads) method (**Mortazavi et al. 2008**) between technical replicates calculated using the method previously described by **Chepelev et al. 2009**. In short, exons from all isoforms of a gene were merged to create one meta-transcript. The number of reads falling in the meta-transcript was counted and normalized by the size of the meta-transcript and by the size of the library. The lack of biological replicates in the NGS experiment necessitates additional steps in the estimation of gene expression. The expression variance for each gene was estimated using the variance across the four sequencings for one breed (two technical replicates for the control group and two for PUFAs enriched diet group) using the 'blind' method of dispersion (**Anders and Huber 2010)**. The RNA-Seq raw data of PL purebred were deposited in NCBI' GEO (Gene Expression Omnibus) (**Barrett et al. 2013**) under accession number **GSE72123**. The RNA-Seq raw data of PL x Duroc crossbred will be deposited in NCBI' GEO (Gene Expression Omnibus) **(Barrett et al. 2013)** after the submission of the Ph.D. dissertation to reviewers.

3.2.4.3. Gene expression analysis of the porcine liver transcriptome using CLC Genomics workbench

Gene expression analysis of DEGs (comparison of breeds and diets): Differentially expressed genes (DEGs) were identified using CLC Genomics Workbench v. 6.0. The normalized RNA-Seq data was used as the value of gene expression. The statistical significance was adjusted using the Benjamini and Hochberg correction test as an error rate and false discovery rate (FDR) correction test for multiple comparisons. Genes were considered to be differentially expressed with highly significant if their adjusted *p*-value (FDR) was lower than 0.0001 ($p<0.0001$).

Based on the RNA-Seq experimental design (**TABLE 5**), four different gene expression comparisons were performed to identify DEGs:

1. First Comparison of standard (control) diet vs healthy PUFA supplementary diet in PL purebred
2. Second Comparison of standard (control) diet vs healthy PUFA supplementary diet in PLxDuroc crossbred
3. Third Comparison of PL purebred vs PL x Duroc crossbred fed with standard (control) diet
4. Fourth Comparison of PL purebred vs PL x Duroc crossbred fed with healthy PUFA supplementary diet

3.2.4.4. Excel Filtering of the porcine liver transcriptome DEGs data representing Polish Landrace purebred pigs and Polish Landrace x Duroc crossbred pigs

The final lists of DEGs were filtered three times (3 stages of filtering) according to the following filtering criteria:

1. According to Bonferroni p-values, p-values, and FDR values parameters (without cutoff values, and with cutoff p-values<0.0001) of the up-regulated and down-regulated genes
2. According to the absolute value of log_2FC and FC values parameters (without cutoff values, and with two fold cutoff values) of the up-regulated and down-regulated genes.
3. According to both Bonferroni p-values and the absolute value of fold change (FC) and log2FC

Filtering criterion:

In all four DEGs comparison analysis, three stages filtering were performed to the output file of DEGs analysis from CLC pipeline:

Under the first filtering criterion, the DEGs output files of each comparison were filtered into two categories: i) the all DEGs (non-significant and significant) without cutoff values, and ii) highly significant DEGs according to Bonferroni p-values, p-values, and FDR values.

Under the second Filtering criterion, the first filtered Excel files were further filtered both i) all DEGs without cutoff values, and ii) highly significant DEGs according to cutoff values of log_2FC and FC (with two fold, four folds, and nine folds cutoff values) of the up-regulated and down-regulated genes.

Under the third filtering criterion, the first and second filtered Excel files were further filtered according to both p-values and the absolute value of fold change (FC) and log2FC.

3.2.4.5. Cytoscape biological networks analysis of the porcine liver transcriptome

Cytoscape biological networks: The biological interaction networks of DEGs between PUFAs enriched diet groups as compared to the control groups for PL and PL x Duroc were carried out using Cytoscape v. 3.1.0 software (http://www.cytoscape.org/) **(Saito et al.,**

2012). The visualizations of pathways and associated genes were done for similarly and reversely regulated pathways for two breeds. The interaction networks were created on the base of gene expression data. The first set of DEGs included commonly deregulated genes for two breeds where the direction of regulation (up- or down-regulated genes) for purebred and crossbred was the same. The second set of DEGs included commonly deregulated genes, which were regulated in the opposite direction for PL and PL x Duroc. Functional analysis was done through the CluePedia Cytoscape application. Ontology analysis was done through ClueGO v 2.2.0. (for regulation in the same direction, up or down) and ClueGO v 2.3.2. Cytoscape application (for regulation in opposite directions). The results were created for *Homo sapiens* as an analyzed organism for gene annotation as the most comprehensive genome comparing to the annotations available for other species. The ClueGO analysis referred to the data incorporated in the following databases: KEGG, REACTOME, WikiPathways, InterPro Protein Domains, and Gene Ontology (GO Immune System Process, GO Molecular Function, GO Cellular Component, and GO Biological Process).

Kappa coefficient was used to define relations (lines, connections) between annotated functional groups based on shared genes in ClueGO networks to study the functional correlations among pathways. Kappa score threshold ≥0.97 (high agreement) was used to study similar regulation (for common DEGs regulated in the same direction). The selection parameters for ClueGO in this analysis were at least 2 genes in one pathway, and a minimum 5% of genes found in the pathway from all assigned to the pathway. The adjusted parameters for the analysis of common DEGs regulated in the opposite direction for two breeds were: kappa coefficient ≥0.4 (medium agreement), at least 2 genes in one pathway and minimum 6% of genes found in the pathway from all assigned genes to the pathway. Statistical significance was considered at p-values<0.05 by a two-side hypergeometric test followed by Bonferroni step down test to correct the p-value of the enrichment terms in both ClueGO Cytoscape analysis.

3.2.5. Validation of gene expression analysis results by Quantitative RT-PCR

Selected DEGs identified in the transcriptomic sequencing analysis were validated by qRT-PCR for two pig breeds – PL purebred (n = 30) and PL x Duroc crossbred (n = 20). Validation was performed on individual liver samples, covering the samples from the RNA-Seq experiment. Differentially expressed genes were analyzed using relative gene expression analysis.

Gene expression levels were determined on individual samples for 12 DEGs: acyl-CoA synthetase long-chain family member 1 (ACSL1), apolipoprotein A4 (APOA4), apolipoprotein A5 (APOA5), diacylglycerol O-acyltransferase 2 (DGAT2), exostosin like glycosyltransferase 1 (EXTL1), fatty acid desaturase 1 (FADS1), fatty acid desaturase 2 (FADS2), acetyl-CoA carboxylase alpha (ACACA), ELOVL fatty acid elongase 6 (ELOVL6), matrix metalloproteinase-2 (MMP2), fatty acid synthase (FASN), and collagen type I alpha 1 (COL1A1). The majority of the selected target genes were involved in lipid and lipoprotein metabolism, especially in fatty acyl-CoA biosynthesis (FASN, ACSL1, ELOVL6, ACACA, FADS1, FADS2), ALA and LA metabolism (ACSL1, FADS1, FADS2), lipid signaling and chylomicron mediated lipid transport (APOA4, APOA5), triacylglycerol biosynthesis (DGAT2, ACSL1, ELOVL6), lipid metabolism regulation by PPARα (ACSL1, APOA5, FADS1, DGAT2, ELOVL6), and cholesterol biosynthesis regulation by SREBP (ELOVL6, ACACA).

Selection of appropriate reference genes for the studied tissue under given experimental conditions was performed using NormFinder software (http://moma.dk/normfinder-software; **Andersen et al. 2004**) prior to the validation experiment. The reference genes were selected from the panel of five candidates and tested against expression stability in the liver. The set included glyceraldehyde-3-phosphate dehydrogenase (GAPDH), glutathione reductase (GSR), ribosomal protein S18 (RPS18), TATA-box binding protein (TBP/LOC100125545), topoisomerase (DNA) II beta (TOP2B). NormFinder indicated GSR and RPS18 with the most stable expression in the studied tissue in this preliminary analysis. Thus GSR and RPS18 were further used in relative quantification of target genes for gene expression normalization.

The primer sequences used in this study were designed with Primer3 Input version 4.1.0 (**Koressaar and Remm, 2007; Untergasser et al., 2012**; http://primer3.ut.ee/) and Primer-BLAST tool (**Ye et al., 2012**; www.ncbi.nlm.nih.gov/tools/primer-blast/?). Primer sequences, amplicon length, and exonic location for target and reference genes are listed in **TABLE 16**.

3.2.5.1. Laboratory procedures in quantitative real-time PCR

Total RNA for qRT-PCR was extracted from the frozen liver samples using the guanidinium thiocyanate-phenol-chloroform method (**Chomczynski and Sacchi, 1987; Chomczynski and Sacchi, 2006**). The liver samples (20 mg) were homogenized using MagNA Lyser (Roche Diagnostics, Mannheim, Germany) with Trizol Reagent (Invitrogen, Carlsbad CA, USA). Total RNA was purified using chloroform, isopropanol, and 75% ethanol, and eluted with RNase free water. The RNA extracts were incubated with RQ1 RNase-free DNase (Promega, Madison, WI, USA) for 15 min at 37ºC to remove residues of genomic DNA. Purification was repeated using phenol:chloroform:isoamyl alcohol (25:24:1 v/v, Sigma-Aldrich, St Louis, USA), 100% ethanol, and 75% ethanol. The RNA extracts were again resuspended in nuclease-free water, and checked against DNA contamination on 1,5% agarose gel. RNA concentration and extracts purity against phenol and protein contamination were determined by NanoDrop spectrophotometer (Thermo Scientific, USA). RNA integrity number was evaluated using the Agilent 2100 Bioanalyzer instrument and RNA 6000 Nano Kit (chips and reagents, Agilent Technologies, Santa Clara, CA, USA). Samples were frozen in -80ºC for further processing.

Total RNA (2 μg) was reverse transcribed to cDNA using the Transcriptor First Strand cDNA Synthesis Kit (Roche Applied Science, Penzberg, Germany) in a final volume of 20 μl using random hexamer primers, according to the manufacturer's instructions.

Gene expression analysis was conducted on a LightCycler 96 instrument (Roche Applied Science, Mannheim, Germany) using SYBR Green I Master mix (Roche Diagnostics, Mannheim, Germany). Quantitative RT-PCR was carried out in triplicates for all samples and negative controls (NTC) without the cDNA template were included for all genes.

Prior to the experiment, standard curves were run for all tested genes for relative quantification analysis, and after reaction optimization resulted in a correlation coefficient greater than 0.97 and the efficiency value greater than 80% (E=1.8) as automatically calculated in LightCycler 96 software. The reaction mixture consisted of 3 μl of the cDNA template diluted 40 times, 5 pmol of the reaction primers, 5 μl of SYBR Green I, and water to a final volume of 10 μl. Amplification was performed in a 96-well optical plate (Roche

Diagnostics, Mannheim, Germany). The thermal profile used in the analysis was: initial denaturation at 95°C for 5 min followed by 40 amplification cycles at 95°C for 10 sec during denaturation step, primer hybridization in a range of 57°C to 62°C for 10 sec depending on the primer pair used, and elongation at 72°C for 10 sec. Reaction specificity including amplicon length and absence of primer-dimer peaks were verified by melting curve analysis at 95°C for 5 sec, 65°C for 15 sec, heating to 95°C with fluorescence acquisition, and cooling step at 37°C for 30 sec. The presence of a single peak in the melting curve graph of each analyzed gene showed the specificity of amplification (data not shown). Additionally, the specificity of designed primer pairs to each cDNA template (resulted in one specific PCR product) and PCR amplicon length was checked on 1.5% agarose gel.

Quantitative real-time PCR was performed following the MIQE guidelines (**Hugget et al., 2013; Bustin et al., 2013)**.

3.2.5.2. Statistical analysis of Quantitative real-time PCR

Raw data, including cycle thresholds (Ct) for a total of 17 tested genes and around 100 cDNA templates for each gene, were extracted from LightCycler 96 software. Relative expression ratio (R) was calculated according to Pfaffl model (**Pfaffl, 2001**) using Microsoft Excel. The cycle thresholds values analyzed for each cDNA and transcript, were reported as the mean and standard error of the mean (SE). Shapiro-Wilk statistics were used for testing the normal distribution of data. Levene's test using the median was used to evaluate the equality of variances. The statistical differences between PUFAs enriched diet group (containing linseed 2% and rapeseed 1%) and control group were assessed using Student's t-test, and statistical significance was considered at $p<0.05$ and $p<0.01$. Data were analyzed for two PL purebred, and two PL x Duroc crossbred feeding groups.

Table 16. Genes selected for real-time PCR, primer sequences, amplicon length and exonic location of the sequences amplified in real-time PCR.

Gene symbol	Gene name	Primer sequence (5' – 3')	Exonic position	Amplicon size (base pairs)	Chromosome location	Transcript length (base pairs)	Accession number (NCBI GeneBank)
APOA4	apolipoprotein A4	For. CAGCAGCTCAACACTCTCTT Rev. GAATCTCCTCCTTCAGCTTCTC	2/3 3	142	9	1388	NM_214388.1
APOA5	apolipoprotein A5	For. GGAAGAGAAGGGAAGAAGGAAG Rev. CATCGGCCAACAGGGATATT	3 3	83	9	1875	NM_001159308.1
ACSL1	acyl-CoA synthetase long-chain family member 1	For. TCAGAAGGTTGCCAGTGAAG Rev. CTGGAGGAGAGGATCAGAGAATA	21 21	115	15	3133 3799 3605 3605 3604 3857 4062 3791	NM_001167629.2 XM_005671709.3 (transcript variant X1) XM_021074704.1 (transcript variant X2) XM_021074705.1 (transcript variant X3) XM_021074706.1 (transcript variant X4) XM_005671708.3 (transcript variant X5)

						3885	XM_005671707.3 (transcript variant X6) XM_021074707.1 (transcript variant X7) XM_021074708.1 (transcript variant X8
ELOVL 6	ELOVL fatty acid elongase 6	For. GAACACGTAGCGACTCCGAA Rev. ATGCCGACCGCCAAAGATAA	2 3	178	8	4921 4902 4933	XM_021100705.1 (transcript variant X1) XM_021100706.1 (transcript variant X2) XM_021100707.1 (transcript variant X3)
DGAT2	diacylglycerol O-acyltransferase 2	For. GACCCTCATAGCTGCCTACTC Rev. CAGCACGGAGATGACCTGTA	1 3	136	9	1481	NM_001160080.1
FADS1	fatty acid desaturase 1	For. GGGCCTTGTGAGGAAGTATATG Rev. GGAACTCATCTGTCAGCTCTTT	2 3	104	2	1338	NM_001113041.1

FADS2	fatty acid desaturase 2	For. CCTTACAACCACCAGCATGA Rev. CCAAGTCCACCCAGTCTTTAC	7 8/9	118	2	1489	NM_001171750
ACACA	acetyl-CoA carboxylase alpha	For. ATCCGCCTCTTCCTGACAAA Rev. CCTAAGGACTGTGCCTGGAA	38 39 (X1) 37 38 (X2) 38 39 (X3) 39 40 (X4) 39 40 (X5) 38 39 (X6) 38 39 (X7) 38 39 (X8) 38 39 (X9) 37 38 (X10) 37 38 (X11)	200	12	7382 8887 9741 10817 9207 8997 9107 9090 8917 9192 9066	NM_001114269.1 XM_021066227.1 (transcript variant X1) XM_021066228.1 (transcript variant X2) XM_021066229.1 (transcript variant X3) XM_021066230.1 (transcript variant X4) XM_021066231.1 (transcript variant X5) XM_021066233.1 (transcript variant X6) XM_021066234.1 (transcript variant

						8718	X7) XM_021066235.1 (transcript variant X8) XM_021066236.1 (transcript variant X9) XM_021066237.1 (transcript variant X10) XM_021066238.1 (transcript variant X11)
EXTL1	exostosin like glycosyltransferase 1	For. TGGGATGGGCACTGTGAGC Rev. GCAGAAGGTGGCATTGGGTA	1 2	78	6	3964	XM_003356212
MMP2	matrix metallopeptitase 2	For. CGGACAAAGAGTTGGCTGTG Rev. CATGGTCTCGATGGTGCTCT	2/3 3	158	6	3082	NM_214192
FASN	fatty acid synthase	For. CTTGTCCTGGGAAGAGTGTAAG Rev. AGATGGTCACCGTGTCTTTG	11	83	12	8044	NM_001099930
COL1A1	collagen, type I, alpha 1	For. TTCAGCTTTGTGGACCTCCG Rev. CGTTCTGTACGCAGGTGACT	1	136	12	1481	XM_005668927
GSR	glutathione-disulfide reductase	For. CACAGCTCCTCACATCCTGA Rev. GGGCAATTCTTCCAGCTGAA	5 6	121	15	2818	XM_003483635
RPS18	ribosomal protein S18	For. AGGAAAGCAGACATCGACCT Rev. ACCTGGCTGTACTTCCCATC	3 4/5	158	7	528	NM_213940.1
GAPDH	glyceraldehyde-3-	For.	11	100	5	1341	NM_001206359.

	phosphate dehydrogenase	ACTCACTCTTCTACCTTTGATGCT Rev. TGTTGCTGTAGCCAAATTCA	12				1
TBP	TATA-box binding protein	For. GATGGACGTTCGGTTTAGG Rev. AGCAGCACAGTACGAGCAA	3 3	124	1	1792	XM_021085497.1
TOP2B	topoisomerase (DNA) II beta	For. AACTGGATGATGCTAATGATGCT Rev. TGGAAAAACTCCGTATCTGTCTC	11 12	137	13	5187	NM_001258386.1

3.2.6. Statistical analysis

3.2.6.1. Cytoscape: Kappa score threshold ≥0.97 (high agreement) was used for the analysis of common DEGs regulated in similar directions for both breeds. Minimum 2 genes in one pathway and min. 5% of genes found in the pathway from all assigned to the pathway were included in this analysis. The adjusted parameters for the analysis of common DEGs regulated in the opposite direction for two breeds were: kappa coefficient ≥0.4 (medium agreement), at least 2 genes in one pathway and a minimum 6% of genes found in the pathway from all assigned genes to the pathway. *P*-values<0.05 were considered significant by a two-side hypergeometric test followed by Bonferroni step down test to correct the *p*-value of the enrichment terms in both ClueGO Cytoscape analysis.

3.2.6.2. qRT-PCR: All values from each analyzed gene were checked for normal distribution (Shapiro-Wilk test) and equality of variances (Levene's test using median). Values are reported as the mean and standard error of the mean. Student's t-test for groups with unequal variances was used and differences in relative gene expression were considered statistically significant at $p<0.05$ and $p<0.01$.

4. Results

4.1. Feeding experiment including Polish Landrace purebred and Polish Landrace x Duroc crossbred pigs

4.1.1. Linseed and rapeseed oil supplementation reduces the hepatic omega-6/omega-3 ratio

The effect of different diet compositions (different PUFAs enriched diets) on fatty acids profiles in the liver was first tested in both PL purebred and PL x Duroc crossbred in order to select an appropriate PUFAs enriched diet effectively affecting the omega-6/omega-3 fatty acids ratio in the liver. The fatty acids profiling included thirteen various fatty acids. The possible differences in fatty acids liver profiles between PL and PL x Duroc under the control diet were excluded by comparing the two fatty acids profiles between purebreed and crossbreed. The analysis showed that control diet effects were comparable between purebreed and crossbreed pigs liver as no significant differences between particular fatty acids in the liver were revealed. The fatty acids contents of the three PUFAs enriched diet groups (R, RL, and LR) were compared to the control group (C) within each of the purebred or crossbred pigs.

The results for PL purebred demonstrated significant differences in fatty acids content in liver under LR diet (PUFA enriched diet containing 2% linseed oil and 1% rapeseed oil), for LA (C18:2n6), ALA (C18:3n3), EPA (C20:5n3), and DHA (C22:6n3). The percentage of LA in LR group in comparison to C group increased from 13.7% to 15.61% ($p<0.05$), ALA from 0.82% to 3.32% ($p<0.001$), EPA from 0.87% to 3.16% ($p<0.01$), and DHA from 1.88% to 3.38% ($p<0.001$). The only significant differences revealed in the RL group were shown for ALA and DHA percentage, and none of those fatty acid values were different between R and C groups (**TABLE 17**).

The significant differences in fatty acids percentage evaluated in PL x Duroc between LR and C groups were found for ALA (C18:3n3), AA (C20:4n6), and EPA(C20:5n3). The percentage of ALA increased from 1.53% to 3.43% ($p<0.01$), AA decreased from 13.55% to 8.86% ($p<0.001$), and EPA increased from 1.46% to 2.27% ($p<0.01$). Significant differences were

shown for myristic (C14:0) and arachidonic acid (C20:4n6) between R and C groups, and no differences were shown between RL and C group for PL x Duroc (**TABLE 18**).

The PUFA enriched diet consisting of 2% linseed oil and 1% rapeseed oil (LR group) compared to C group effectively reduced the omega-6/omega-3 ratio from 32.73 to 4.25 ($p<0.001$) for PL purebred (**TABLE 19**) and from 14.42 to 4.74 ($p<0.01$) for PL x Duroc (**TABLE 20**). Additionally, the PUFA/SFA ratio was changed from 0.63 to 0.80 ($p<0.001$) for PL purebred between the above-mentioned dietary groups. The PUFAs enriched diet LR and the control diet contained 660 mg of LA and 64 mg of ALA per 100 g of fodder, and 268 mg of LA and 25 mg of ALA per 100 g of fodder, respectively. The growth performance, carcass characteristics, and slaughter weight were not affected by linseed and rapeseed oils supplementation (data not shown). The PUFAs enriched diet LR were chosen for further analysis as a diet, which most effectively changed the fatty acids profile and decreased the omega-6/omega-3 ratio either in PL and PL x Duroc pigs liver. Samples from LR and C group were processed for RNA-Seq and qRT-PCR analysis. The selected samples from PUFAs enriched diet LR were characterized by low omega-6/omega-3 fatty acids ratio (<7), while from the control group (C) by high (>7) ratio.

Table 17. Liver fatty acids profiles (g/100 g FAME) of Polish Landrace (n = 99). Data presented as mean and standard deviation (SD). Differences between tested groups were evaluated using the Kruskal-Wallis test. Post-hoc statistics for p-value calculations were assessed using Dunn's test. Significance level between supplemented groups compared to control group – *p<0.05; **p<0.01, ***p<0.001. #saturated fatty acids from C4:0 to C12:0

FATTY ACID	COMMON NAME	POLISH LANDRACE – Mean (SD)			
		Control	Rapeseed oil 2%	Rapeseed oil 2% Linseed oil 1%	Linseed oil 2% Rapeseed oil 1%
≤ C12:0	Lauric acid and SFA# from C4:0	3.21 (2.44)	2.25 (1.48)	2.83 (1.35)	2.31 (1.90)
C14:0	Myristic acid	0.62 (0.28)	0.71 (0.27)	0.60 (0.28)	0.58 (0.27)
C16:0	Palmitic acid	17.93 (4.61)	18.41 (4.22)	16.37 (3.52)	16.17 (2.48)
C16:1n7	Palmitoleic acid	3.47 (4.62)	2.39 (0.56)	2.25 (0.56)	1.85 (0.75)
C18:0	Stearic acid	21.77 (5.80)	20.69 (6.19)	20.90 (6.25)	23.42 (4.64)
C18:1n9	Oleic acid	17.56 (5.42)	19.34 (6.06)	18.15 (6.20)	16.30 (4.67)
C18:1n7	Vaccenic acid	1.93 (0.42)	2.02 (0.29)	1.87 (0.20)	1.64 (0.23)
C18:2n6 LA	Linoleic acid	13.70 (3.40)	14.43 (3.36)	15.10 (3.26)	**15.61*** (2.27)
C18:3n3 ALA	α-linolenic acid	0.82 (1.17)	1.59 (0.66)	**2.32***** (1.81)	**3.32***** (1.17)
C20:3n6 ETA	Eicosatrienoic acid	3.02 (6.09)	0.50 (0.46)	0.67 (0.59)	1.57 (2.61)
C20:4n6 AA	Arachidonic acid	12.66 (4.18)	11.64 (3.34)	10.85 (3.45)	9.41 (2.87)
C20:5n3 EPA	Eicosapentaenoic acid	0.87 (0.74)	0.74 (0.60)	1.12 (0.57)	**3.16**** (0.92)

C22:6n3 DHA	Docosahexaenoic acid	1.88 (1.08)	2.20 (0.74)	**2.89*** ** (0.82)	**3.38*** ** (1.02)

Table 18. Liver fatty acids profiles (g/100 g FAME) of Polish Landrace x Duroc (n = 102). Data presented as mean and standard deviation (SD). Differences between tested groups were evaluated using Kruskal-Wallis test. Post-hoc statistics for p-value calculations were assessed using Dunn's test. Significance level between supplemented groups compared to control group – *p<0.05; **p<0.01, ***p<0.001; #saturated fatty acids from C4:0 to C12:0

FATTY ACID	**COMMON NAME**	**POLISH LANDRACE x DUROC – Mean (SD)**			
		Control	**Rapeseed oil 2%**	**Rapeseed oil 2% Linseed oil 1%**	**Linseed oil 2% Rapeseed oil 1%**
≤ C12:0	Lauric acid and SFA# from C4:0	1.44 (1.10)	2.75 (2.07)	2.03 (1.48)	1.98 (1.73)
C14:0	Myristic acid	0.46 (0.33)	**0.81*** (0.44)	0.78 (0.38)	1.07 (0.97)
C16:0	Palmitic acid	19.43 (2.34)	19.29 (3.52)	18.75 (2.24)	19.32 (3.82)
C16:1n7	Palmitoleic acid	3.04 (3.97)	2.44 (0.86)	2.42 (0.80)	2.04 (0.64)
C18:0	Stearic acid	24.43 (3.26)	17.80 (5.11)	21.08 (5.71)	21.22 (4.19)
C18:1n9	Oleic acid	17.84 (3.81)	21.23 (6.26)	20.97 (4.86)	18.38 (3.48)
C18:1n7	Vaccenic acid	2.50 (2.86)	2.19 (0.25)	1.99 (0.38)	2.47 (3.25)
C18:2n6 LA	Linoleic acid	14.90 (1.41)	14.83 (2.68)	16.05 (1.65)	15.58 (3.13)
C18:3n3 ALA	α-linolenic acid	1.53 (1.55)	2.16 2.06)	2.26 (0.74)	**3.43**** (2.21)
C20:3n6 ETA	Eicosatrienoic acid	0.73 (0.43)	1.14 (1.67)	2.04 (3.38)	0.71 (0.67)
C20:4n6 AA	Arachidonic acid	13.55 (2.93)	**9.38**** (3.23)	10.56 (4.63)	**8.86*** ** (2.72)

C20:5n3 EPA	Eicosapentaenoic acid	1.46 (1.18)	0.71 (0.48)	1.47 (1.32)	**2.27**** (1.28)
C22:6n3 DHA	Docosahexaenoic acid	2.12 (1.33)	1.85 (0.62)	2.29 (0.79)	2.45 (0.97)

Table 19. Sum of fatty acids within classes for Polish Landrace (n = 99). Data presented as mean and standard deviation (SD). Differences between tested groups were evaluated using the Kruskal-Wallis test. Post-hoc statistics for p-value calculations were assessed using Dunn's test. Significance level between supplemented groups compared to control group – *p<0.05; **p<0.01, ***p<0.001; SFA – total saturated fatty acids, MUFA – total monounsaturated fatty acids, PUFA – total polyunsaturated fatty acids, ∑ n-6 PUFA – total n-6 (sum of LA+ETA+AA), ∑ n-3 PUFA – total n-3 (sum of ALA+EPA+DHA)

FATTY ACID CLASS	**POLISH LANDRACE – Mean (SD)**			
	Control	**Rapeseed oil 2%**	**Rapeseed oil 2% Linseed oil 1%**	**Linseed oil 2% Rapeseed oil 1%**
∑ SFA	25.63 (7.72)	26.31 (5.24)	25.83 (6.90)	25.69 (4.13)
∑ MUFA	2.16 (1.83)	3.21 (1.49)	5.58 (2.25)	8.22 (3.50)
∑ PUFA	27.23 (8.05)	29.40 (5.46)	31.42 (6.64)	**33.90**** (6.28)
∑ n-6 PUFA	22.96 (7.20)	23.67 (6.58)	22.17 (6.51)	19.65 (5.38)
∑ n-3 PUFA	43.18 (9.12)	41.75 (7.22)	40.60 (7.71)	42.35 (5.09)
n-6/n-3 RATIO	32.73 (62.02)	19.25 (45.64)	**6.14**** (5.64)	**4.25***** (3.93)
PUFA/SFA RATIO	0.63 (0.17)	0.71 (0.08)	**0.77***** (0.09)	**0.80***** (0.12)

Table 20. Sum of fatty acids within classes for Polish Landrace x Duroc (n = 102). Data presented as mean and standard deviation (SD). Differences between tested groups were evaluated using the Kruskal-Wallis test. Post-hoc statistics for p-value calculations were assessed using Dunn's test. Significance level between supplemented groups compared to control group – *p<0.05; **p<0.01, ***p<0.001; SFA – total saturated fatty acids, MUFA – total monounsaturated fatty acids, PUFA – total polyunsaturated fatty acids, ∑ n-6 PUFA – total n-6 (sum of LA+ETA+AA), ∑ n-3 PUFA – total n-3 (sum of ALA+EPA+DHA)

FATTY ACID CLASS	**POLISH LANDRACE x DUROC – Mean (SD)**			
	Control	**Rapeseed oil 2%**	**Rapeseed oil 2% Linseed oil 1%**	**Linseed oil 2% Rapeseed oil 1%**
∑ SFA	27.78 (4.53)	**24.37**** (4.94)	**27.16**** (3.63)	24.85 (3.68)
∑ MUFA	3.82 (2.93)	3.81 (2.52)	4.56 (2.41)	7.01 (3.22)
∑ PUFA	31.14 (5.17)	28.03 (4.96)	31.36 (4.21)	31.85 (5.07)
∑ n-6 PUFA	23.25 (7.36)	25.86 (7.00)	25.38 (5.86)	22.90 (4.23)
∑ n-3 PUFA	44.92 (3.93)	40.48 (8.02)	42.43 (3.12)	43.46 (2.92)
n-6/n-3 RATIO	14.42 (15.35)	9.03 (5.66)	7.53 (4.17)	**4.74**** (3.39)
PUFA/SFA RATIO	0.69 (0.10)	0.71 (0.12)	0.74 (0.09)	0.74 (0.13)

4.2. NGS based RNA-Seq experiment of porcine liver representing Polish Landrace purebred and Polish Landrace x Duroc crossbred pigs

4.2.1. Preprocessing and post-processing of porcine liver RNA-Seq data representing Polish Landrace purebred and Polish Landrace x Duroc crossbred pigs

Preprocessing of the RNA-Seq data (FASTq): NCBI submission:

The NGS experiment yielded two RNA-Seq data using MiSeq (PL purebred) and HiSeq (PL x Duroc crossbred) Illumina platform. The MiSeq FASTq RNA-Seq data of PL purebred pig were submitted to NCBI (https://www.ncbi.nlm.nih.gov/geo/query/acc.cgi?acc=GSE72123) under BioProject ID: PRJNA293108 (https://www.ncbi.nlm.nih.gov/bioproject/PRJNA293108), and SRA ID: SRP062497 (https://www.ncbi.nlm.nih.gov/sra?term=SRP062497), as well as two pooled group with PUFA enriched diet (H: https://www.ncbi.nlm.nih.gov/sra/SRX1155630[accn], GSM18555718, and control diet (L: https://www.ncbi.nlm.nih.gov/sra/SRX1155631[accn], GSM1855719). The HiSeq FASTq RNA-seq data of PLxDuroc crossbred pig will be submitted to NCBI after the publication of the Ph.D. dissertation.

Postprocessing of the RNA-Seq data (normalization of mapped reads): The number of reads per sample obtained from the NGS from PL purebred liver samples was 13,509,248 sequences using paired-end libraries. Among these, 9,812,246 (72.63%) reads were mapped in pairs, 381,668 (2.83%) were mapped in broken pairs and 3,315,334 (24.54%) reads were not mapped. The average read was 151 base-pairs lengths. With regard to the fragment counting, the total number of fragments was 6,754,624, in which 1,848,501 (27.37%) remained uncounted. Among 4,906,123 counted fragments (72.63% of total fragments), 4,401,376 (65.16%) were unique and 504,747 (7.47%) were non-specific. An intact pair was counted as one, broken pairs were ignored.

The total number of transcripts, which are defined in the whole reference genome of *Sus scrofa*, was 22,861. The number of transcripts identified in the PL was 13,159 in the control group and 13,342 in the experimental group, while in PL x Duroc were 15,297 in the control group and 15,241 in the experimental group (**TABLE 21**).

Table 21. Sum of identified transcripts.

Group	Number of identified transcripts
Total number of trancripts defined in *Sus scrofa* reference genome	22,861
Polish Landrace	
PUFAs enriched diet group	13,342
Control group	13,159
Polish Landrace x Duroc	
PUFAs enriched diet group	15,241
Control group	15,297

4.2.2. DEGs analysis of porcine liver by comparing the standard (control) diet versus experimental nutritional PUFAs diets within Polish Landrace purebred pigs (MiSeq RNA-Seq data) using CLC Genomics workbench:

4.2.2.1. Identification of DEGs and Excel filtering of highly significant DEGs with cutoff p-values p<0.0001:

A complete gene expression profile representing within the breed DEGs comparison between standard (control) diet *versus* supplementary healthy diet enriched with omega-6 and omega-3 fatty acids (PUFAs) on the liver transcriptome in PL purebred pigs is presented in **SUPPLEMENTARY TABLE S1**. Results revealed the identification of 14,117 DEGs without cutoff values including non-significant and significant (cutoff values: $p<0.01$, $p<0.001$) and highly significant (cutoff value $p<0.0001$) DEGs. After the first Microsoft-Excel filtering of all these DEGs (n=14,117), a total of 665, 1,236, and 1,762 highly significant ($p<0.0001$) DEGs were according to Bonferroni p-values, p-values, and FDR values, respectively. The results presented in the Venn diagram (**FIGURE 6**) revealed that highly significant ($p<0.0001$) Bonferroni p-values (n=665) were commonly sheared among all three p-values. However, a total of 570 highly significant ($p<0.0001$) DEGs were commonly sheared between FDR adjusted p-value and standard p-value. Overall, a total of 527 highly significant ($p<0.0001$) DEGs were uniquely identified with the standard p-value.

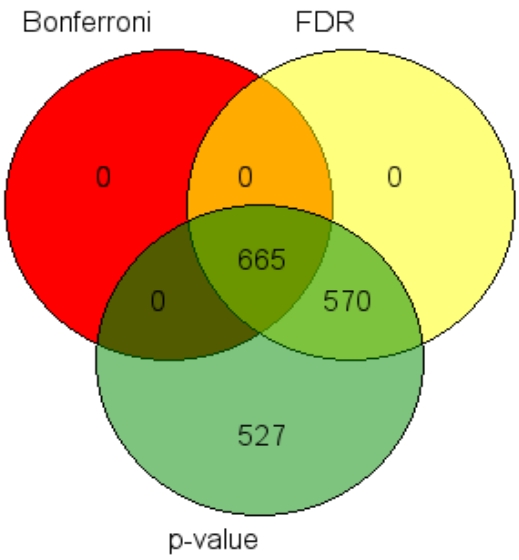

Figure 6. Identification of highly significant (p<0.0001) DEGs according to Bonferroni p-values (n=665), p-values (n=527), and FDR values (n=570), respectively by comparing the standard (control) diet *versus* supplementary healthy diet enriched with omega-6 and omega-3 fatty acids (PUFAs) on the liver transcriptome in PL purebred pigs.

4.2.2.2. Identification of highly significant upregulated and downregulated DEGs in Polish Landrace purebred pigs

Based on the **SUPPLEMENTARY TABLE S1**., upregulated and downregulated DEGs were further filtered (second Microsoft- Excel filtering) according to log2FC and FC values and presented in **SUPPLEMENTARY TABLE S2**. and **SUPPLEMENTARY TABLE S3**. Results revealed the identification of 6,756 upregulated (**SUPPLEMENTARY TABLE S2**) and 7,258 downregulated (**SUPPLEMENTARY TABLE S3**) DEGs (without cutoff values of log2FC and FC) that were expressed in the liver transcriptome PL purebred pigs. Identification of both up-regulated and downregulated DEGs according to log2FC and FC values in liver transcriptome by within breed comparing the standard (control) diet *versus* supplementary healthy diet enriched with omega-6 and omega-3 fatty acids (PUFAs) in PL purebred pigs are presented in **TABLE 22**.

Table 22. Identification of upregulated and downregulated DEGs according to log2FC and FC values in liver transcriptome by within breed comparing the standard (control) diet *versus* supplementary healthy diet enriched with omega-6 and omega-3 fatty acids (PUFAs) in Polish Landrace purebred pigs.

Venn diagram circle representing DEGs	Upregulated			Downregulated		
	all DEGs	log2FC (>2FC)	FC (>2FC)	all DEGs	log2FC (>2FC)	FC (>2FC)
Bonferroni p<0.0001	386	30*	199	279	20*	159
FDR p<0.0001	683	46	274	552	46	277
p-value p<0.0001	961	56	329	801	62	364

*Gene symbols and full gene names of DEGs are listed in the separate tables.

Based on the log2FC (>2FC) values of **TABLE 22**, Venn diagram (**FIGURE 7**) results revealed a total of 30 (log2FC) highly significant upregulated DEGs with Bonferroni p-values (p<0.0001) were commonly sheared among all three p-values (a complete list of upregulated DEGs (n=30*) with gene symbol and full names is further presented in **TABLE 23**). However, a total of 16 (log2FC) highly significant (p<0.0001) upregulated DEGs were commonly sheared between FDR adjusted p-value and standard p-value. Overall, a total of 10 (log2FC) highly significant (p<0.0001) upregulated DEGs were uniquely identified with the standard p-value. Similarly, based on the log2FC (>2FC) values of **TABLE 22**, a Venn diagram (**FIGURE 8**) results revealed a total of 20 (log2FC) highly significant downregulated DEGs with Bonferroni p-values (p<0.0001), which were commonly sheared among all three p-values (a complete list of downregulated DEGs (n=20*) with gene symbol and full names is presented in **TABLE 24**). However, a total of 26 (log2FC) highly significant (p<0.0001) downregulated DEGs were commonly sheared between FDR adjusted p-value and standard p-value. Overall, a total of 16 (log2FC) highly significant (p<0.0001) downregulated DEGs were uniquely identified with the standard p-value.

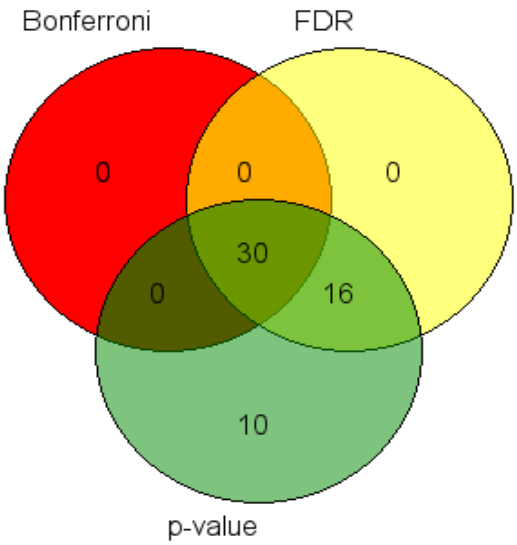

Figure 7. Highly significant (p<0.0001) upregulated DEGs revealed by comparing the standard (control) diet *versus* supplementary healthy diet enriched with omega-6 and omega-3 fatty acids (PUFAs) in the liver transcriptome of Polish Landrace purebred pigs, according to log_2FC and FC values.

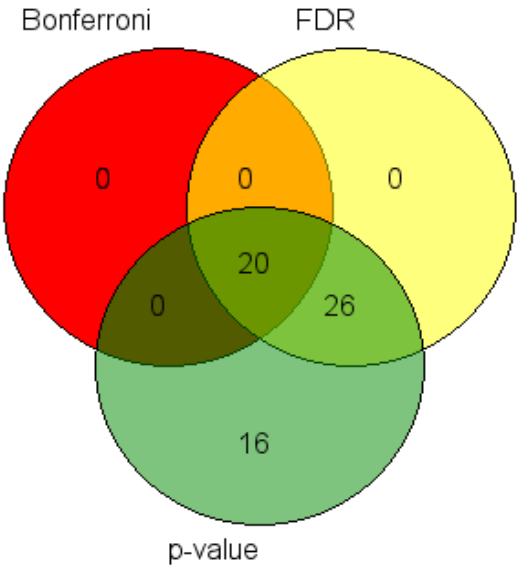

Figure 8. Highly significant (p<0.0001) downregulated DEGs revealed by comparing the standard (control) diet *versus* supplementary healthy diet enriched with omega-6 and omega-3 fatty acids (PUFAs) in the liver transcriptome of Polish Landrace purebred pigs, according to log_2FC and FC values.

Table 23. List of identified highly significant (p<0.0001) upregulated (n=30) **(Figure 7)** DEGs according to log2FC (>2x) values in the liver transcriptome by comparing the standard (control) diet *versus* supplementary healthy diet enriched with omega-6 and omega-3 fatty acids (PUFAs) in Polish Landrace purebred pigs.

Highly significant (Bonferroni p <0.0001) upregulated DEGs with log2FC (>2x) values			
Gene stable ID	Gene symbol	Gene description	Chromosome
ENSSSCG00000000164	CRY1	cryptochrome circadian regulator 1 [Source:NCBI gene;Acc:100520380]	5
ENSSSCG00000001235	TRIM15	tripartite motif containing 15 [Source:NCBI gene;Acc:100144461]	7
ENSSSCG00000001906	CYP1A1	cytochrome P450 1A1 [Source:NCBI gene;Acc:403103]	7
ENSSSCG00000002294	ARG2	arginase 2 [Source:NCBI gene;Acc:100155893]	7
ENSSSCG00000002743	IST1	IST1, ESCRT-III associated factor [Source:NCBI gene;Acc:100626669]	6
ENSSSCG00000003410	MASP2	mannan-binding lectin serine peptidase 2 [Source:NCBI gene;Acc:100302537]	6
ENSSSCG00000003789	CTH	cystathionine gamma-lyase [Source:NCBI gene;Acc:733654]	6
ENSSSCG00000004195	ARG1	arginase 1 [Source:NCBI gene;Acc:397115]	1
ENSSSCG00000004702	STRC	stereocilin [Source:NCBI gene;Acc:100519812]	1
ENSSSCG00000006141	CA3	carbonic anhydrase 3 [Source:NCBI	4

		gene;Acc:494016]	
ENSSSCG00000006238	CYP7A1	cytochrome P450, family 7, subfamily A, polypeptide 1 [Source:NCBI gene;Acc:448985]	4
ENSSSCG00000006582	S100A14	S100 calcium binding protein A14 [Source:NCBI gene;Acc:100153930]	4
ENSSSCG00000006588	S100A9	S100 calcium-binding protein A9 [Source:NCBI gene;Acc:100127489]	4
ENSSSCG00000008119	KCNIP3	potassium voltage-gated channel interacting protein 3 [Source:NCBI gene;Acc:100524248]	3
ENSSSCG00000012071	ENSSSCG00000012071	immunoglobulin superfamily member 5 [Source:NCBI gene;Acc:100517006]	13
ENSSSCG00000015268	FMO1	Flavin-containing monooxygenase 1 [Source:NCBI gene;Acc:397132]	9
ENSSSCG00000015391	CROT	carnitine O-octanoyltransferase [Source:NCBI gene;Acc:100521142]	9
ENSSSCG00000015699	ACMSD	aminocarboxymuconate semialdehyde decarboxylase [Source:NCBI gene;Acc:100154768]	15
ENSSSCG00000022331	ENSSSCG00000022331	fibroblast growth factor 13 [Source:NCBI gene;Acc:100523833]	X
ENSSSCG00000026427	RORC	RAR related orphan receptor C	4

		[Source:NCBI gene;Acc:100622477]	
ENSSSCG00000026850	SNCG	synuclein gamma [Source:NCBI gene;Acc:100125343]	14
ENSSSCG00000029558	EXTL1	exostosin like glycosyltransferase 1 [Source:NCBI gene;Acc:100623848]	6
ENSSSCG00000004170	ENSSSCG00000004170	Not listed (annotated) in NCBI resources	1
ENSSSCG00000001231	ENSSSCG00000001231	Not listed (annotated) in NCBI resources	7
ENSSSCG00000006985	ENSSSCG00000006985	Not listed (annotated) in NCBI resources	17
ENSSSCG00000009871	SDS		Not listed (annotated)
ENSSSCG00000000134	MPST		Not listed (annotated)
ENSSSCG00000001652	GNMT		Not listed (annotated)
ENSSSCG00000011148	ENSSSCG00000011148	Not listed (annotated) in NCBI resources	Not listed (annotated)
ENSSSCG00000014945	TAF1D		Not listed (annotated)

Table 24. List of Identified highly significant (p<0.0001) downregulated (n=20) **(Figure 8)** DEGs according to log2FC (>2x) values in liver transcriptome by comparing the standard (control) diet *versus* supplementary healthy diet enriched with omega-6 and omega-3 fatty acids (PUFAs) in Polish Landrace purebred pigs.

Highly significant (Bonferroni p <0.0001) downregulated DEGs with log2FC (>2x) values			
Gene stable ID	Gene symbol	Gene description	Chromosome
ENSSSCG00000000779	KIF21A	kinesin family member 21A [Source:NCBI gene;Acc:100520674]	5
ENSSSCG00000001004	SLC22A23	solute carrier family 22 member 23 [Source:NCBI gene;Acc:100152838]	7
ENSSSCG00000001045	ELOVL2	ELOVL fatty acid elongase 2 [Source:NCBI gene;Acc:100153368]	7
ENSSSCG00000001844	PLIN1	perilipin 1 [Source:NCBI gene;Acc:654411]	7
ENSSSCG00000002355	ENTPD5	ectonucleoside triphosphate diphosphohydrolase 5 [Source:NCBI gene;Acc:100154506]	7
ENSSSCG00000002425	ENSSSCG00000002425	protein tyrosine phosphatase, non-receptor type 21 [Source:NCBI gene;Acc:100152076]	7
ENSSSCG00000002515	SLC25A47	solute carrier family 25 member 47 [Source:NCBI gene;Acc:100515556]	7
ENSSSCG00000003971	SCMH1	Scm polycomb group protein homolog 1 [Source:NCBI gene;Acc:100525880]	6
ENSSSCG00000006988	PDGFRL	platelet-derived growth factor receptor-like	17

		[Source:NCBI gene;Acc:100736738]	
ENSSSCG00000008237	RETSAT	retinol saturase [Source:NCBI gene;Acc:100519138]	3
ENSSSCG00000010442	LIPK	lipase family member K [Source:HGNC Symbol;Acc:HGNC:23444]	14
ENSSSCG00000014900	RAB30	RAB30, member RAS oncogene family [Source:NCBI gene;Acc:100626412]	9
ENSSSCG00000017300	ENSSSCG00000017300	mannose receptor C type 2 [Source:NCBI gene;Acc:100516106]	12
ENSSSCG00000002626	ENSSSCG00000002626	Not listed (annotated) in NCBI resources	Not listed (annotated)
ENSSSCG00000011289	ACKR2	Not listed (annotated) in NCBI resources	Not listed (annotated)
ENSSSCG00000014442	PDGFRB	Not listed (annotated) in NCBI resources	Not listed (annotated)
ENSSSCG00000016729	IGFBP3	Not listed (annotated) in NCBI resources	Not listed (annotated)
ENSSSCG00000022884	ENSSSCG00000022884	Not listed (annotated) in NCBI resources	Not listed (annotated)
ENSSSCG00000025541	ELOVL6	Not listed (annotated) in NCBI resources	Not listed (annotated)
ENSSSCG00000028994	ENSSSCG00000028994	Not listed (annotated) in NCBI resources	Not listed (annotated)

4.2.3. DEGs analysis of porcine liver by comparing the standard (control) diet *versus* experimental nutritional PUFAs diets within Polish Landrace x Duroc crossbred pigs (HiSeq RNA-Seq data) using CLC Genomics workbench

4.2.3.1. Identification of DEGs and Excel filtering of highly significant DEGs with cutoff p-values p<0.0001:

A complete gene expression profile representing within breed DEGs comparison between standard (control) diet *versus* supplementary healthy diet enriched with omega-6 and omega-3 fatty acids (PUFAs) on the liver transcriptome in PL x Duroc crossbred pigs are presented in **SUPPLEMENTARY TABLE S4.** Results revealed the identification of 16,226 DEGs without cutoff values including non-significant and significant ($p<0.01$, $p<0.001$) and highly significant ($p<0.0001$) DEGs. After the first Microsoft- Excel filtering of all these DEGs (n=16,226), a total of 738, 1,493, and 2,104 highly significant ($p<0.0001$) DEGs were found according to Bonferroni p-values, p-values, and FDR values, respectively. The results are presented in the Venn diagram (**FIGURE 9**), which revealed that highly significant ($p<0.0001$) Bonferroni p-values (n=737) were commonly sheared among all three p-values. However, a total of 756 highly significant ($p<0.0001$) DEGs were commonly sheared between FDR adjusted p-value and standard p-value. Overall, a total of 611 highly significant ($p<0.0001$) DEGs were uniquely identified with the standard p-value.

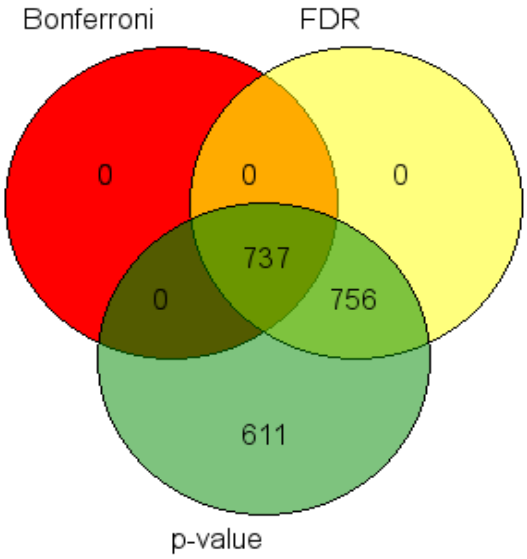

Figure 9. Identification of highly significant (p<0.0001) DEGs according to Bonferroni p-values, p-values, and FDR values, respectively by comparing the standard (control) diet *versus* supplementary healthy diet enriched with omega-6 and omega-3 fatty acids (PUFAs) on the liver transcriptome in Polish Landrace x Duroc crossbred pigs.

4.2.3.2. Identification of highly significant upregulated and downregulated DEGs in Polish Landrace x Duroc crossbred pigs:

Based on the **SUPPLEMENTARY TABLE S4**, upregulated and downregulated DEGs were further filtered (second Microsoft- Excel filtering) according to log2FC and FC values and presented in **SUPPLEMENTARY TABLE S5** and **SUPPLEMENTARY TABLE S6.** Results revealed the identification of 6,756 upregulated (**SUPPLEMENTARY TABLE S5**) and 7,258 downregulated (**SUPPLEMENTARY TABLE S6**) DEGs (without cutoff values of log2FC and FC) that were expressed in the liver transcriptome PL x Duroc crossbred pigs. Identification of both upregulated and downregulated DEGs according to log2FC and FC values in liver transcriptome by within breed comparing the standard (control) diet *versus* supplementary healthy diet enriched with omega-6 and omega-3 fatty acids (PUFAs) in PL x Duroc crossbred pigs: are presented in **TABLE 25.**

Table 25. Identification of upregulated and downregulated DEGs according to log2FC and FC values in liver transcriptome by comparing the standard (control) diet *versus* supplementary healthy diet enriched with omega-6 and omega-3 fatty acids (PUFAs) in Polish Landrace x Duroc crossbred pigs.

Venn diagram circle representing DEGs	Upregulated			Downregulated		
	all DEGs	log2FC (>2FC)	FC (>2FC)	all DEGs	log2FC (>2FC)	FC (>2FC)
Bonferroni p< 0.0001	330	29*	93	407	18*	153
FDR p< 0.0001	716	43	149	777	39	238
p-value p< 0.0001	1020	53	183	1083	51	299

*Gene symbols and full gene names of DEGs are listed in the separate tables.

Based on the log2FC (>2FC) values of **TABLE 25**, Venn diagram (**FIGURE 10**) results revealed a total of 29 (log2FC) highly significant upregulated DEGs with Bonferroni p-values (p<0.0001), which were commonly sheared among all three p-values (a complete list of upregulated DEGs (n=29*) with gene symbol and full names is further presented in **TABLE 26**). However, a total of 14 (log2FC) highly significant (p<0.0001) upregulated DEGs were commonly sheared between FDR adjusted p-value and standard p-value. Overall, a total of 10 (log2FC) highly significant (p<0.0001) upregulated DEGs were uniquely identified with the standard p-value. Similarly, based on the log2FC (>2FC) values of **TABLE 25**, a Venn diagram (**FIGURE 11)** results revealed a total of 18 (log2FC) highly significant down-regulated DEGs with Bonferroni p-values (p<0.0001) were commonly sheared among all three p-values (a complete list of downregulated DEGs (n=18*) with gene symbol and full names is presented in **TABLE 27).** However, a total of 21 (log2FC) highly significant (p<0.0001) downregulated DEGs were commonly sheared between FDR adjusted p-value and standard p-value. Overall, a total of 12 (log2FC) highly significant (p<0.0001) downregulated DEGs were uniquely identified with the standard p-value.

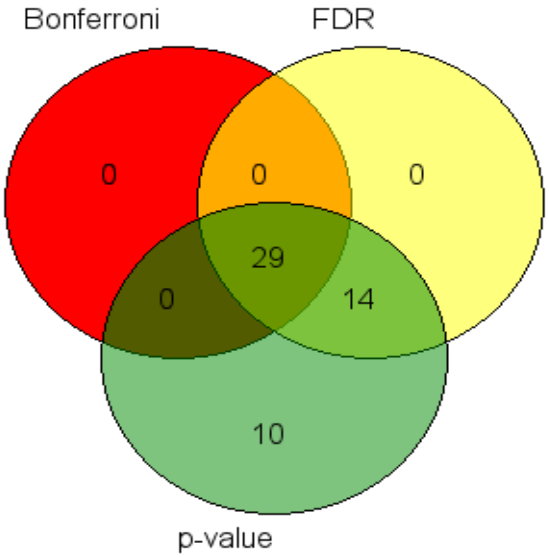

Figure 10. Identification of highly significant ($p<0.0001$) upregulated DEGs by comparing the standard (control) diet *versus* supplementary healthy diet enriched with omega-6 and omega-3 fatty acids (PUFAs) in the liver transcriptome of Polish Landrace x Duroc crossbred, according to log_2FC and FC values.

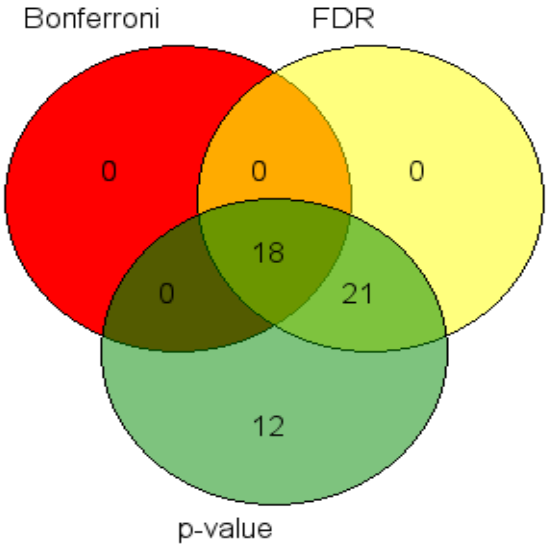

Figure 11. Identification of highly significant ($p<0.0001$) downregulated DEGs by comparing the standard (control) diet *versus* supplementary healthy diet enriched with omega-6 and omega-3 fatty acids (PUFAs) in the liver transcriptome of Polish Landrace x Duroc crossbred, according to log_2FC and FC values.

Table 26. List of identified highly significant (p<0.0001) upregulated (n=29) **(Figure 10)** DEGs according to log2FC (>2x) values in liver transcriptome by comparing the standard (control) diet *versus* supplementary healthy diet enriched with omega-6 and omega-3 fatty acids (PUFAs) in Polish Landrace x Duroc crossbred pigs.

Highly significant (Bonferroni p <0.0001) upregulated DEGs with log2FC (>2x) values			
Gene stable ID	Gene symbol	Gene description	Chromosome
ENSSSCG00000001045	ELOVL2	ELOVL fatty acid elongase 2 [Source:NCBI gene;Acc:100153368]	7
ENSSSCG00000003278	ENSSSCG00000003278	leukocyte immunoglobulin-like receptor subfamily B member 3-like [Source:NCBI gene;Acc:100511639]	6
ENSSSCG00000003318	GALP	galanin like peptide [Source:NCBI gene;Acc:396772]	6
ENSSSCG00000005067	CCDC198	coiled-coil domain containing 198 [Source:NCBI gene;Acc:100513515]	1
ENSSSCG00000005196	DMAC1	distal membrane arm assembly complex 1 [Source:NCBI gene;Acc:100155846]	1
ENSSSCG00000010432	ENSSSCG00000010432	N-acylsphingosine amidohydrolase 2 [Source:NCBI gene;Acc:100157065]	14
ENSSSCG00000011307	ENSSSCG00000011307	zinc finger protein 501 [Source:NCBI gene;Acc:100738134]	13

ENSSSCG00000013060	SCGB1A1	secretoglobin family 1A member 1 [Source:NCBI gene;Acc:102164135]	2
ENSSSCG00000013369	SAA1	Serum Amyloid A1	2
ENSSSCG00000013370	ENSSSCG00000013370	serum amyloid A-2 protein [Source:NCBI gene;Acc:100525680]	2
ENSSSCG00000016504	TBXAS1	thromboxane A synthase 1 [Source:NCBI gene;Acc:397112]	18
ENSSSCG00000016678	NOD1	nucleotide binding oligomerization domain containing 1 [Source:NCBI gene;Acc:100135660]	18
ENSSSCG00000022724	ENSSSCG00000022724	UDP-glucuronosyltransferase 2B18-like [Source:NCBI gene;Acc:100516628]	8
ENSSSCG00000024310	F13A1	coagulation factor XIII A chain [Source:NCBI gene;Acc:100153504]	7
ENSSSCG00000029515	PON3	paraoxonase 3 [Source:NCBI gene;Acc:733674]	9
ENSSSCG00000030198	ENV_1	viral gene that encodes the protein forming the viral envelope	1
ENSSSCG00000001134	ENSSSCG00000001134	Not listed (annotated) in NCBI resources	Not listed (annotated)
ENSSSCG00000003824	ENSSSCG00000003824	Not listed (annotated) in NCBI resources	Not listed (annotated)
ENSSSCG00000008588	FKBP1B	Not listed (annotated) in NCBI resources	Not listed (annotated)

ENSSSCG00000008886	ENSSSCG00000008886	Not listed (annotated) in NCBI resources	Not listed (annotated)
ENSSSCG00000011148	ENSSSCG00000011148	Not listed (annotated) in NCBI resources	Not listed (annotated)
ENSSSCG00000021940	CYP2J34	Not listed (annotated) in NCBI resources	Not listed (annotated)
ENSSSCG00000021965	ENV_2	Not listed (annotated) in NCBI resources	Not listed (annotated)
ENSSSCG00000023038	ENSSSCG00000023038	Not listed (annotated) in NCBI resources	Not listed (annotated)
ENSSSCG00000028525	ENSSSCG00000028525	Not listed (annotated) in NCBI resources	Not listed (annotated)
ENSSSCG00000028994	ENSSSCG00000028994	Not listed (annotated) in NCBI resources	Not listed (annotated)
ENSSSCG00000029028	FGF23	Not listed (annotated) in NCBI resources	Not listed (annotated)
ENSSSCG00000030730	IGLV-4	Not listed (annotated) in NCBI resources	Not listed (annotated)
ENSSSCG00000030738	IGKV-5	Not listed (annotated) in NCBI resources	Not listed (annotated)

Table 27. List of identified highly significant (p<0.0001) downregulated (n=18) **(Figure 11)** DEGs according to log2FC (>2x) values in liver transcriptome by comparing the standard (control) diet *versus* supplementary healthy diet enriched with omega-6 and omega-3 fatty acids (PUFAs) in Polish Landrace x Duroc crossbred pigs.

Highly significant (Bonferroni p <0.0001) downregulated DEGs with log2FC (>2x) values			
Gene stable ID	Gene symbol	Gene description	Chromosome
ENSSSCG00000000216	ASIC1	acid-sensing ion channel subunit 1 [Source:NCBI gene;Acc:100517467]	5
ENSSSCG00000002270	ENSSSCG00000002270	coiled-coil domain-containing protein 170-like [Source:NCBI gene;Acc:100522152]	7
ENSSSCG00000002720	CLEC18A	C-type lectin domain family 18 member C [Source:NCBI gene;Acc:100525922]	6
ENSSSCG00000003889	ENSSSCG00000003889	cytochrome P450 4A25-like [Source:NCBI gene;Acc:110261409]	6
ENSSSCG00000003967	ZMYND12	zinc finger MYND-type containing 12 [Source:NCBI gene;Acc:100524028]	6
ENSSSCG00000005474	SAL1	salivary lipocalin [Source:NCBI gene;Acc:396739]	1
ENSSSCG00000006238	CYP7A1	cytochrome P450, family 7, subfamily A, polypeptide 1 [Source:NCBI gene;Acc:448985]	4
ENSSSCG00000009789	HCAR1	hydroxycarboxylic acid receptor 1 [Source:NCBI	14

		gene;Acc:100153287]	
ENSSSCG00000010427	MBL2	mannose-binding lectin 2 [Source:NCBI gene;Acc:397230]	14
ENSSSCG00000014314	FBXL21	F-box and leucine-rich repeat protein 21, pseudogene [Source:NCBI gene;Acc:100517085]	2
ENSSSCG00000024537	CYP2C42	cytochrome P450 C42 [Source:NCBI gene;Acc:403111]	14
ENSSSCG00000030271	GSTO2	glutathione S-transferase omega-2 [Source:NCBI gene;Acc:100152209]	14
ENSSSCG00000007500	CH242-266P8.1	Not listed (annotated) in NCBI resources	17
ENSSSCG00000008620	ENSSSCG00000008620	Not listed (annotated) in NCBI resources	Not listed (annotated)
ANHX	ENSSSCG00000009724	Not listed (annotated) in NCBI resources	Not listed (annotated)
ENSSSCG00000022796	ENSSSCG00000022796	Not listed (annotated) in NCBI resources	Not listed (annotated)
ENSSSCG00000026923	ENSSSCG00000026923	Not listed (annotated) in NCBI resources	Not listed (annotated)
ENSSSCG00000030298	ENSSSCG00000030298	Not listed (annotated) in NCBI resources	Not listed (annotated)

4.2.4. DEGs analysis of porcine liver by comparing the Polish Landrace purebred pigs (MiSeq RNA-Seq data) and Polish Landrace x Duroc crossbred pigs (HiSeq RNA-Seq data) after experimental feeding with standard (control) diet using CLC Genomics workbench

4.2.4.1. Identification of DEGs and Excel filtering of highly significant DEGs with cutoff p-values p<0.0001

A complete gene expression profile representing the between breed comparison of PL purebred *versus* PL x Duroc crossbred pigs liver transcriptome fed with standard (control) diet is presented in **SUPPLEMENTARY TABLE S7.** Results revealed the identification of 16,032 DEGs without cutoff values including non-significant and significant ($p<0.01$, $p<0.001$) and highly significant ($p<0.0001$) DEGs. After the first Microsoft- Excel filtering of all these DEGs (n=16,032), a total of 5,614, 7,154, and 7,445 highly significant ($p< 0.0001$) DEGs were identified according to Bonferroni p-values, p-values, and FDR values, respectively. The results presented in the Venn diagram (**FIGURE 12**) revealed that highly significant ($p<0.0001$) Bonferroni p-values (n=5,614) were commonly sheared among all three p-values. However, a total of 1,540 highly significant ($p<0.0001$) DEGs were commonly sheared between FDR adjusted p-value and standard p-value. Overall, a total of 291 highly significant ($p<0.0001$) DEGs were uniquely identified with the standard p-value.

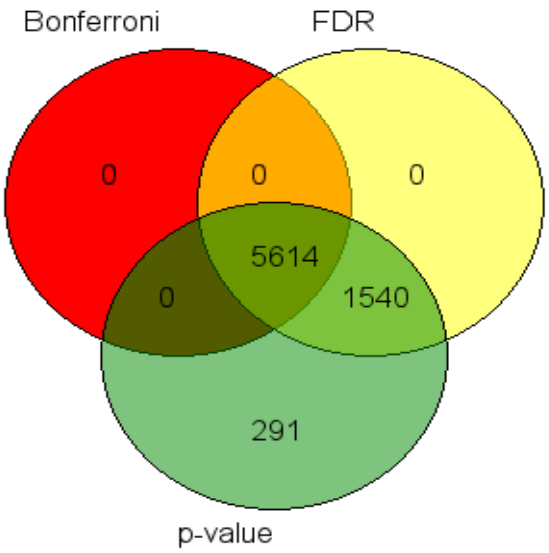

Figure 12. Identification of highly significant (p<0.0001) DEGs according to Bonferroni p-values, p-values, and FDR values, respectively by comparing the Polish Landrace purebred *versus* Polish Landrace x Duroc crossbred pigs liver transcriptome after experimental feeding with standard (control) diet.

4.2.4.2. Identification of highly significant upregulated and downregulated DEGs in purebred and crossbred pigs after experimental feeding with standard (control) diet.

Based on the **SUPPLEMENTARY TABLE S7**, upregulated and downregulated DEGs were further filtered (second Microsoft- Excel filtering) according to log2FC and FC values and presented in **SUPPLEMENTARY TABLE S8** and **SUPPLEMENTARY TABLE S9.** Results revealed the identification of 8,871 upregulated (**SUPPLEMENTARY TABLE S8**) and 6,877 downregulated (**SUPPLEMENTARY TABLE S9**) DEGs (without cutoff values of log2FC and FC) that were expressed in the liver transcriptome of PL purebred and PL x Duroc crossbred pigs after feeding with standard (control) diet. Identification of both **up-regulated and downregulated DEGs** according to log_2FC and FC values in liver transcriptome by comparing the liver transcriptome of PL purebred *versus* PL x Duroc crossbred pigs after experimental feeding with standard (control) diet are presented in **TABLE 28**.

Table 28. Identification of upregulated and downregulated DEGs according to log2FC and FC values in liver transcriptome by comparing the liver transcriptome of Polish Landrace purebred *versus* Polish Landrace x Duroc crossbred pigs after feeding with standard (control) diet.

Venn diagram circle representing DEGs	Upregulated			Downregulated		
	log2FC (>2FC)	FC (>2FC)	log2FC (>9FC)	log2FC (>2FC)	FC (>2FC)	log2FC (>9FC)
Bonferroni p< 0.0001	1451	2443	43*	1385	2372	42*
FDR p< 0.0001	1673	2880	43*	1583	2770	70
p-value p< 0.0001	1714	2945	43*	1618	2837	76

*Gene symbols and full gene names of DEGs are listed in the separate tables.

Based on the log2FC (>9FC) values of **TABLE 28**, Venn diagram (**FIGURE 13**) results revealed all identified highly significant (p<0.0001) upregulated DEGs (n=43) with **log2FC values of >9x** were commonly sheared among all three highly significant p-values (p<0.0001) when we compared the liver transcriptome of PL purebred and PL x Duroc crossbred pigs after feeding with standard (control) diet (a complete list of upregulated DEGs (n=43*) with gene symbol and full names is further presented in **TABLE 29**). However, based on the log2FC (>9FC) values of **TABLE 28**, Venn diagram (**FIGURE 14**) results revealed a total of 42 highly significant (p<0.0001) downregulated DEGs with log2FC values of <9x were commonly sheared among all three p-values (a complete list of downregulated DEGs (n=42*) with gene symbol and full names is further presented in **TABLE 30**). Whereas, a total of 28 highly significant (p<0.0001) downregulated DEGs with log2FC values of <9x were commonly sheared between FDR adjusted p-value and standard p-value. Overall, a total of 6 highly significant (p<0.0001) downregulated DEGs with log2FC values of <9x were uniquely identified with the standard p-value.

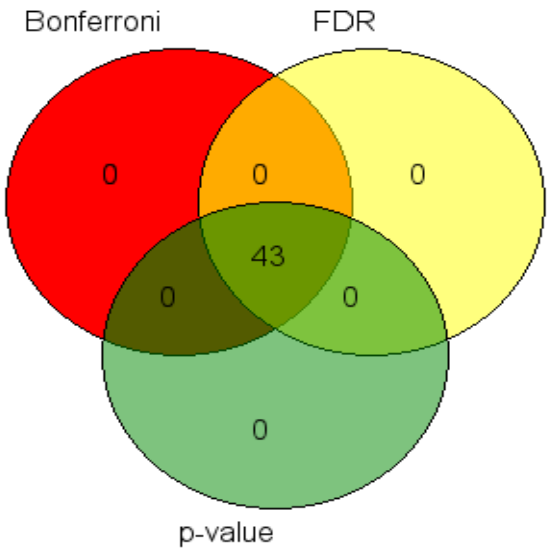

Figure 13. Highly significant ($p<0.0001$) upregulated DEGs identified by comparing the liver transcriptome of Polish Landrace purebred and Polish Landrace x Duroc crossbred pigs after feeding with standard (control) diet, according to log_2FC and FC values.

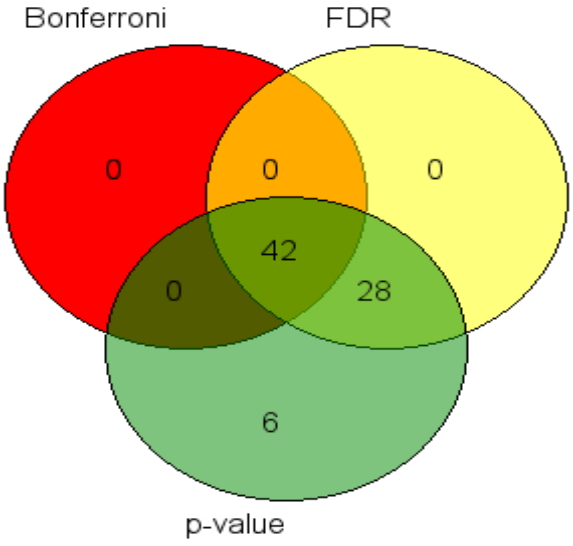

Figure 14. Highly significant ($p<0.0001$) downregulated DEGs identified by comparing the liver transcriptome of Polish Landrace purebred and Polish Landrace x Duroc crossbred pigs after feeding with standard (control) diet, according to log_2FC and FC values.

Table 29. List of identified highly significant (p<0.0001) upregulated (n=43) **(Figure 13)** DEGs according to log2FC (>9x) values in the liver transcriptome by comparing the liver transcriptome of Polish Landrace purebred and Polish Landrace x Duroc crossbred pigs after feeding with standard (control) diet.

Highly significant (all p <0.0001) upregulated DEGs with log2FC (>9x) values			
Gene stable ID	Gene symbol	Gene description	Chromosome
ENSSSCG00000000749	SLC6A12	solute carrier family 6 member 12 [Source:NCBI gene;Acc:100512716]	5
ENSSSCG00000000856	PAH	phenylalanine hydroxylase [Source:NCBI gene;Acc:100521900]	5
ENSSSCG00000001411	APOM	apolipoprotein M [Source:NCBI gene;Acc:692188]	7
ENSSSCG00000001901	CYP1A2	cytochrome P450, family 1, subfamily A, polypeptide 2 [Source:NCBI gene;Acc:100152910]	7
ENSSSCG00000002475	SERPINA6	serpin family A member 6 [Source:NCBI gene;Acc:396736]	7
ENSSSCG00000002476	SERPINA1	serpin family A member 1 [Source:NCBI gene;Acc:397688]	7
ENSSSCG00000002481	SERPINA5	serpin family A member 5 [Source:NCBI	7

		gene;Acc:100153513]	
ENSSSCG00000003835	C8A	complement C8 alpha chain [Source:NCBI gene;Acc:100037953]	6
ENSSSCG00000004001	A1BG	alpha-1-B glycoprotein [Source:NCBI gene;Acc:100516980]	6
ENSSSCG00000005485	AMBP	alpha-1-microglobulin/bikunin precursor [Source:NCBI gene;Acc:397593]	1
ENSSSCG00000005488	ENSSSCG00000005488	orosomucoid 1 [Source:NCBI gene;Acc:396901]	1
ENSSSCG00000006621	CGN	cingulin [Source:NCBI gene;Acc:100157963]	4
ENSSSCG00000007671	TFR2	transferrin receptor 2 [Source:NCBI gene;Acc:100517580]	3
ENSSSCG00000008948	ALB	albumin [Source:NCBI gene;Acc:396960]	8
ENSSSCG00000009805	HPD	4-hydroxyphenylpyruvate dioxygenase [Source:NCBI gene;Acc:397443]	14
ENSSSCG00000009942	DAO	D-amino acid oxidase [Source:NCBI gene;Acc:397134]	14
ENSSSCG00000010008	SEC14L3	SEC14-like protein 3 [Source:NCBI gene;Acc:100156470]	14

ENSSSCG00000010427	MBL2	mannose-binding lectin 2 [Source:NCBI gene;Acc:397230]	14
ENSSSCG00000011450	ITIH1	inter-alpha-trypsin inhibitor heavy chain 1 [Source:NCBI gene;Acc:396963]	13
ENSSSCG00000011799	AHSG	alpha 2-HS glycoprotein [Source:NCBI gene;Acc:397585]	13
ENSSSCG00000011800	FETUB	fetuin B [Source:NCBI gene;Acc:100517609]	13
ENSSSCG00000011801	HRG	histidine rich glycoprotein [Source:NCBI gene;Acc:100152095]	13
ENSSSCG00000013665	ENSSSCG00000013665	complement C3 [Source:NCBI gene;Acc:100517145]	2
ENSSSCG00000015799	KLKB1	kallikrein B1 [Source:NCBI gene;Acc:397144]	15
ENSSSCG00000016728	IGFBP1	insulin like growth factor binding protein 1 [Source:NCBI gene;Acc:397270]	18
ENSSSCG00000017700	CCL3L1	chemokine (C-C motif) ligand 3-like 1 [Source:NCBI gene;Acc:494459]	12
ENSSSCG00000021847	ENSSSCG00000021847	serum amyloid A-4 protein [Source:NCBI	2

		gene;Acc:100526034]	
ENSSSCG00000021938	UPP2	uridine phosphorylase 2 [Source:NCBI gene;Acc:100522709]	15
ENSSSCG00000023686	TTR	transthyretin [Source:NCBI gene;Acc:397419]	6
ENSSSCG00000023693	PROC	protein C, inactivator of coagulation factors Va and VIIIa [Source:NCBI gene;Acc:396954]	15
ENSSSCG00000024520	PGP3	ATP binding cassette subfamily B member 4 [Source:NCBI gene;Acc:100144586]	9
ENSSSCG00000027439	HAO1	hydroxyacid oxidase 1 [Source:NCBI gene;Acc:100627803]	17
ENSSSCG00000027926	FTCD	formimidoyltransferase cyclodeaminase [Source:NCBI gene;Acc:397517]	AEMK02000328.1
ENSSSCG00000023305	ENSSSCG00000023305	Not listed (annotated) in NCBI resources	6
ENSSSCG00000028901	ENSSSCG00000028901	Not listed (annotated) in NCBI resources	8
ENSSSCG00000000852	ENSSSCG00000000852	Not listed (annotated) in NCBI resources	Not listed (annotated)
ENSSSCG00000003087	APOC4	Not listed (annotated) in NCBI resources	Not listed (annotated)
ENSSSCG00000005395	ENSSSCG00000005395	Not listed (annotated) in NCBI resources	Not listed (annotated)

ENSSSCG00000017704	CCL16	Not listed (annotated) in NCBI resources	Not listed (annotated)
ENSSSCG00000022156	ENSSSCG00000022156	Not listed (annotated) in NCBI resources	Not listed (annotated)
ENSSSCG00000022808	ENSSSCG00000022808	Not listed (annotated) in NCBI resources	Not listed (annotated)
ENSSSCG00000024079	ENSSSCG00000024079	Not listed (annotated) in NCBI resources	Not listed (annotated)
ENSSSCG00000024682	ENSSSCG00000024682	Not listed (annotated) in NCBI resources	Not listed (annotated)

Table 30. List of identified highly significant (p<0.0001) downregulated (n=42) **(Figure 14)** DEGs, according to log2FC (>9x) values in the liver transcriptome by comparing the liver transcriptome of Polish Landrace purebred and Polish Landrace x Duroc crossbred pigs after experimental feeding with standard (control) diet.

Highly significant (Bonferroni p <0.0001) downregulated DEGs with log2FC (>9x) values			
Gene stable ID	Gene symbol	Gene description	Chromosome
ENSSSCG00000000866	MYBPC1	myosin binding protein C, slow type [Source:NCBI gene;Acc:100523187]	5
ENSSSCG00000004094	PPP1R14C	protein phosphatase 1 regulatory inhibitor subunit 14C [Source:NCBI gene;Acc:100521302]	1
ENSSSCG00000004703	ENSSSCG00000004703	creatine kinase, mitochondrial 1A [Source:NCBI gene;Acc:100519994]	1
ENSSSCG00000006390	CASQ1	calsequestrin 1 [Source:NCBI gene;Acc:100156448]	4
ENSSSCG00000006725	TBX15	T-box 15 [Source:NCBI gene;Acc:100158194]	4
ENSSSCG00000006829	SYPL2	synaptophysin like 2 [Source:NCBI gene;Acc:100514960]	4
ENSSSCG00000007231	MYLK2	myosin light chain kinase 2 [Source:NCBI gene;Acc:100524288]	17
ENSSSCG00000007424	TNNC2	troponin C2, fast skeletal type [Source:NCBI gene;Acc:414905]	17

ENSSSCG00000007757	TRIM72	tripartite motif containing 72 [Source:NCBI gene;Acc:100511188]	3
ENSSSCG00000007949	SRL	sarcalumenin [Source:NCBI gene;Acc:100514098]	3
ENSSSCG00000008200	ANKRD23	ankyrin repeat domain 23 [Source:NCBI gene;Acc:100525457]	3
ENSSSCG00000008215	SMYD1	SET and MYND domain containing 1 [Source:NCBI gene;Acc:100294702]	3
ENSSSCG00000009004	SFRP2	secreted frizzled related protein 2 [Source:NCBI gene;Acc:100516027]	8
ENSSSCG00000009281	SGCG	sarcoglycan gamma [Source:NCBI gene;Acc:100623668]	11
ENSSSCG00000010304	MYOZ1	myozenin 1 [Source:NCBI gene;Acc:574060]	14
ENSSSCG00000010317	DUPD1	dual specificity phosphatase and pro isomerase domain containing 1 [Source:NCBI gene;Acc:100155430]	14
ENSSSCG00000010461	ANKRD1	ankyrin repeat domain 1 [Source:NCBI gene;Acc:396959]	14
ENSSSCG00000011238	ARPP21	cAMP regulated	13

		phosphoprotein 21 [Source:NCBI gene;Acc:100512986]	
ENSSSCG00000011286	KLHL40	kelch like family member 40 [Source:NCBI gene;Acc:100523695]	13
ENSSSCG00000011325	MYL3	myosin light chain 3 [Source:NCBI gene;Acc:100515755]	13
ENSSSCG00000011622	KBTBD12	kelch repeat and BTB domain containing 12 [Source:NCBI gene;Acc:100156499]	13
ENSSSCG00000012584	CAPN6	calpain 6 [Source:NCBI gene;Acc:100522971]	X
ENSSSCG00000013354	CSRP3	cysteine and glycine rich protein 3 [Source:NCBI gene;Acc:100337687]	2
ENSSSCG00000014324	MYOT	myotilin [Source:NCBI gene;Acc:100101550]	2
ENSSSCG00000014443	CAMK2A	calcium/calmodulin dependent protein kinase II alpha [Source:NCBI gene;Acc:100626014]	2
ENSSSCG00000014560	COX8H	COX8H protein [Source:NCBI gene;Acc:100038031]	2
ENSSSCG00000014570	NRIP3	TMEM9 domain family member B [Source:NCBI gene;Acc:100519788]	9
ENSSSCG00000017583	SGCA	sarcoglycan alpha	12

		[Source:NCBI gene;Acc:100240723]	
ENSSSCG00000020953	ATP1A4		4
ENSSSCG00000026533	MYF6	myogenic factor 6 [Source:NCBI gene;Acc:397005]	5
ENSSSCG00000027613	TRDN		1
ENSSSCG00000027684	TRIM63	tripartite motif containing 63 [Source:NCBI gene;Acc:100431101]	6
ENSSSCG00000029651	SLN	sarcolipin [Source:NCBI gene;Acc:733627]	9
ENSSSCG00000010359	LDB3	Not listed (annotated) in NCBI resources	14
ENSSSCG00000006036	ABRA	Not listed (annotated) in NCBI resources	Not listed (annotated)
ENSSSCG00000009830	MLC-2V	Not listed (annotated) in NCBI resources	Not listed (annotated)
ENSSSCG00000010389	C10orf71	Not listed (annotated) in NCBI resources	Not listed (annotated)
ENSSSCG00000011265	XIRP1	Not listed (annotated) in NCBI resources	Not listed (annotated)
ENSSSCG00000013379	KCNJ11	Not listed (annotated) in NCBI resources	Not listed (annotated)
ENSSSCG00000014795	ART1	Not listed (annotated) in NCBI resources	Not listed (annotated)
ENSSSCG00000015481	MYOC	Not listed (annotated) in NCBI resources	Not listed (annotated)
ENSSSCG00000022342	ENSSSCG00000022342	Not listed (annotated) in NCBI resources	Not listed (annotated)

4.2.5. DEGs analysis of porcine liver by comparing the Polish Landrace purebred pigs (MiSeq RNA-Seq data) and Polish Landrace x Duroc crossbred pigs (HiSeq RNA-Seq data) after experimental feeding with the supplementary healthy diet enriched with omega-6 and omega-3 fatty acids (PUFAs) diet using the CLC Genomics workbench

4.2.5.1. Identification of DEGs and Excel filtering of highly significant DEGs with cutoff p-values p<0.0001

A complete gene expression profile representing the between breed comparison of PL purebred *versus* PL x Duroc crossbred pigs liver transcriptome fed with omega-6 and omega-3 fatty acids (PUFAs) supplementary healthy diet is presented in **SUPPLEMENTARY TABLE S10.** Results revealed the identification of 15,966 DEGs without cutoff values including non-significant and significant ($p<0.01$, $p<0.001$) and highly significant ($p<0.0001$) DEGs. After the first Microsoft- Excel filtering of all these DEGs (n=15,966), a total of 5,522, 7,054, and 7,370 highly significant ($p<0.0001$) DEGs were according to Bonferroni p-values, p-values, and FDR values, respectively. The results presented in the Venn diagram (**FIGURE 15**) revealed that highly significant ($p<0.0001$) Bonferroni p-values (n=5522) were commonly sheared among all three p-values. However, a total of 1,532 highly significant ($p<0.0001$) DEGs were commonly sheared between FDR adjusted p-value and standard p-value. Overall, a total of 316 highly significant ($p<0.0001$) DEGs were uniquely identified with the standard p-value.

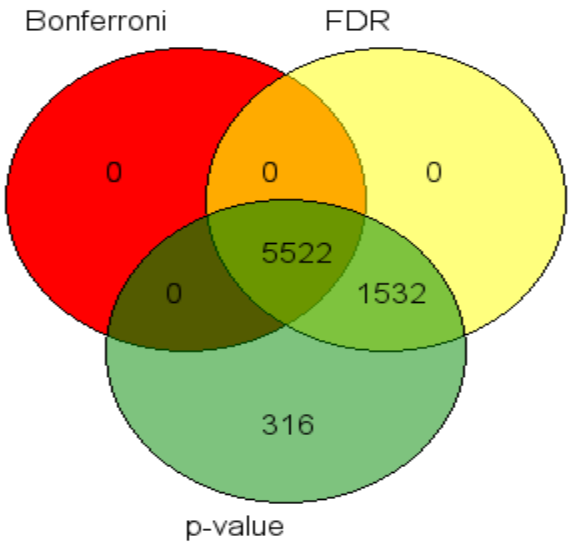

Figure 15. Identification of highly significant (p<0.0001) DEGs according to Bonferroni p-values, p-values, and FDR values, respectively by comparing the Polish Landrace purebred *versus* Polish Landrace x Duroc crossbred pigs liver transcriptome after experimental feeding with the diet enriched with omega-6 and omega-3 fatty acids (PUFAs)

4.2.5.2. Identification of highly significant upregulated and downregulated DEGs in purebred and crossbred pigs after experimental feeding with the diet enriched with omega-6 and omega-3 fatty acids (PUFAs) diet.

Based on the **SUPPLEMENTARY TABLE S10**, upregulated and downregulated DEGs were further filtered (second Microsoft- Excel filtering) according to log2FC and FC values and presented in **SUPPLEMENTARY TABLE S11** and **SUPPLEMENTARY TABLE S12**. Results revealed the identification of 8,871 upregulated (**SUPPLEMENTARY TABLE** S11) and 6,877 downregulated (**SUPPLEMENTARY TABLE** S12) DEGs (without cutoff values of log2FC and FC) that were expressed in the liver transcriptome of PL purebred and PL x Duroc crossbred pigs after experimental feeding with the diet enriched with omega-6 and omega-3 fatty acids (PUFAs). Identification of both up-regulated and downregulated DEGs according to log_2FC and FC values in liver transcriptome by comparing the liver transcriptome of PL purebred *versus* PL x Duroc crossbred pigs after experimental feeding with the diet enriched with omega-6 and omega-3 fatty acids (PUFAs) are presented in **TABLE 31**.

Table 31. Identification of upregulated and downregulated DEGs according to log2FC and FC values in liver transcriptome by comparing the Polish Landrace purebred *versus* Polish Landrace x Duroc crossbred pigs liver transcriptome after experimental feeding with the diet enriched with omega-6 and omega-3 fatty acids (PUFAs).

Venn diagram circle representing DEGs	Upregulated			Downregulated		
	log2FC (>2FC)	FC (>2FC)	log2FC (>9FC)	log2FC (>2FC)	FC (>2FC)	log2FC (>9FC)
Bonferroni p< 0.0001	1395	2364	123*	1457	2430	61*
FDR p< 0.0001	1620	2805	123	1658	2793	88
p-value p< 0.0001	1683	2902	124	1699	2872	94

*Gene symbols and full gene names of DEGs are listed in the separate tables.

Based on the log2FC (>9FC) values of **TABLE 31** and Venn diagram (**FIGURE 16**) results revealed that the majority of the 123 highly significant down-regulated DEGs (log2FC values of <9x) were commonly sheared among all three p-values (a complete list of upregulated DEGs (n=123*) with gene symbol and full names is further presented in **TABLE 32**). However, one highly significant (p<0.0001) downregulated DEGs (log2FC values of <9x) were uniquely identified with the standard p-value. Furthermore, based on the log2FC (>9FC) values of **TABLE 31** and a Venn diagram (**FIGURE 17**) results revealed a total of 61 highly significant down-regulated DEGs (log2FC values of <9) with Bonferroni p-values (p<0.0001) were commonly sheared among all three p-values (a complete list of downregulated DEGs (n=61*) with gene symbol and full names is further presented in **TABLE 33**). However, a total of 27 highly significant (p<0.0001) downregulated DEGs(log2FC values of <9x) were commonly sheared between FDR adjusted p-value and standard p-value. Overall, a total of 6 (log2FC values of <9x) highly significant (p<0.0001) downregulated DEGs were uniquely identified with the standard p-value.

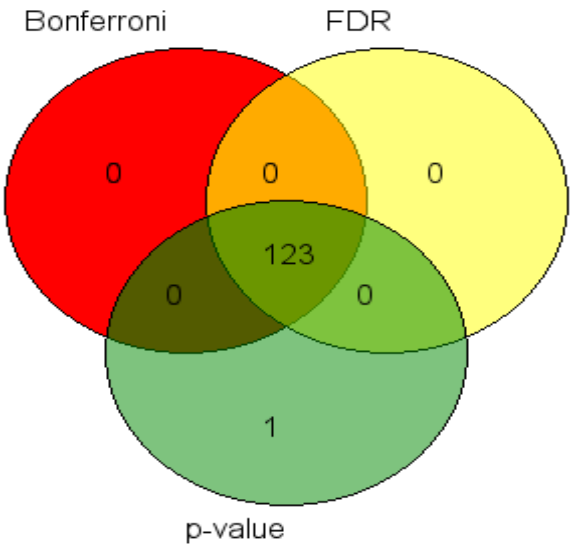

Figure 16. Identified highly significant (p<0.0001) upregulated DEGs by comparing the liver transcriptome of Polish Landrace purebred and Polish Landrace x Duroc crossbred pigs after experimental feeding with the diet enriched with omega-6 and omega-3 fatty acids (PUFAs) according to log_2FC and FC values.

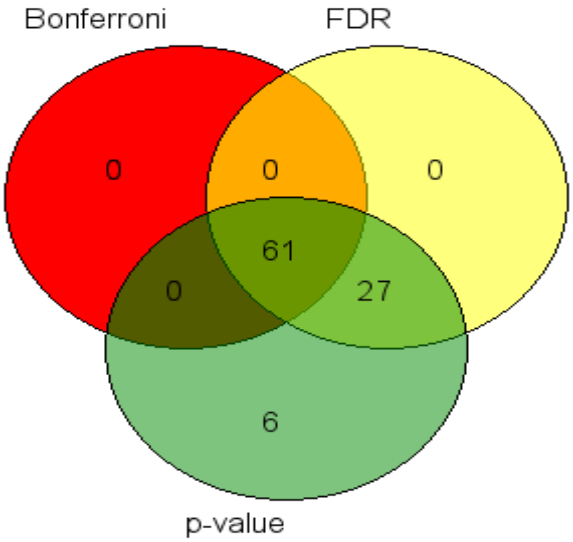

Figure 17. Identified highly significant (p<0.0001) downregulated DEGs by comparing the liver transcriptome of Polish Landrace purebred and Polish Landrace x Duroc crossbred pigs after experimental feeding with the diet enriched with omega-6 and omega-3 fatty acids (PUFAs) according to log_2FC and FC values.

Table 32: List of identified highly significant (p<0.0001) upregulated (n=123) (**Figure 16**) DEGs according to log2FC (>9x) values in liver transcriptome by comparing the Polish Landrace purebred *versus* Polish Landrace x Duroc crossbred pigs liver transcriptome after experimental feeding with the diet enriched with omega-6 and omega-3 fatty acids (PUFAs).

Highly significant (all p <0.0001) upregulated DEGs with log2FC (>9x) values			
Gene stable ID	Gene symbol	Gene description	Chromosome
ENSSSCG00000000046	CYP2D25	vitamin D3 25-Hydroxylase [Source:NCBI gene;Acc:397687]	5
ENSSSCG00000000253	KRT18	keratin 18 [Source:NCBI gene;Acc:100126286]	5
ENSSSCG00000000398	APOF	apolipoprotein F [Source:NCBI gene;Acc:445462]	5
ENSSSCG00000000577	GYS2	glycogen synthase 2 [Source:NCBI gene;Acc:100157080]	5
ENSSSCG00000000584	SLCO1A2	solute carrier organic anion transporter family member 1A2 [Source:NCBI gene;Acc:397534]	5
ENSSSCG00000000660	A2M	alpha-2-macroglobulin [Source:NCBI gene;Acc:403166]	5
ENSSSCG00000000749	SLC6A12	solute carrier family 6 member 12 [Source:NCBI gene;Acc:100512716]	5
ENSSSCG00000000856	PAH	phenylalanine hydroxylase [Source:NCBI gene;Acc:100521900]	5
ENSSSCG00000000892	HAL	histidine ammonia-lyase [Source:NCBI gene;Acc:100154617]	5

ENSSSCG00000001823	UROC1	urocanate hydratase 1 [Source:NCBI gene;Acc:100157217]	7
ENSSSCG00000002009	PCK2	phosphoenolpyruvate carboxykinase 2, mitochondrial [Source:NCBI gene;Acc:403165]	7
ENSSSCG00000002476	SERPINA1	serpin family A member 1 [Source:NCBI gene;Acc:397688]	7
ENSSSCG00000002483	SERPINA3-3	serpin A3-8 [Source:NCBI gene;Acc:106504545]	7
ENSSSCG00000002486	ENSSSCG00000002486	serpin A3-5 [Source:NCBI gene;Acc:396684]	7
ENSSSCG00000002487	SERPINA3-2	alpha-1-antichymotrypsin 2 [Source:NCBI gene;Acc:396686]	7
ENSSSCG00000002749	HP	haptoglobin [Source:NCBI gene;Acc:397061]	6
ENSSSCG00000002913	PRODH2	proline dehydrogenase 2 [Source:HGNC Symbol;Acc:HGNC:17325]	6
ENSSSCG00000003463	AGMAT	agmatinase [Source:NCBI gene;Acc:100519548]	6
ENSSSCG00000003669	MFSD2A	major facilitator superfamily domain containing 2A [Source:NCBI gene;Acc:100518612]	6
ENSSSCG00000004001	A1BG	alpha-1-B glycoprotein [Source:NCBI gene;Acc:100516980]	6

ENSSSCG00000004038	PLG	plasminogen [Source:NCBI gene;Acc:733660]	1
ENSSSCG00000004041	SLC22A1	solute carrier family 22 member 1 [Source:NCBI gene;Acc:397049]	1
ENSSSCG00000004597	AQP9	aquaporin 9 [Source:NCBI gene;Acc:100127153]	1
ENSSSCG00000005485	AMBP	alpha-1-microglobulin/bikunin precursor [Source:NCBI gene;Acc:397593]	1
ENSSSCG00000005512	C5	complement C5 [Source:NCBI gene;Acc:414437]	1
ENSSSCG00000005609	GARNL3	GTPase activating Rap/RanGAP domain like 3 [Source:NCBI gene;Acc:100156351]	1
ENSSSCG00000005840	C8G	complement C8 gamma chain [Source:NCBI gene;Acc:100037955]	AEMK02000682.1
ENSSSCG00000006353	NR1I3	nuclear receptor subfamily 1 group I member 3 [Source:NCBI gene;Acc:654317]	4
ENSSSCG00000006355	APOA2	apolipoprotein A2 [Source:NCBI gene;Acc:100153243]	4
ENSSSCG00000006403	CRP	C-reactive protein, pentraxin-related [Source:NCBI gene;Acc:396842]	4
ENSSSCG00000006455	CD5L	CD5 molecule like	4

		[Source:NCBI gene;Acc:100154019]	
ENSSSCG00000006716	HMGCS2		4
ENSSSCG00000007507	PCK1	phosphoenolpyruvate carboxykinase 1 [Source:NCBI gene;Acc:100144531]	17
ENSSSCG00000007671	TFR2	transferrin receptor 2 [Source:NCBI gene;Acc:100517580]	3
ENSSSCG00000008522	XDH	xanthine dehydrogenase [Source:NCBI gene;Acc:100515259]	3
ENSSSCG00000008700	HGFAC	HGF activator [Source:NCBI gene;Acc:100739841]	8
ENSSSCG00000008935	ENSSSCG00000008935	UDP-glucuronosyltransferase 2B31 [Source:NCBI gene;Acc:100623255]	8
ENSSSCG00000008948	ALB	albumin [Source:NCBI gene;Acc:396960]	8
ENSSSCG00000008997	FGB	fibrinogen beta chain [Source:NCBI gene;Acc:100514354]	8
ENSSSCG00000009225	HSD17B13	estradiol 17-beta-dehydrogenase 11 [Source:NCBI gene;Acc:100520923]	8
ENSSSCG00000009413	CPB2	carboxypeptidase B2 [Source:NCBI gene;Acc:100155038]	11
ENSSSCG00000009558	F10	coagulation factor X	11

		[Source:NCBI gene;Acc:733662]	
ENSSSCG00000009805	HPD	4-hydroxyphenylpyruvate dioxygenase [Source:NCBI gene;Acc:397443]	14
ENSSSCG00000009942	DAO	D-amino acid oxidase [Source:NCBI gene;Acc:397134]	14
ENSSSCG00000010008	SEC14L3	SEC14-like protein 3 [Source:NCBI gene;Acc:100156470]	14
ENSSSCG00000010337	MAT1A	methionine adenosyltransferase 1A [Source:NCBI gene;Acc:100156922]	14
ENSSSCG00000010479	RBP4	retinol binding protein 4 [Source:NCBI gene;Acc:397124]	14
ENSSSCG00000010543	ABCC2	ATP binding cassette subfamily C member 2 [Source:NCBI gene;Acc:397535]	14
ENSSSCG00000010545	CPN1	carboxypeptidase N subunit 1 [Source:NCBI gene;Acc:100157984]	14
ENSSSCG00000010780	CYP2E1	cytochrome P450, family 2, subfamily E, polypeptide 1 [Source:NCBI gene;Acc:403216]	14
ENSSSCG00000011147	AKR1C1	aldo-keto reductase family 1, member C1 [Source:NCBI gene;Acc:733634]	10

ENSSSCG00000011450	ITIH1	inter-alpha-trypsin inhibitor heavy chain 1 [Source:NCBI gene;Acc:396963]	13
ENSSSCG00000011451	ITIH3	inter-alpha-trypsin inhibitor heavy chain 3 [Source:NCBI gene;Acc:100157235]	13
ENSSSCG00000011640	TF	transferrin [Source:NCBI gene;Acc:396996]	13
ENSSSCG00000011700	CP	ceruloplasmin [Source:NCBI gene;Acc:406870]	13
ENSSSCG00000011799	AHSG	alpha 2-HS glycoprotein [Source:NCBI gene;Acc:397585]	13
ENSSSCG00000011801	HRG	histidine rich glycoprotein [Source:NCBI gene;Acc:100152095]	13
ENSSSCG00000012236	OTC	ornithine carbamoyltransferase [Source:NCBI gene;Acc:397438]	X
ENSSSCG00000012394	GJB1	gap junction protein beta 1 [Source:NCBI gene;Acc:100519581]	X
ENSSSCG00000013252	F2	coagulation factor II, thrombin [Source:NCBI gene;Acc:100144442]	2
ENSSSCG00000013370	ENSSSCG00000013370	serum amyloid A-2 protein [Source:NCBI gene;Acc:100525680]	2
ENSSSCG00000013842	CYP4F3	docosahexaenoic acid	2

		omega-hydroxylase CYP4F3-like [Source:NCBI gene;Acc:110259329]	
ENSSSCG00000014108	BHMT	betaine--homocysteine S-methyltransferase [Source:NCBI gene;Acc:397371]	2
ENSSSCG00000014110	DMGDH	dimethylglycine dehydrogenase [Source:NCBI gene;Acc:100525563]	2
ENSSSCG00000014626	HPX	hemopexin [Source:NCBI gene;Acc:396998]	9
ENSSSCG00000015039	BCO2	beta-carotene oxygenase 2 [Source:NCBI gene;Acc:100517547]	9
ENSSSCG00000015067	APOA5	apolipoprotein A5 [Source:NCBI gene;Acc:100286807]	9
ENSSSCG00000015069	APOC3	apolipoprotein C3 [Source:NCBI gene;Acc:406187]	9
ENSSSCG00000015276	ETNK2	ethanolamine kinase 2 [Source:NCBI gene;Acc:100622861]	9
ENSSSCG00000015493	SERPINC1	serpin family C member 1 [Source:NCBI gene;Acc:100125972]	9
ENSSSCG00000015662	C4BPA	complement component 4 binding protein, alpha [Source:NCBI gene;Acc:396982]	9

ENSSSCG00000016159	CPS1	carbamoyl-phosphate synthase 1 [Source:NCBI gene;Acc:100157716]	15
ENSSSCG00000016315	SPP2	secreted phosphoprotein 2 [Source:NCBI gene;Acc:396669]	15
ENSSSCG00000016402	AGXT	alanine--glyoxylate and serine--pyruvate aminotransferase [Source:NCBI gene;Acc:100517616]	15
ENSSSCG00000016829	AGXT2	alanine--glyoxylate aminotransferase 2 [Source:NCBI gene;Acc:100513890]	16
ENSSSCG00000016856	C9	complement C9 [Source:NCBI gene;Acc:100037951]	16
ENSSSCG00000021867	HPN	hepsin [Source:NCBI gene;Acc:100624088]	6
ENSSSCG00000021998	ENSSSCG00000021998	solute carrier organic anion transporter family member 1B3 [Source:NCBI gene;Acc:100620829]	5
ENSSSCG00000022390	RGN	regucalcin [Source:NCBI gene;Acc:768107]	X
ENSSSCG00000022739	DSG2	desmoglein 2 [Source:NCBI gene;Acc:100625833]	6
ENSSSCG00000023472	FMO3	flavin containing monooxygenase 3 [Source:NCBI gene;Acc:100523562]	9

ENSSSCG00000023684	MT1A	metallothionein-1E-like [Source:NCBI gene;Acc:102166944]	6
ENSSSCG00000023686	TTR	transthyretin [Source:NCBI gene;Acc:397419]	6
ENSSSCG00000023693	PROC	protein C, inactivator of coagulation factors Va and VIIIa [Source:NCBI gene;Acc:396954]	15
ENSSSCG00000024179	NAGS	N-acetylglutamate synthase [Source:NCBI gene;Acc:100048960]	12
ENSSSCG00000024305	MT3	metallothionein 3 [Source:NCBI gene;Acc:397123]	6
ENSSSCG00000024314	FGG	fibrinogen gamma chain [Source:NCBI gene;Acc:403164]	8
ENSSSCG00000024402	ENSSSCG00000024402	pregnancy zone protein [Source:NCBI gene;Acc:100153288]	5
ENSSSCG00000024911	ENSSSCG00000024911	metallothionein-1E [Source:NCBI gene;Acc:100037920]	6
ENSSSCG00000024914	BF	complement factor B [Source:NCBI gene;Acc:100124383]	7
ENSSSCG00000027609	GC	GC, vitamin D binding protein [Source:NCBI gene;Acc:448964]	8
ENSSSCG00000027801	VTN	vitronectin [Source:NCBI gene;Acc:397192]	12
ENSSSCG00000027854	HSD17B6	17-beta-hydroxysteroid	5

		dehydrogenase type 6 [Source:NCBI gene;Acc:100620470]	
ENSSSCG00000027926	FTCD	formimidoyltransferase cyclodeaminase [Source:NCBI gene;Acc:397517]	AEMK02000328.1
ENSSSCG00000028203	ICA	transferrin [Source:NCBI gene;Acc:396845]	13
ENSSSCG00000028758	LBP	lipopolysaccharide binding protein [Source:NCBI gene;Acc:397303]	17
ENSSSCG00000030033	ACSM4	acyl-CoA synthetase medium-chain family member 4 [Source:NCBI gene;Acc:100512595]	3
ENSSSCG00000030300	MT2A	metallothionein-2A [Source:NCBI gene;Acc:396827]	6
ENSSSCG00000030371	ENSSSCG00000030371	serpin A3-8 [Source:NCBI gene;Acc:396685]	7
ENSSSCG00000010549	ENSSSCG00000010549	Not listed (annotated) in NCBI resources	14
ENSSSCG00000013369	SAA1	Not listed (annotated) in NCBI resources	2
ENSSSCG00000015068	APOA4	Not listed (annotated) in NCBI resources	9
ENSSSCG00000028901	ENSSSCG00000028901	Not listed (annotated) in NCBI resources	8
ENSSSCG00000001652	GNMT	Not listed (annotated) in NCBI resources	Not listed (annotated)
ENSSSCG00000002482	ENSSSCG00000002482	Not listed (annotated) in NCBI resources	Not listed (annotated)

ENSSSCG00000003130	SULT2A1	Not listed (annotated) in NCBI resources	Not listed (annotated)
ENSSSCG00000005394	ALDOB	Not listed (annotated) in NCBI resources	Not listed (annotated)
ENSSSCG00000005395	ENSSSCG00000005395	Not listed (annotated) in NCBI resources	Not listed (annotated)
ENSSSCG00000006990	FGL1	Not listed (annotated) in NCBI resources	Not listed (annotated)
ENSSSCG00000008596	ENSSSCG00000008596	Not listed (annotated) in NCBI resources	Not listed (annotated)
ENSSSCG00000010944	FBP1	Not listed (annotated) in NCBI resources	Not listed (annotated)
ENSSSCG00000017704	CCL16	Not listed (annotated) in NCBI resources	Not listed (annotated)
ENSSSCG00000021186	CRP_1	Not listed (annotated) in NCBI resources	Not listed (annotated)
ENSSSCG00000021602	TTC36	Not listed (annotated) in NCBI resources	Not listed (annotated)
ENSSSCG00000022156	ENSSSCG00000022156	Not listed (annotated) in NCBI resources	Not listed (annotated)
ENSSSCG00000024682	ENSSSCG00000024682	Not listed (annotated) in NCBI resources	Not listed (annotated)
ENSSSCG00000023414	ENSSSCG00000023414	Not listed (annotated) in NCBI resources	Not listed (annotated)
ENSSSCG00000024079	ENSSSCG00000024079	Not listed (annotated) in NCBI resources	Not listed (annotated)
ENSSSCG00000024213	ENSSSCG00000024213	Not listed (annotated) in NCBI resources	Not listed (annotated)
ENSSSCG00000024919	RDH16	Not listed (annotated) in NCBI resources	Not listed (annotated)
ENSSSCG00000026314	ENSSSCG00000026314	Not listed (annotated) in NCBI resources	Not listed (annotated)
ENSSSCG00000030385	ENSSSCG00000030385	Not listed (annotated) in	Not listed

		NCBI resources	(annotated)
ENSSSCG00000030522	ENSSSCG00000030522	Not listed (annotated) in NCBI resources	Not listed (annotated)

Table 33: List of identified highly significant (p<0.0001) downregulated (n=61) **(Figure 17)** DEGs according to log2FC (>9x) values in liver transcriptome by comparing the Polish Landrace purebred *versus* Polish Landrace x Duroc crossbred pigs liver transcriptome after experimental feeding with the diet enriched with omega-6 and omega-3 fatty acids (PUFAs).

Highly significant (Bonferroni p <0.0001) downregulated DEGs with log2FC (>9x) values			
Gene stable ID	Gene symbol	Gene description	Chromosome
ENSSSCG00000000866	MYBPC1	myosin binding protein C, slow type [Source:NCBI gene;Acc:100523187]	5
ENSSSCG00000001068	CAP2	cyclase associated actin cytoskeleton regulatory protein 2 [Source:NCBI gene;Acc:100523257]	7
ENSSSCG00000001487	KLHL31	kelch like family member 31 [Source:NCBI gene;Acc:100152767]	7
ENSSSCG00000002029	MYH7	myosin heavy chain 7 [Source:NCBI gene;Acc:396860]	7
ENSSSCG00000002831	IRX3	iroquois homeobox 3 [Source:NCBI gene;Acc:100518611]	6
ENSSSCG00000004255	VGLL2	vestigial like family member 2 [Source:NCBI gene;Acc:100739384]	1
ENSSSCG00000005087	SIX1	SIX homeobox 1 [Source:NCBI gene;Acc:100156847]	1
ENSSSCG00000006174	JPH1	junctophilin 1 [Source:NCBI gene;Acc:100155368]	4

ENSSSCG00000006216	TRIM55	tripartite motif containing 55 [Source:NCBI gene;Acc:100152010]	4
ENSSSCG00000006391	ATP1A2	ATPase Na+/K+ transporting subunit alpha 2 [Source:NCBI gene;Acc:396828]	4
ENSSSCG00000006725	TBX15	T-box 15 [Source:NCBI gene;Acc:100158194]	4
ENSSSCG00000007231	MYLK2	myosin light chain kinase 2 [Source:NCBI gene;Acc:100524288]	17
ENSSSCG00000007424	TNNC2	troponin C2, fast skeletal type [Source:NCBI gene;Acc:414905]	17
ENSSSCG00000007462	KCNB1	potassium voltage-gated channel subfamily B member 1 [Source:NCBI gene;Acc:397433]	17
ENSSSCG00000007757	TRIM72	tripartite motif containing 72 [Source:NCBI gene;Acc:100511188]	3
ENSSSCG00000008200	ANKRD23	ankyrin repeat domain 23 [Source:NCBI gene;Acc:100525457]	3
ENSSSCG00000008806	YIPF7	Yip1 domain family member 7 [Source:NCBI gene;Acc:100516500]	8
ENSSSCG00000010144	ACTN2	actinin alpha 2 [Source:NCBI gene;Acc:100157406]	14

ENSSSCG00000010190	ACTA1	actin, alpha 1, skeletal muscle [Source:NCBI gene;Acc:100154254]	14
ENSSSCG00000010304	MYOZ1	myozenin 1 [Source:NCBI gene;Acc:574060]	14
ENSSSCG00000010317	DUPD1	dual specificity phosphatase and pro isomerase domain containing 1 [Source:NCBI gene;Acc:100155430]	14
ENSSSCG00000010522	ANKRD2	ankyrin repeat domain 2 [Source:HGNC Symbol;Acc:HGNC:495]	14
ENSSSCG00000010578	PITX3	paired like homeodomain 3 [Source:NCBI gene;Acc:100154216]	14
ENSSSCG00000010947	FBP2	fructose-bisphosphatase 2 [Source:NCBI gene;Acc:100134828]	10
ENSSSCG00000011238	ARPP21	cAMP regulated phosphoprotein 21 [Source:NCBI gene;Acc:100512986]	13
ENSSSCG00000011325	MYL3	myosin light chain 3 [Source:NCBI gene;Acc:100515755]	13
ENSSSCG00000013354	CSRP3	cysteine and glycine rich protein 3 [Source:NCBI gene;Acc:100337687]	2
ENSSSCG00000014324	MYOT	myotilin [Source:NCBI gene;Acc:100101550]	2

ENSSSCG00000014560	COX8H	COX8H protein [Source:NCBI gene;Acc:100038031]	2
ENSSSCG00000014834	UCP3	uncoupling protein 3 [Source:NCBI gene;Acc:397116]	9
ENSSSCG00000015796	PDLIM3	PDZ and LIM domain 3 [Source:NCBI gene;Acc:414421]	15
ENSSSCG00000015835	DUSP26	dual specificity phosphatase 26 [Source:NCBI gene;Acc:100525894]	AEMK02000697.1
ENSSSCG00000016605	LMOD2	leiomodin 2 [Source:NCBI gene;Acc:100525195]	18
ENSSSCG00000016701	HOXA7	homeobox A7 [Source:NCBI gene;Acc:100519456]	18
ENSSSCG00000017500	TCAP	titin-cap [Source:NCBI gene;Acc:100271745]	12
ENSSSCG00000017583	SGCA	sarcoglycan alpha [Source:NCBI gene;Acc:100240723]	12
ENSSSCG00000017624	CUEDC1	CUE domain containing 1 [Source:NCBI gene;Acc:100511955]	12
ENSSSCG00000017717	UNC45B	unc-45 myosin chaperone B [Source:NCBI gene;Acc:100134956]	12
ENSSSCG00000020785	DES	desmin [Source:NCBI gene;Acc:396725]	15

ENSSSCG00000024061	TNNI1	troponin I1, slow skeletal type [Source:NCBI gene;Acc:396947]	10
ENSSSCG00000025353	TNNT1	troponin T1, slow skeletal type [Source:NCBI gene;Acc:396579]	6
ENSSSCG00000026600	KLHL30	kelch like family member 30 [Source:NCBI gene;Acc:100623077]	15
ENSSSCG00000027684	TRIM63	tripartite motif containing 63 [Source:NCBI gene;Acc:100431101]	6
ENSSSCG00000028047	DTNA	dystrobrevin alpha [Source:NCBI gene;Acc:100627907]	6
ENSSSCG00000029311	MYPN	myopalladin [Source:NCBI gene;Acc:100624901]	14
ENSSSCG00000010359	LDB3	Not listed (annotated) in NCBI resources	14
ENSSSCG00000020953	ATP1A4	Not listed (annotated) in NCBI resources	4
NKAIN1	ENSSSCG00000003593	Not listed (annotated) in NCBI resources	Not listed (annotated)
MYOZ2	ENSSSCG00000009110	Not listed (annotated) in NCBI resources	Not listed (annotated)
MLC-2V	ENSSSCG00000009830	Not listed (annotated) in NCBI resources	Not listed (annotated)
DUSP13	ENSSSCG00000010318	Not listed (annotated) in NCBI resources	Not listed (annotated)

ENSSSCG00000014118	ENSSSCG00000014118	Not listed (annotated) in NCBI resources	Not listed (annotated)
ART1	ENSSSCG00000014795	Not listed (annotated) in NCBI resources	Not listed (annotated)
MYOC	ENSSSCG00000015481	Not listed (annotated) in NCBI resources	Not listed (annotated)
HSPB3	ENSSSCG00000016896	Not listed (annotated) in NCBI resources	Not listed (annotated)
ENSSSCG00000022342	ENSSSCG00000022342	Not listed (annotated) in NCBI resources	Not listed (annotated)
ENSSSCG00000024577	ENSSSCG00000024577	Not listed (annotated) in NCBI resources	Not listed (annotated)
NMRK2	ENSSSCG00000025409	Not listed (annotated) in NCBI resources	Not listed (annotated)
ENSSSCG00000028103	ENSSSCG00000028103	Not listed (annotated) in NCBI resources	Not listed (annotated)
ENSSSCG00000028808	ENSSSCG00000028808	Not listed (annotated) in NCBI resources	Not listed (annotated)
ENSSSCG00000029128	ENSSSCG00000029128	Not listed (annotated) in NCBI resources	Not listed (annotated)

4.2.6. Overall comparisons of identified up- and down-regulated genes (Third filtering)

Based on the second filtering data of all four DEGs comparisons, a third Excel filtering was performed to identify the „Unique" as well as the „Commonly shared" diet-specific and breed-specific DEGs. A complete gene expression profile representing third filtering of all four DEGs comparison between standard (control) diet *versus* supplementary healthy diet enriched with omega-6 and omega-3 fatty acids (PUFAs) on the liver transcriptome in PL purebred and PL x Duroc Crossbred pigs is presented (**SUPPLEMENTARY TABLES S1–S4** and Venn Diagrams in **FIGURES 18–25**) and described in the subsection below subsection.

4.2.6.1. Comparison of identified upregulated DEGs in purebred *versus* crossbred pigs.

A Venn diagram results in **FIGURE 18** revealed the identification of 192 and 89 unique upregulated DEGs ($p<0.0001$, and <2FC) specific to PL purebred *versus* PL x Duroc crossbred, respectively (**SUPPLEMENTARY TABLE S1**, and **FIGURE 18**). Furthermore, a total of 7 upregulated DEGs ($p<0.0001$, and <2FC) were identified represented in both PL purebred and PL x Duroc crossbred, respectively (**TABLE 34**, and **FIGURE 18**).

However, the Venn diagram results in **FIGURE 19** revealed the identification of 29 and 28 unique upregulated DEGs ($p<0.0001$, and <2 log2FC) specific to PL purebred *versus* PL x Duroc crossbred, respectively, whereas only one upregulated DEGs ($p<0.0001$, and <2 log2FC) identified that was shared in both PL purebred and PL x Duroc crossbred, respectively (**TABLE 35**, and **FIGURE 19**).

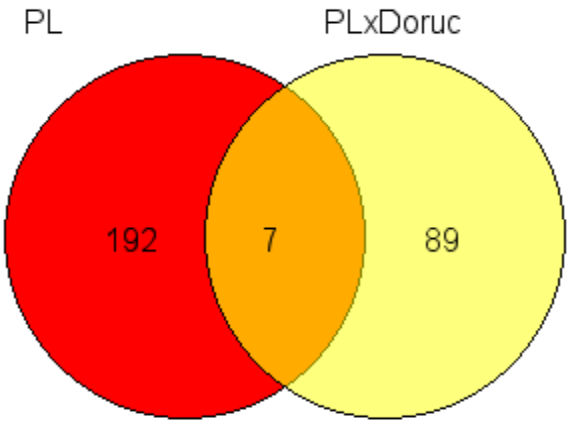

Figure 18. Upregulated DEGs with FC (<2FC) values with Bonferroni p <0.0001 by comparing the PL vs PL-Duroc breeds.

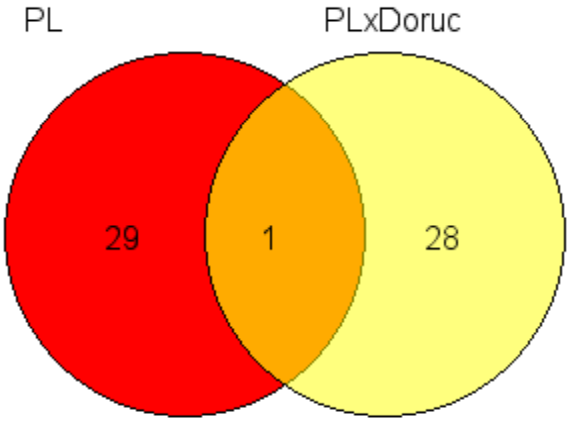

Figure 19. Upregulated DEGs with Log2FC (<2FC) values with Bonferroni p <0.0001 by comparing the PL vs PL-Duroc breeds.

Supplementary Table S1: Unique DEGs

Table 34. List of upregulated in both PL and PL x Duroc DEGs FC (<2FC) values with Bonferroni p<0.0001 by comparing Polish Landrace purebred *versus* Polish Landrace x Duroc crossbred.

Common DEGs	Gene name	Gene description	Chromosome
ENSSSCG00000002743	IST1	IST1, ESCRT-III associated factor [Source:NCBI gene;Acc:100626669]	6
ENSSSCG00000010464	PPP1R3C	protein phosphatase 1 regulatory subunit 3C [Source:NCBI gene;Acc:641349]	14
ENSSSCG00000013380	NUCB2	nucleobindin 2 [Source:NCBI gene;Acc:100512826]	2
ENSSSCG00000015054	NNMT	nicotinamide N-methyltransferase [Source:NCBI gene;Acc:100144485]	9
ENSSSCG00000022797	PPP1R3B	protein phosphatase 1 regulatory subunit 3B [Source:NCBI gene;Acc:100515931]	15
ENSSSCG00000011148	Not listed (annotated)	Not listed (annotated) in NCBI resources	Not listed (annotated)
ENSSSCG00000001134	Not listed (annotated)	Not listed (annotated) in NCBI resources	Not listed (annotated)

Table 35. List of upregulated in both Pl and PL x Duroc and unique DEGs log2FC (<2FC) values with Bonferroni p<0.0001 by comparing Polish Landrace purebred *versus* Polish Landrace x Duroc crossbred.

Common DEGs (1)	Gene name	Gene description	Chromosome
ENSSSCG00000011148	ENSSSCG00000011148	Not listed (annotated) in NCBI resources	Not listed (annotated)
Unique PL DEGs (29)	**Gene name**	**Gene description**	**Chromosome**
ENSSSCG00000000164	CRY1	cryptochrome circadian regulator 1 [Source:NCBI gene;Acc:100520380]	5
ENSSSCG00000001235	TRIM15	tripartite motif containing 15 [Source:NCBI gene;Acc:100144461]	7
ENSSSCG00000001906	CYP1A1	cytochrome P450 1A1 [Source:NCBI gene;Acc:403103]	7
ENSSSCG00000002294	ARG2	arginase 2 [Source:NCBI gene;Acc:100155893]	7
ENSSSCG00000002743	IST1	IST1, ESCRT-III associated factor [Source:NCBI gene;Acc:100626669]	6
ENSSSCG00000003410	MASP2	mannan binding lectin serine peptidase 2 [Source:NCBI gene;Acc:100302537]	6
ENSSSCG00000003789	CTH	cystathionine gamma-lyase [Source:NCBI gene;Acc:733654]	6
ENSSSCG00000004195	ARG1	arginase 1 [Source:NCBI gene;Acc:397115]	1
ENSSSCG00000004702	STRC	stereocilin [Source:NCBI gene;Acc:100519812]	1
ENSSSCG00000006141	CA3	carbonic anhydrase 3 [Source:NCBI gene;Acc:494016]	4
ENSSSCG00000006238	CYP7A1	cytochrome P450, family 7, subfamily A, polypeptide 1 [Source:NCBI gene;Acc:448985]	4
ENSSSCG00000006582	S100A14	S100 calcium binding protein A14	4

		[Source:NCBI gene;Acc:100153930]	
ENSSSCG00000006588	S100A9	S100 calcium binding protein A9 [Source:NCBI gene;Acc:100127489]	4
ENSSSCG00000008119	KCNIP3	potassium voltage-gated channel interacting protein 3 [Source:NCBI gene;Acc:100524248]	3
ENSSSCG00000012071	ENSSSCG00000012071	immunoglobulin superfamily member 5 [Source:NCBI gene;Acc:100517006]	13
ENSSSCG00000015268	FMO1	flavin containing monooxygenase 1 [Source:NCBI gene;Acc:397132]	9
ENSSSCG00000015391	CROT	carnitine O-octanoyltransferase [Source:NCBI gene;Acc:100521142]	9
ENSSSCG00000015699	ACMSD	aminocarboxymuconate semialdehyde decarboxylase [Source:NCBI gene;Acc:100154768]	15
ENSSSCG00000022331	ENSSSCG00000022331	fibroblast growth factor 13 [Source:NCBI gene;Acc:100523833]	X
ENSSSCG00000026427	RORC	RAR related orphan receptor C [Source:NCBI gene;Acc:100622477]	4
ENSSSCG00000026850	SNCG	synuclein gamma [Source:NCBI gene;Acc:100125343]	14
ENSSSCG00000029558	EXTL1	exostosin like glycosyltransferase 1 [Source:NCBI gene;Acc:100623848]	6
ENSSSCG00000001231	ENSSSCG00000001231	Not listed (annotated) in NCBI resources	7
ENSSSCG00000004170	ENSSSCG00000004170	Not listed (annotated) in NCBI resources	1
ENSSSCG00000006985	ENSSSCG00000006985	Not listed (annotated) in NCBI resources	17
ENSSSCG00000000134	ENSSSCG00000000134	Not listed (annotated) in NCBI resources	Not listed (annotated)
ENSSSCG00000001652	ENSSSCG00000001652	Not listed (annotated) in NCBI resources	Not listed (annotated)

ENSSSCG00000009871	ENSSSCG00000009871	Not listed (annotated) in NCBI resources	Not listed (annotated)
ENSSSCG00000014945	ENSSSCG00000014945	Not listed (annotated) in NCBI resources	Not listed (annotated)
Unique PL x Duroc (28)	**Gene name**	**Gene description**	**Chromosome**
ENSSSCG00000001045	ELOVL2	ELOVL fatty acid elongase 2 [Source:NCBI gene;Acc:100153368]	7
ENSSSCG00000003278	ENSSSCG00000003278	leukocyte immunoglobulin-like receptor subfamily B member 3-like [Source:NCBI gene;Acc:100511639]	6
ENSSSCG00000003318	GALP	galanin like peptide [Source:NCBI gene;Acc:396772]	6
ENSSSCG00000005067	CCDC198	coiled-coil domain containing 198 [Source:NCBI gene;Acc:100513515]	1
ENSSSCG00000005196	DMAC1	distal membrane arm assembly complex 1 [Source:NCBI gene;Acc:100155846]	1
ENSSSCG00000010432	ENSSSCG00000010432	N-acylsphingosine amidohydrolase 2 [Source:NCBI gene;Acc:100157065]	14
ENSSSCG00000011307	ENSSSCG00000011307	zinc finger protein 501 [Source:NCBI gene;Acc:100738134]	13
ENSSSCG00000013060	SCGB1A1	secretoglobin family 1A member 1 [Source:NCBI gene;Acc:102164135]	2
ENSSSCG00000013370	ENSSSCG00000013370	serum amyloid A-2 protein [Source:NCBI gene;Acc:100525680]	2
ENSSSCG00000016504	TBXAS1	thromboxane A synthase 1 [Source:NCBI gene;Acc:397112]	18
ENSSSCG00000016678	NOD1	nucleotide binding oligomerization domain containing 1 [Source:NCBI gene;Acc:100135660]	18
ENSSSCG00000022724	ENSSSCG00000022724	UDP-glucuronosyltransferase 2B18-like [Source:NCBI gene;Acc:100516628]	8
ENSSSCG00000024310	F13A1	coagulation factor XIII A chain	7

		[Source:NCBI gene;Acc:100153504]	
ENSSSCG00000029515	PON3	paraoxonase 3 [Source:NCBI gene;Acc:733674]	9
ENSSSCG00000013369	ENSSSCG00000013369	Not listed (annotated) in NCBI resources	2
ENSSSCG00000030198	ENSSSCG00000030198	Not listed (annotated) in NCBI resources	1
ENSSSCG00000001134	ENSSSCG00000001134	Not listed (annotated) in NCBI resources	Not listed (annotated)
ENSSSCG00000003824	ENSSSCG00000003824	Not listed (annotated) in NCBI resources	Not listed (annotated)
ENSSSCG00000008588	ENSSSCG00000008588	Not listed (annotated) in NCBI resources	Not listed (annotated)
ENSSSCG00000008886	ENSSSCG00000008886	Not listed (annotated) in NCBI resources	Not listed (annotated)
ENSSSCG00000021940	ENSSSCG00000021940	Not listed (annotated) in NCBI resources	Not listed (annotated)
ENSSSCG00000021965	ENSSSCG00000021965	Not listed (annotated) in NCBI resources	Not listed (annotated)
ENSSSCG00000023038	ENSSSCG00000023038	Not listed (annotated) in NCBI resources	Not listed (annotated)
ENSSSCG00000028525	ENSSSCG00000028525	Not listed (annotated) in NCBI resources	Not listed (annotated)
ENSSSCG00000028994	ENSSSCG00000028994	Not listed (annotated) in NCBI resources	Not listed (annotated)
ENSSSCG00000029028	ENSSSCG00000029028	Not listed (annotated) in NCBI resources	Not listed (annotated)
ENSSSCG00000030738	ENSSSCG00000030738	Not listed (annotated) in NCBI resources	Not listed (annotated)
ENSSSCG00000030730	ENSSSCG00000030730	Not listed (annotated) in NCBI resources	Not listed (annotated)

4.2.6.2 Comparison of identified downregulated DEGs in purebred *versus* crossbred pigs.

For the downregulated DEGs, the Venn diagram results in **FIGURE 20** identified a total of 154 and 148 unique downregulated DEGs (p<0.0001, and <2FC) specific to PL purebred *versus* PL x Duroc crossbred, respectively (**SUPPLEMENTARY TABLE S2**, and **FIGURE 20**). Furthermore, a total of 5 downregulated DEGs (p<0.0001, and <2FC) were identified, represented in both PL purebred and PL x Duroc crossbred, respectively (**TABLE 36,** and **FIGURE 20**). However, Venn **FIGURE 21** results revealed the identification of 20 and 18 unique downregulated DEGs (p<0.0001, and <2 log2FC) specific to Polish Landrace purebred *versus* Polish Landrace x Duroc crossbred, respectively, whereas not a single downregulated DEGs (p<0.0001, and <2 log2FC) was identified that was shared in both PL purebred and PL x Duroc crossbred, respectively (**TABLE 37,** and **FIGURE 21**).

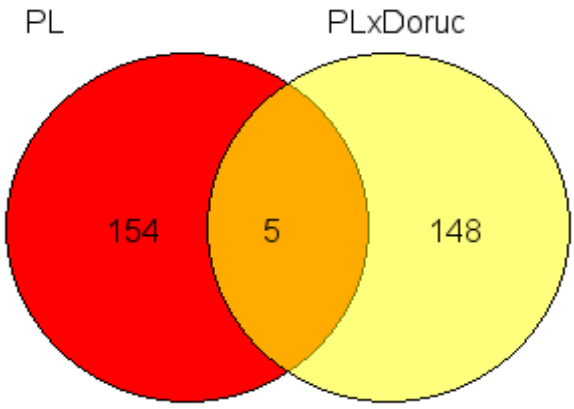

Figure 20. Downregulated DEGs with FC (<2FC) with Bonferroni p <0.0001 by comparing the PL vs PL x Duroc breeds.

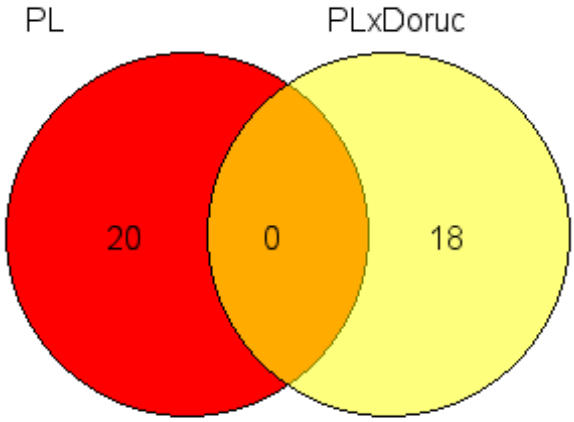

Figure 21. Downregulated DEGs with Log2FC (<2FC) with Bonferroni p <0.0001 by comparing the PL vs PL x Duroc breeds.

Table 36. List of common downregulated DEGs with FC (<2FC) values with Bonferroni p<0.0001 by comparing the PL vs PL-Duroc breeds.

Common DEGs	Gene name	Gene description	Chromosome
ENSSSCG00000004017	FRMD1	FERM domain containing 1 [Source:NCBI gene;Acc:100514201]	1
ENSSSCG00000008397	EFEMP1	EGF containing fibulin extracellular matrix protein 1 [Source:NCBI gene;Acc:100512046]	3
ENSSSCG00000010427	MBL2	mannose binding lectin 2 [Source:NCBI gene;Acc:397230]	14
ENSSSCG00000026819	NID1	nidogen 1 [Source:NCBI gene;Acc:100511351]	14
ENSSSCG00000025831	ENSSSCG00000025831	Not listed (annotated)	Not listed

		in NCBI resources	(annotated)

Table 37. List of unique downregulated DEGs with log2FC (<2FC) values with Bonferroni p<0.0001 by comparing the PL vs PL-Duroc breeds.

Unique PL (20)	Gene name	Gene description	Chromosome
ENSSSCG00000000779	KIF21A	kinesin family member 21A [Source:NCBI gene;Acc:100520674]	5
ENSSSCG00000001004	SLC22A23	solute carrier family 22 member 23 [Source:NCBI gene;Acc:100152838]	7
ENSSSCG00000001045	ELOVL2	ELOVL fatty acid elongase 2 [Source:NCBI gene;Acc:100153368]	7
ENSSSCG00000001844	PLIN1	perilipin 1 [Source:NCBI gene;Acc:654411]	7
ENSSSCG00000002355	ENTPD5	ectonucleoside triphosphate diphosphohydrolase 5 [Source:NCBI gene;Acc:100154506]	7
ENSSSCG00000002425	ENSSSCG00000002425	protein tyrosine phosphatase, non-receptor type 21 [Source:NCBI gene;Acc:100152076]	7
ENSSSCG00000002515	SLC25A47	solute carrier family 25 member 47 [Source:NCBI gene;Acc:100515556]	7
ENSSSCG00000003971	SCMH1	Scm polycomb group protein homolog 1 [Source:NCBI gene;Acc:100525880]	6
ENSSSCG00000006988	PDGFRL	platelet derived growth factor	17

		receptor like [Source:NCBI gene;Acc:100736738]	
ENSSSCG00000008237	RETSAT	retinol saturase [Source:NCBI gene;Acc:100519138]	3
ENSSSCG00000010442	LIPK	lipase family member K [Source:HGNC Symbol;Acc:HGNC:23444]	14
ENSSSCG00000014900	RAB30	RAB30, member RAS oncogene family [Source:NCBI gene;Acc:100626412]	9
ENSSSCG00000017300	ENSSSCG00000017300	mannose receptor C type 2 [Source:NCBI gene;Acc:100516106]	12
ENSSSCG00000002626	ENSSSCG00000002626	Not listed (annotated) in NCBI resources	Not listed (annotated)
ENSSSCG00000011289	ENSSSCG00000011289	Not listed (annotated) in NCBI resources	Not listed (annotated)
ENSSSCG00000014442	ENSSSCG00000014442	Not listed (annotated) in NCBI resources	Not listed (annotated)
ENSSSCG00000016729	ENSSSCG00000016729	Not listed (annotated) in NCBI resources	Not listed (annotated)
ENSSSCG00000022884	ENSSSCG00000022884	Not listed (annotated) in NCBI resources	Not listed (annotated)
ENSSSCG00000025541	ENSSSCG00000025541	Not listed (annotated) in NCBI resources	Not listed (annotated)
ENSSSCG00000028994	ENSSSCG00000028994	Not listed (annotated) in NCBI resources	Not listed (annotated)
Unique PL x Duroc (18)	**Gene name**	**Gene description**	**Chromosome**
ENSSSCG00000000216	ASIC1	acid sensing ion channel subunit 1 [Source:NCBI gene;Acc:100517467]	5
ENSSSCG00000002270	ENSSSCG00000002270	coiled-coil domain-containing	7

		protein 170-like [Source:NCBI gene;Acc:100522152]	
ENSSSCG00000002720	ENSSSCG00000002720	C-type lectin domain family 18 member C [Source:NCBI gene;Acc:100525922]	6
ENSSSCG00000003889	ENSSSCG00000003889	cytochrome P450 4A25-like [Source:NCBI gene;Acc:110261409]	6
ENSSSCG00000003967	ZMYND12	zinc finger MYND-type containing 12 [Source:NCBI gene;Acc:100524028]	6
ENSSSCG00000005474	SAL1	salivary lipocalin [Source:NCBI gene;Acc:396739]	1
ENSSSCG00000006238	CYP7A1	cytochrome P450, family 7, subfamily A, polypeptide 1 [Source:NCBI gene;Acc:448985]	4
ENSSSCG00000007500	ENSSSCG00000007500		17
ENSSSCG00000009789	HCAR1	hydroxycarboxylic acid receptor 1 [Source:NCBI gene;Acc:100153287]	14
ENSSSCG00000010427	MBL2	mannose binding lectin 2 [Source:NCBI gene;Acc:397230]	14
ENSSSCG00000014314	ENSSSCG00000014314	F-box and leucine rich repeat protein 21, pseudogene [Source:NCBI gene;Acc:100517085]	2
ENSSSCG00000024537	CYP2C42	cytochrome P450 C42 [Source:NCBI gene;Acc:403111]	14
ENSSSCG00000030271	GSTO2	glutathione S-transferase omega-2 [Source:NCBI gene;Acc:100152209]	14
ENSSSCG00000008620	ENSSSCG00000008620	Not listed (annotated) in NCBI resources	Not listed (annotated)

ENSSSCG00000009724	ENSSSCG00000009724	Not listed (annotated) in NCBI resources	Not listed (annotated)
ENSSSCG00000022796	ENSSSCG00000022796	Not listed (annotated) in NCBI resources	Not listed (annotated)
ENSSSCG00000026923	ENSSSCG00000026923	Not listed (annotated) in NCBI resources	Not listed (annotated)
ENSSSCG00000030298	ENSSSCG00000030298	Not listed (annotated) in NCBI resources	Not listed (annotated)

4.2.6.3. Comparison of identified upregulated DEGs in experimental feeding with control *versus* PUFAs diets.

The Venn diagram results in **FIGURE 22** the revealed identification of 274 and 384 unique upregulated DEGs (p<0.0001, and <9FC) specific to experimental feeding with standard (control) diet, and with the diet enriched with PUFAs, respectively. Furthermore, a total of 384 upregulated DEGs (p<0.0001, and <9FC) were identified in both experimental feedings with standard (control) diet and with the diet enriched with PUFAs, respectively (**SUPPLEMENTARY TABLE S3**, and **FIGURE 22**). However, Venn **FIGURE 23** results revealed the identification of 21 and 100 unique upregulated DEGs (p<0.0001, and <9 log2FC) specific to experimental feeding with standard (control) diet and with the diet enriched with PUFAs, respectively. This dissertation study identified 22 commonly upregulated DEGs (p<0.0001, and <9 log2FC) that were shared in both experimental feeding with standard (control) diet and with the diet enriched with PUFAs, respectively (**TABLE 38,** and **FIGURE 24**).

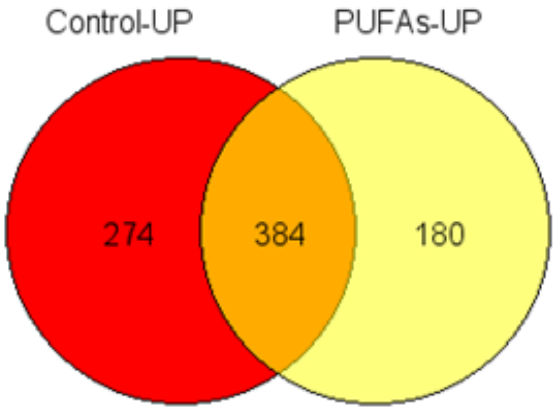

Figure 22. Upregulated DEGs with FC (<9FC) values with Bonferroni p <0.0001 by comparing the standard (control) and PUFAs diets.

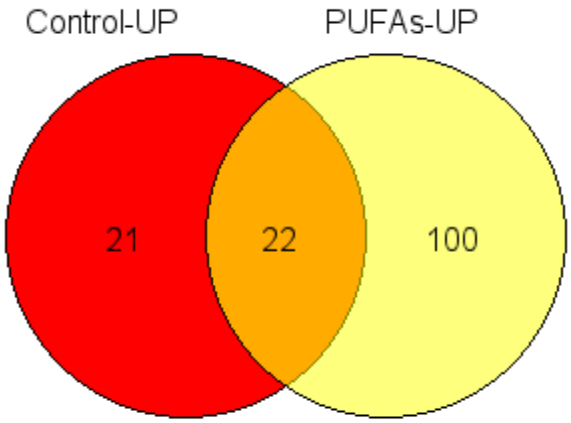

Figure 23. Upregulated DEGs with Log2FC (<9FC) values with Bonferroni p <0.0001 by comparing the standard (control) and PUFAs diets.

Supplementary Table S3

Table 38. List of common upregulated DEGs with log2FC (<9FC) values with Bonferroni p <0.0001 by comparing the control vs PUFAS diets.

Common DEGs (22)	Gene name	Gene description	Chromosome
ENSSSCG00000000749	SLC6A12	solute carrier family 6 member 12 [Source:NCBI gene;Acc:100512716]	5
ENSSSCG00000000856	PAH	phenylalanine hydroxylase [Source:NCBI gene;Acc:100521900]	5
ENSSSCG00000002476	SERPINA1	serpin family A member 1 [Source:NCBI gene;Acc:397688]	7
ENSSSCG00000004001	A1BG	alpha-1-B glycoprotein [Source:NCBI gene;Acc:100516980]	6
ENSSSCG00000005485	AMBP	alpha-1-microglobulin/bikunin precursor [Source:NCBI gene;Acc:397593]	1
ENSSSCG00000007671	TFR2	transferrin receptor 2 [Source:NCBI gene;Acc:100517580]	3
ENSSSCG00000008948	ALB	albumin [Source:NCBI gene;Acc:396960]	8
ENSSSCG00000009805	HPD	4-hydroxyphenylpyruvate dioxygenase [Source:NCBI gene;Acc:397443]	14
ENSSSCG00000009942	DAO	D-amino acid oxidase [Source:NCBI gene;Acc:397134]	14
ENSSSCG00000010008	SEC14L3	SEC14-like protein 3 [Source:NCBI gene;Acc:100156470]	14
ENSSSCG00000011450	ITIH1	inter-alpha-trypsin inhibitor heavy chain 1 [Source:NCBI gene;Acc:396963]	13
ENSSSCG00000011799	AHSG	alpha 2-HS glycoprotein [Source:NCBI gene;Acc:397585]	13

ENSSSCG00000011801	HRG	histidine rich glycoprotein [Source:NCBI gene;Acc:100152095]	13
ENSSSCG00000023686	TTR	transthyretin [Source:NCBI gene;Acc:397419]	6
ENSSSCG00000023693	PROC	protein C, inactivator of coagulation factors Va and VIIIa [Source:NCBI gene;Acc:396954]	15
ENSSSCG00000027926	FTCD	formimidoyltransferase cyclodeaminase [Source:NCBI gene;Acc:397517]	AEMK02000328.1
ENSSSCG00000028901	ENSSSCG00000028901	Not listed (annotated) in NCBI resources	8
ENSSSCG00000005395	ENSSSCG00000005395	Not listed (annotated) in NCBI resources	Not listed (annotated)
ENSSSCG00000017704	ENSSSCG00000017704	Not listed (annotated) in NCBI resources	Not listed (annotated)
ENSSSCG00000022156	ENSSSCG00000022156	Not listed (annotated) in NCBI resources	Not listed (annotated)
ENSSSCG00000024079	ENSSSCG00000024079	Not listed (annotated) in NCBI resources	Not listed (annotated)
ENSSSCG00000024682	ENSSSCG00000024682	Not listed (annotated) in NCBI resources	Not listed (annotated)

4.2.6.4. Comparison of identified downregulated DEGs in experimental feeding with standard *versus* PUFAs diets.

Similarly, for the downregulated DEGs, the Venn diagram results in **FIGURE 24.** identified a total of 165 and 114 unique downregulated DEGs (p<0.0001, and <4FC) specific to experimental feeding with standard (control) diet and with supplementary healthy diet enriched with PUFAs, respectively. Furthermore, a total of 463 downregulated DEGs (p<0.0001, and <4FC) were identified, represented in both experimental feeding with standard (control) diet and with supplementary healthy diet enriched with PUFAs, respectively (**SUPPLEMENTARY TABLE S4**, and **FIGURE 24**). However, Venn **FIGURE 25** shows results revealed identification of 21 and 40 unique downregulated DEGs (p<0.0001, and <9 log2FC) specific to experimental feeding with standard (control) diet and with supplementary healthy diet enriched with PUFAs, respectively. This dissertation study identified 21 common downregulated DEGs (p<0.0001, and <9 log2FC) that were shared in both experimental feeding with standard (control) diet and with supplementary healthy diet enriched with PUFAs, respectively (**TABLE 39**, and **FIGURE 25**).

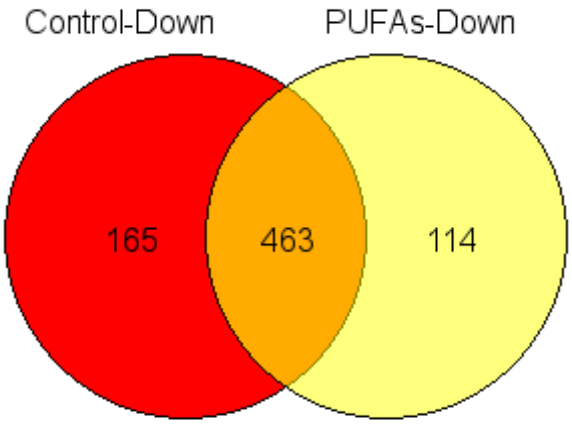

Figure 24. Downregulated DEGs with FC (<4FC) values with Bonferroni p <0.0001 by comparing the standard (control) and PUFAs diets.

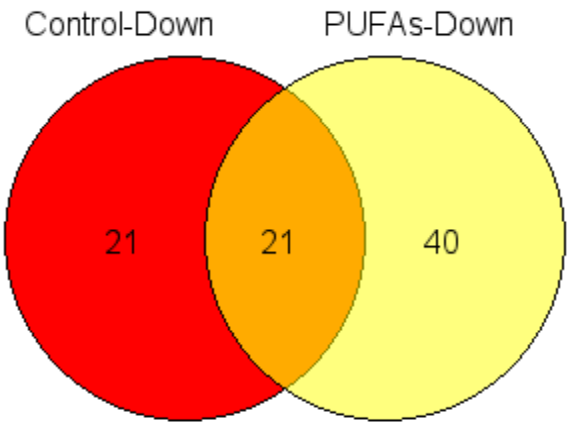

Figure 25. Downregulated DEGs with Log2FC (<9FC) values with Bonferroni p <0.0001 by comparing the standard (control) and PUFAs diets.

Supplementary Table S4:

Table 39. List of common downregulated DEGs with log2FC (<4FC) values with Bonferroni p <0.0001 by comparing the control vs PUFAs diets.

Common DEGs (21)	Gene name	Gene description	Chromosome
ENSSSCG00000000866	MYBPC1	myosin binding protein C, slow type [Source:NCBI gene;Acc:100523187]	5
ENSSSCG00000006725	TBX15	T-box 15 [Source:NCBI gene;Acc:100158194]	4
ENSSSCG00000007231	MYLK2	myosin light chain kinase 2 [Source:NCBI gene;Acc:100524288]	17
ENSSSCG00000007424	TNNC2	troponin C2, fast skeletal type [Source:NCBI gene;Acc:414905]	17
ENSSSCG00000007757	TRIM72	tripartite motif containing 72 [Source:NCBI gene;Acc:100511188]	3
ENSSSCG00000008200	ANKRD23	ankyrin repeat domain 23 [Source:NCBI gene;Acc:100525457]	3
ENSSSCG00000010304	MYOZ1	myozenin 1 [Source:NCBI gene;Acc:574060]	14
ENSSSCG00000010317	DUPD1	dual specificity phosphatase and pro isomerase domain containing 1 [Source:NCBI gene;Acc:100155430]	14
ENSSSCG00000011238	ARPP21	cAMP regulated phosphoprotein 21 [Source:NCBI gene;Acc:100512986]	13
ENSSSCG00000011325	MYL3	myosin light chain 3 [Source:NCBI gene;Acc:100515755]	13
ENSSSCG00000013354	CSRP3	cysteine and glycine rich protein 3 [Source:NCBI gene;Acc:100337687]	2
ENSSSCG00000014324	MYOT	myotilin [Source:NCBI gene;Acc:100101550]	2
ENSSSCG00000014560	COX8H	COX8H protein [Source:NCBI gene;Acc:100038031]	2
ENSSSCG00000001758	SGCA	sarcoglycan alpha [Source:NCBI	12

3		gene;Acc:100240723]	
ENSSSCG00000027684	TRIM63	tripartite motif containing 63 [Source:NCBI gene;Acc:100431101]	6
ENSSSCG00000010359	ENSSSCG00000010359	Not listed (annotated) in NCBI resources	14
ENSSSCG00000020953	ENSSSCG00000020953	Not listed (annotated) in NCBI resources	4
ENSSSCG00000009830	ENSSSCG00000009830	Not listed (annotated) in NCBI resources	Not listed (annotated)
ENSSSCG00000014795	ENSSSCG00000014795	Not listed (annotated) in NCBI resources	Not listed (annotated)
ENSSSCG00000015481	ENSSSCG00000015481	Not listed (annotated) in NCBI resources	Not listed (annotated)
ENSSSCG00000022342	ENSSSCG00000022342	Not listed (annotated) in NCBI resources	Not listed (annotated)

4.3. Visualization of identified upregulated and downregulated DEGs in investigated purebred and crossbred pigs

4.3.1. Visualization of identified upregulated and downregulated DEGs in Volcano plot and in Heatmap

4.3.1.1. Visualization of DEGs by comparing between diets (within breeds)

By comparing the standard (control) diet *versus* supplementary healthy diet enriched with omega-6 and omega-3 fatty acids (PUFAs) in the liver transcriptome, the upregulated and downregulated DEGs were visualized and presented as Volcano plots **FIGURE 26.** (PL purebred pigs), and **FIGURE 27.** (PL x Duroc crossbred pigs). Similarly**,** by comparing the standard (control) diet *versus* supplementary healthy diet enriched with omega-6 and omega-3 fatty acids (PUFAs) in the liver transcriptome, the upregulated and downregulated DEGs were visualized and presented as Heatmap plots **FIGURE 28** (PL purebred pigs), and **FIGURE 29** (PL x Duroc crossbred pigs).

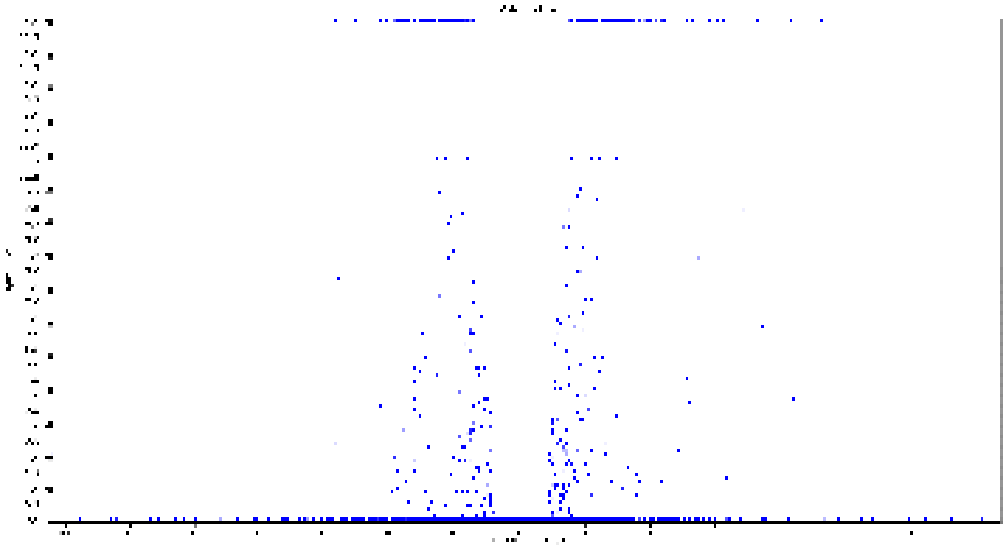

Figure 26. Volcano plot showing the upregulated and downregulated DEGs by comparing the standard (control) diet *versus* supplementary healthy diet enriched with omega-6 and omega-3 fatty acids (PUFAs) in the liver transcriptome PL purebred pigs.

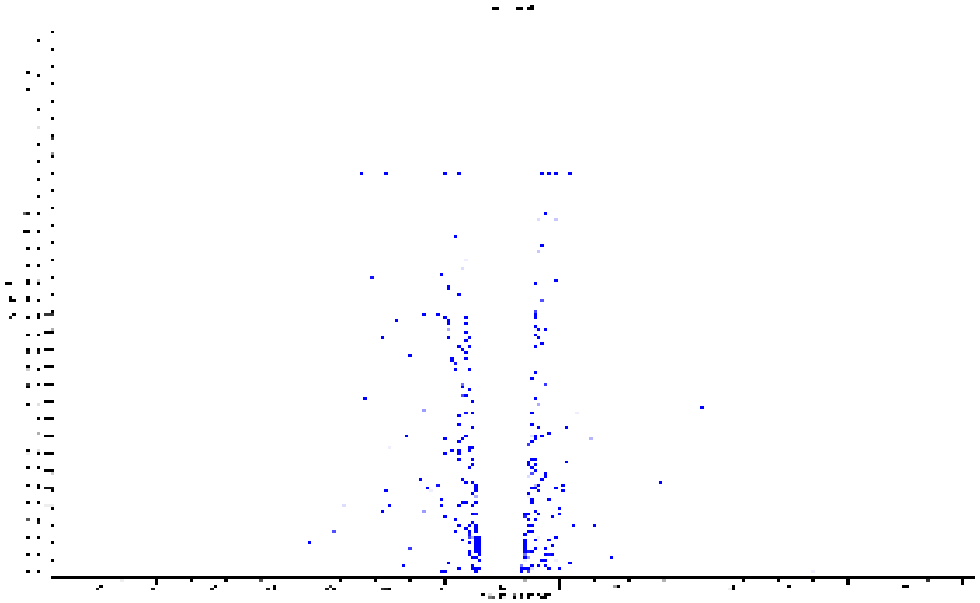

Figure 27. Volcano plot showing the upregulated and downregulated DEGs by comparing the standard (control) diet *versus* supplementary healthy diet enriched with omega-6 and omega-3 fatty acids (PUFAs) in the liver transcriptome of Polish Landrace x Duroc crossbred pigs.

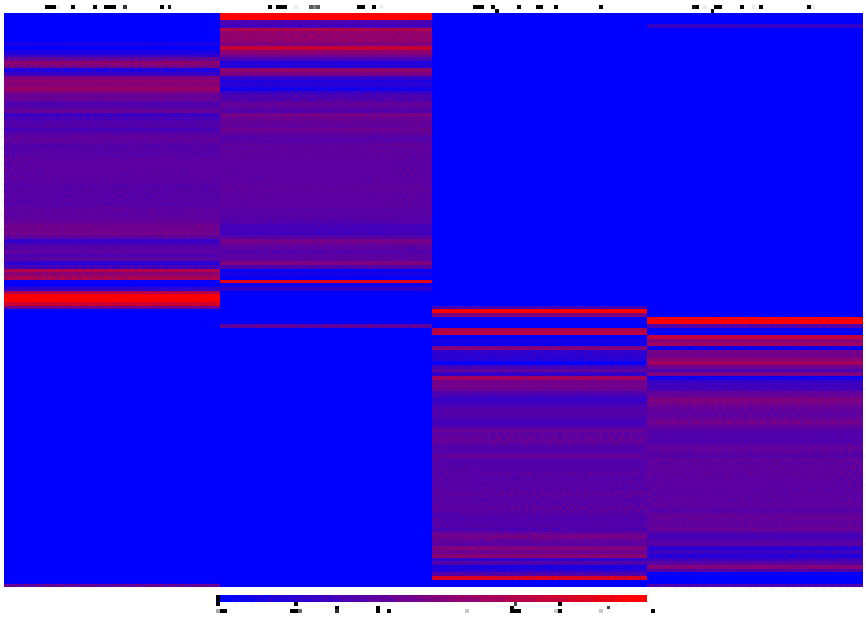

Figure 28. Heatmap showing the upregulated and downregulated DEGs by comparing the standard (control) diet *versus* supplementary healthy diet enriched with omega-6 and omega-3 fatty acids (PUFAs) in the liver transcriptome Polish Landrace purebred pigs. Heatmap shows two technical replicates for each purebred and crossbred.

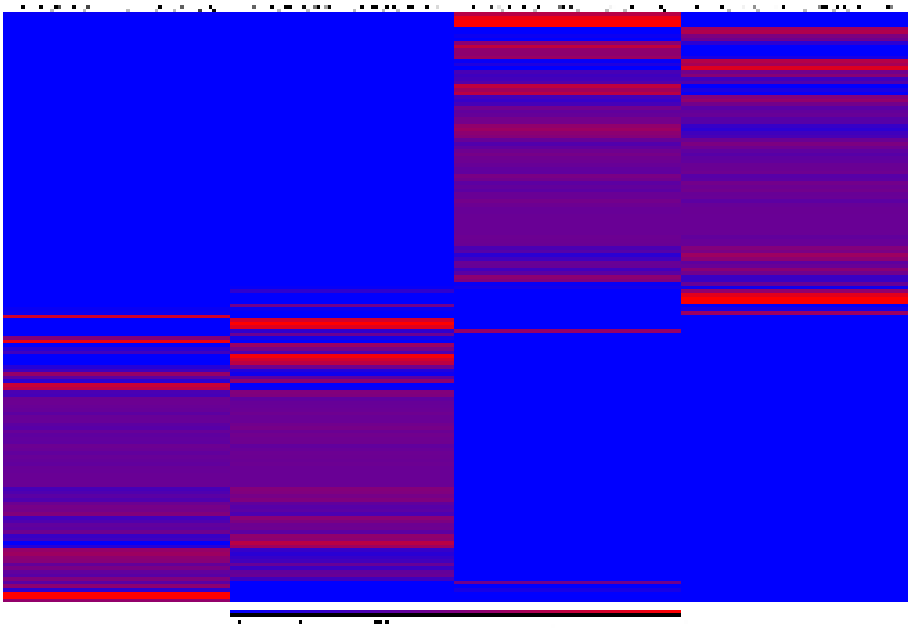

Figure 29. Heatmap showing the upregulated and downregulated DEGs by comparing the standard (control) diet *versus* supplementary healthy diet enriched with omega-6 and omega-3 fatty acids (PUFAs) in the liver transcriptome of Polish Landrace x Duroc crossbred pigs. The heatmap shows two technical replicates for each purebred and crossbred.

4.3.1.2. Visualization of DEGs by comparing between breeds (within diets)

By comparing the PL purebred *versus* PL x Duroc crossbred pigs liver transcriptomes after experimental feeding with standard (control) diet, the upregulated and downregulated DEGs were visualized and presented as Volcano plots **FIGURE 30** (control standard diet), and **FIGURE 31** (healthy PUFAs diet). Similarly, by comparing the PL purebred *versus* PL x Duroc crossbred pigs liver transcriptome after experimental feeding with standard (control) diet, the upregulated and downregulated DEGs were visualized and presented as Heatmap plots **FIGURE 33** (control standard diet), and **FIGURE 34** (healthy PUFAs diet).

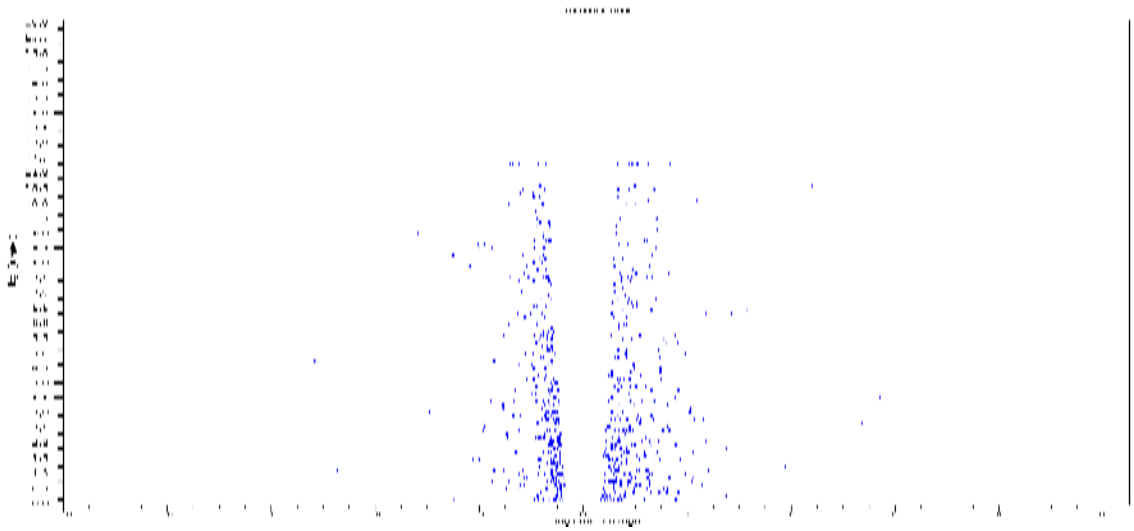

Figure 30. Volcano plot showing the upregulated and downregulated DEGs by comparing the Polish Landrace purebred *versus* Polish Landrace x Duroc crossbred pigs liver transcriptome after experimental feeding with standard (control) diet

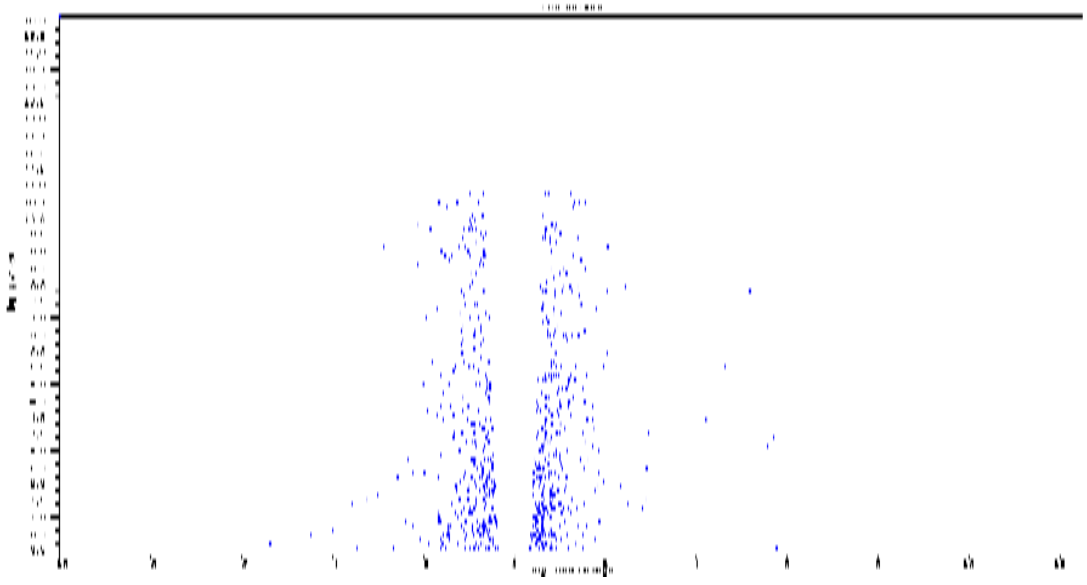

Figure 31. Volcano plot showing the upregulated and downregulated DEGs by comparing the Polish Landrace purebred *versus* Polish Landrace x Duroc crossbred pigs liver transcriptome after experimental feeding with the diet enriched with omega-6 and omega-3 fatty acids (PUFAs)

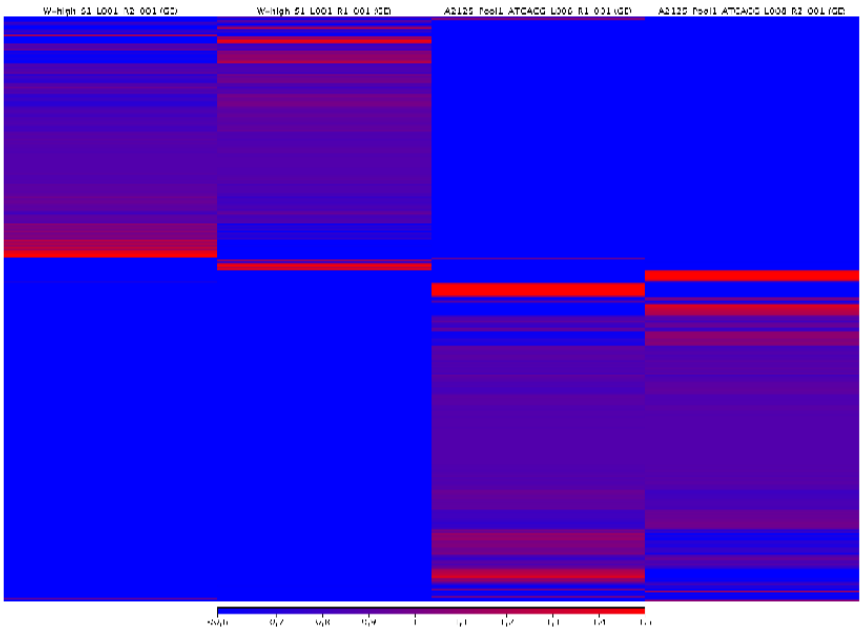

Figure 32. Heatmap showing the upregulated and downregulated DEGs by comparing the Polish Landrace purebred *versus* Polish Landrace x Duroc crossbred pigs liver transcriptome after experimental feeding with standard (control) diet. Heatmap shows two technical replicates for each purebred and crossbred.

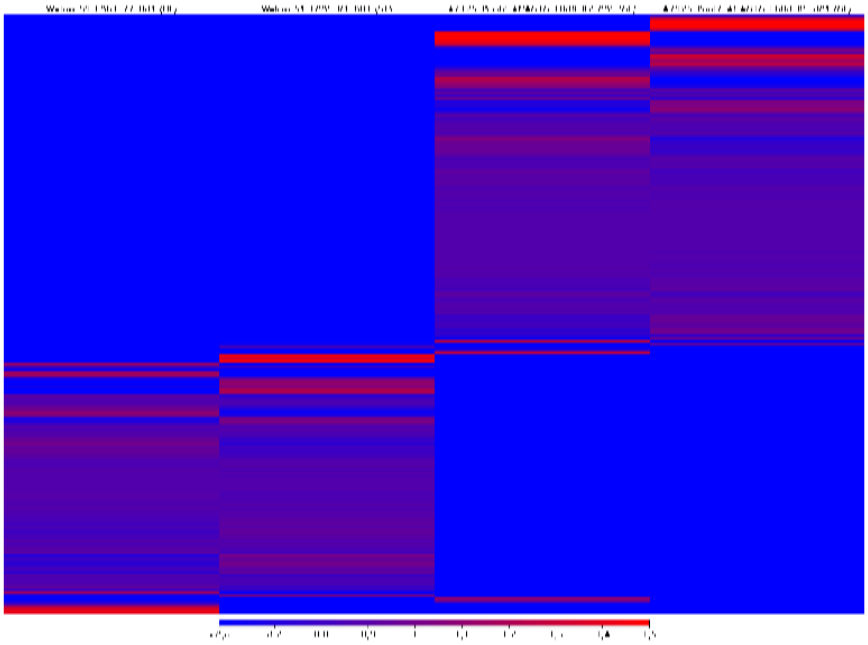

Figure 33. Heatmap showing the upregulated and downregulated DEGs by comparing the Polish Landrace purebred *versus* Polish Landrace x Duroc crossbred pigs liver transcriptome after experimental feeding with the diet enriched with omega-6 and omega-3 fatty acids (PUFAs). The heatmap shows two technical replicates for each purebred and crossbred.

4.4. Biological gene networks and pathways analysis of DEGs using Cytoscape ClueGO

The biological functions of up- and down-regulated genes were evaluated using the ClueGO application of Cytoscape and presented in **SUPPLEMENTARY TABLES S1-S4**.

4.4.1. Identification of biological gene networks and pathways analysis by comparing the standard (control) diet *versus* supplementary healthy diet enriched with omega-6 and omega-3 fatty acids (PUFAs) in liver transcriptome Polish Landrace purebred pigs (First comparison).

Identification of GO/pathway terms: For upregulated hepatic genes ClueGO identified a total of six functional groups with 12 specific terms: namely: Trans-sulfuration pathway, prespliceosome, Urea cycle and metabolism of amino groups, Urea cycle, Phenylalanine and tyrosine catabolism, phenylalanine catabolic process, Tryptophan catabolism, tryptophan catabolic process, Methylation Pathways, Methylation, Aromatic amines can be N-hydroxylated or N-dealkylated by CYP1A2, and Metabolism of ingested SeMet, Sec, MeSec into H2Se (**SUPPLEMENTARY TABLE S1** and **FIGURE 34**). Furthermore, a total of six GO/pathway terms namely: Trans-sulfuration pathway, prespliceosome, Urea cycle and metabolism of amino groups, Phenylalanine and tyrosine catabolism, Tryptophan catabolism, and Methylation, (**SUPPLEMENTARY TABLE S1** and **FIGURE 35**) were identified.

Similarly, for downregulated hepatic genes, ClueGO identified a total of four functional groups with 7 specific term namely: Linoleic acid (LA) metabolism, Chylomicron-mediated lipid transport, ATF6 (ATF6-alpha) activates chaperones, Scavenging by Class A Receptors, GP1b-IX-V activation signaling, regulation of triglyceride catabolic process, and positive regulation of lipoprotein lipase activity (**SUPPLEMENTARY TABLE S1** and **FIGURE 36**). Furthermore, a total of four GO/pathway terms: namely: Linoleic acid (LA) metabolism, Chylomicron-mediated lipid transport, Scavenging by Class A Receptors, and regulation of triglyceride catabolic process (**SUPPLEMENTARY TABLE S1** and **FIGURE 37**) were identified.

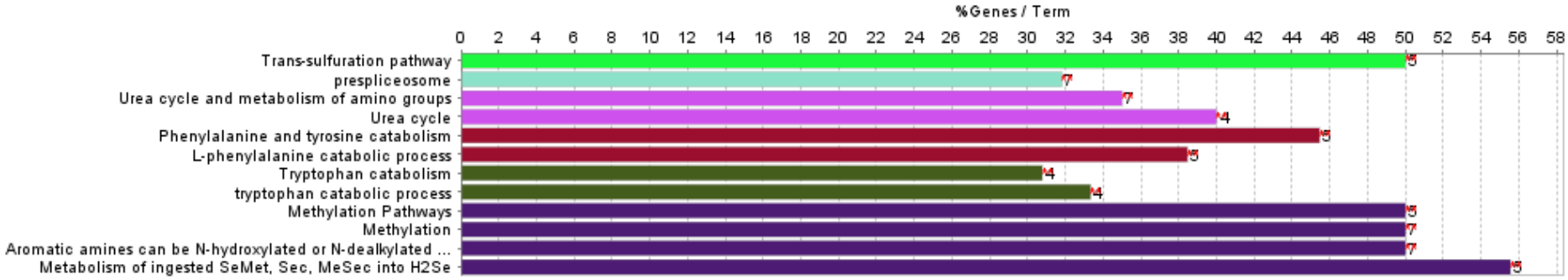

Figure 34. ClueGO analysis of hepatic expression upregulated DEGs in the First comparison: The Figure shows the GO/pathway terms specific for upregulated genes. The bars represent the number of genes associated with the terms. The percentage of genes per term is shown as the bar label.

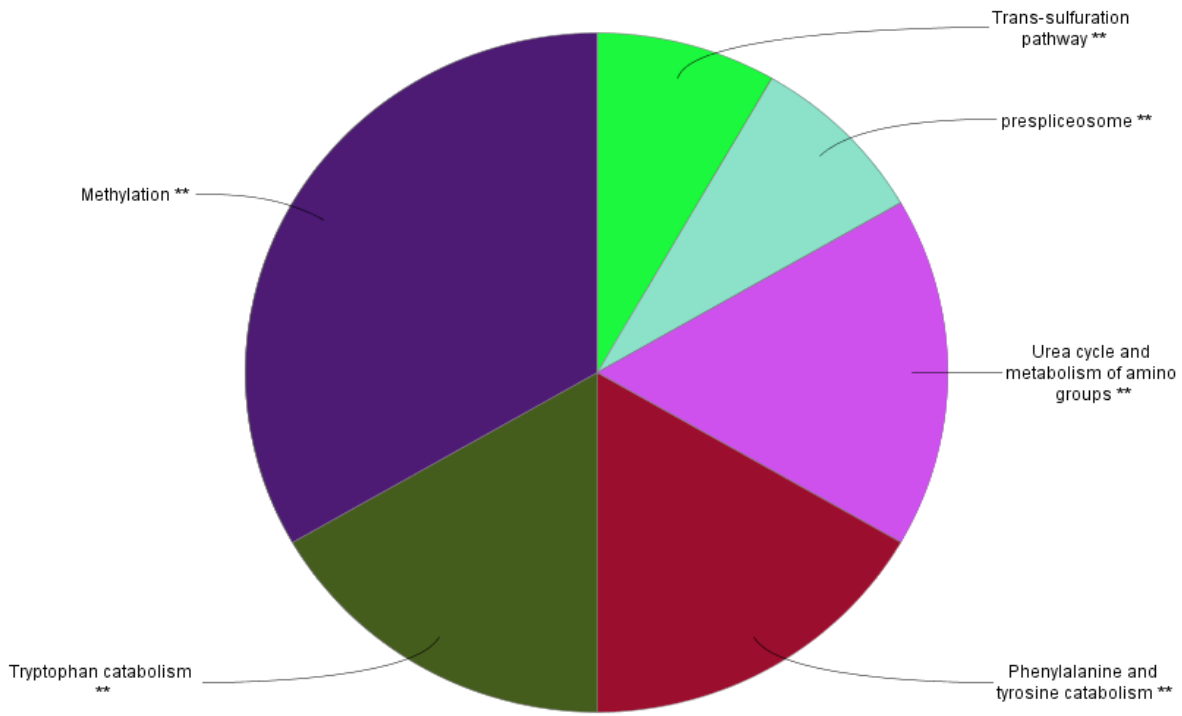

Figure 35. ClueGO analysis of hepatic expression upregulated DEGs in the First comparison: The Figure shows an overview chart with functional groups including specific terms for upregulated genes.

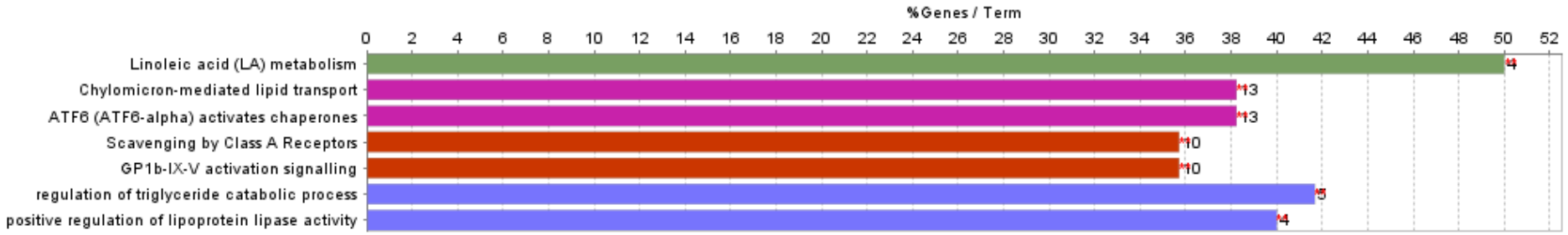

Figure 36. ClueGO analysis of hepatic expression downregulated DEGs in the First comparison: The Figure shows the GO/pathway terms specific for downregulated genes. The bars represent the number of genes associated with the terms. The percentage of genes per term is shown as bar label.

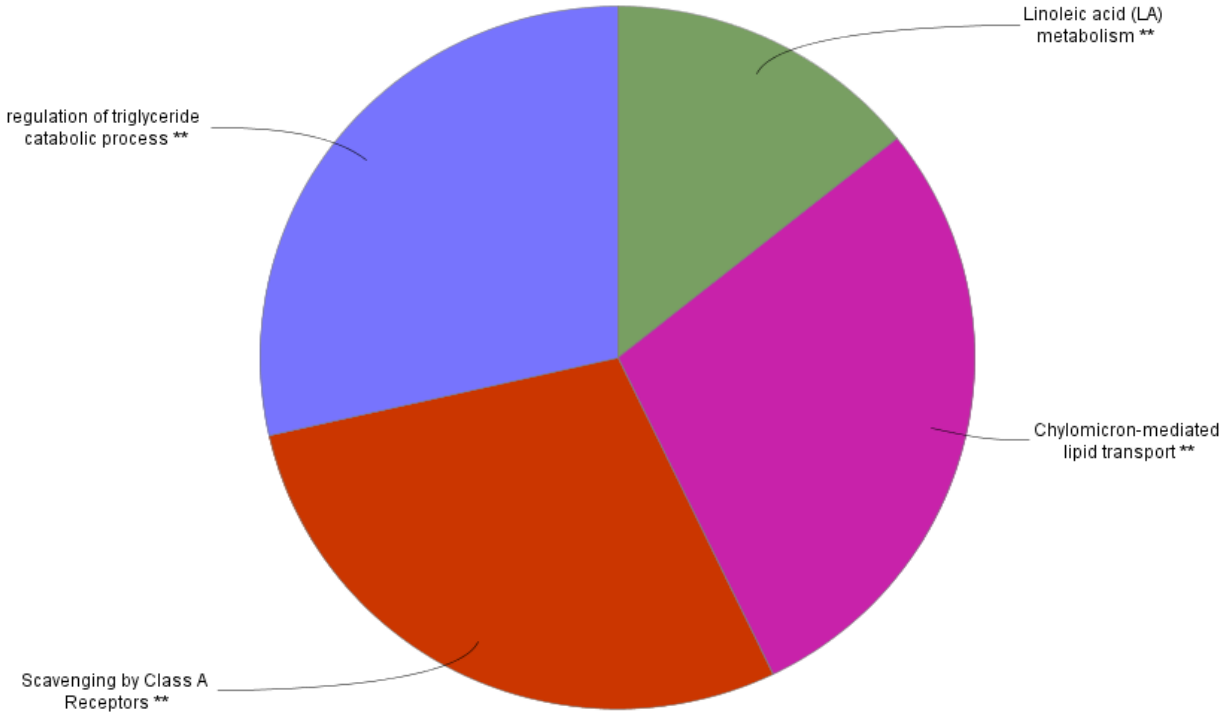

Figure 37. ClueGO analysis of hepatic expression downregulated DEGs in the First comparison: The Figure shows an overview chart with functional groups including specific terms for upregulated genes.

Identification of functional annotation of hepatic DEGs clusters: Functional annotations (GO, KEGG, BioCarta) of hepatic up and downregulated genes were performed and visualized with ClueGO (kappa score ≥0.3). For the hepatic upreguled DEGs, six upregulated gene networks namely: Methylation; Trans-sulfuration pathway, and Urea cycle and metabolism of amino groups, Phenylalanine and tyrosine catabolism and Tryptophan catabolism, and prespliceosome were identified. For the hepatic downregulated DEGs, four downregulation networks namely: Chylomicron-mediated lipid transport, Scavenging by Class A Receptors, regulation of triglyceride catabolic process; Linoleic acid (LA) metabolism were identified. One network pathway namely: Alanine aspartate metabolism with the equal proportion of two DEGs clusters was identified (**FIGURE 38).**

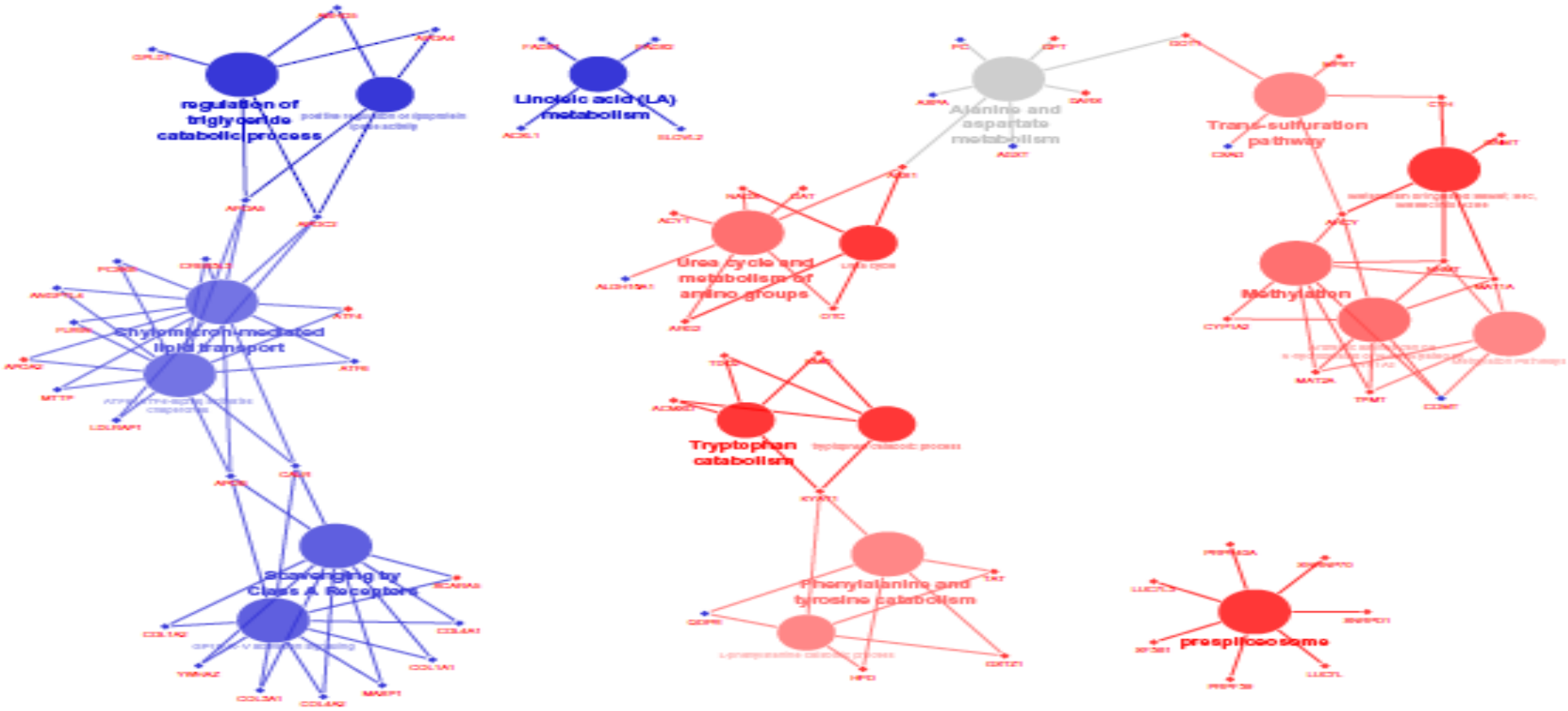

Figure 38. The distribution of two clusters (upregulated and downregulated DEGs) visualized on the network (First comparison). The Figure shows the functionally grouped network with terms as nodes (hubs) linked based on their kappa score level (≥0.3), where only the label of the most significant term per group is shown. The node size represents the term enrichment significance. Not grouped terms (equal proportions of the two clusters) are shown in gray color. Node color represents the functional groups; node size reflects the p-value, with the smaller the node size indicating less significant p-values, while the larger node size represents more significant p-values. The red hubs represent the upregulated DEGs; the blue hubs represent the downregulated DEGs; the lines represent the interactions between the genes.

4.4.2. Identification of biological gene networks and pathways analysis by comparing the standard (control) diet *versus* supplementary healthy diet enriched with omega-6 and omega-3 fatty acids (PUFAs) in the liver transcriptome of Polish Landrace x Duroc crossbred pigs

Identification of GO/pathway terms: For upregulated hepatic genes ClueGO identified a total of four functional groups with 7 specific terms namely: Very-low-density lipoprotein particle remodeling, Protein export, Scavenging of heme from plasma, Binding and Uptake of Ligands by Scavenger receptors, Scavenging by Class F Receptors, Scavenging by Class H Receptors and Platelet sensitization by LDL (**SUPPLEMENTARY TABLE S2 and FIGURE 39**). Furthermore, a total of four GO/pathway terms: namely: very-low-density lipoprotein particle remodeling, Protein export, Scavenging of heme from plasma, and Scavenging by Class F Receptors, (**SUPPLEMENTARY TABLE S2** and **FIGURE 40**) were identified.

Similarly, for downregulated hepatic genes, genes ClueGO identified a total of three functional groups with 3 specific terms namely: Glomerular visceral epithelial cell development, Cholesterol Biosynthesis and Estrogen Receptor Pathway (**SUPPLEMENTARY TABLE S2** and **FIGURE 41**). Furthermore, a total of three GO/pathway terms namely: Glomerular visceral epithelial cell development, Cholesterol Biosynthesis and Estrogen Receptor Pathway (**SUPPLEMENTARY TABLE S2** and **FIGURE 42**) were identified.

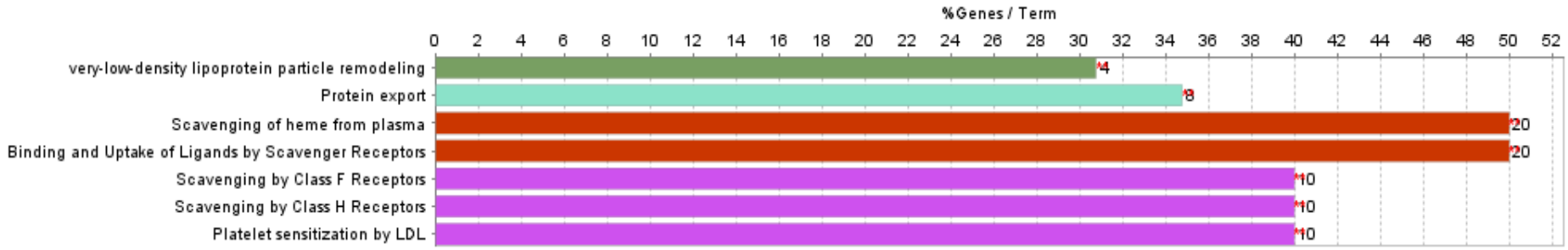

Figure 39. ClueGO analysis of hepatic expression upregulated DEGs in the Second comparison: The Figure shows the GO/pathway terms specific for upregulated genes. The bars represent the number of genes associated with the terms. The percentage of genes per term is shown as a bar label.

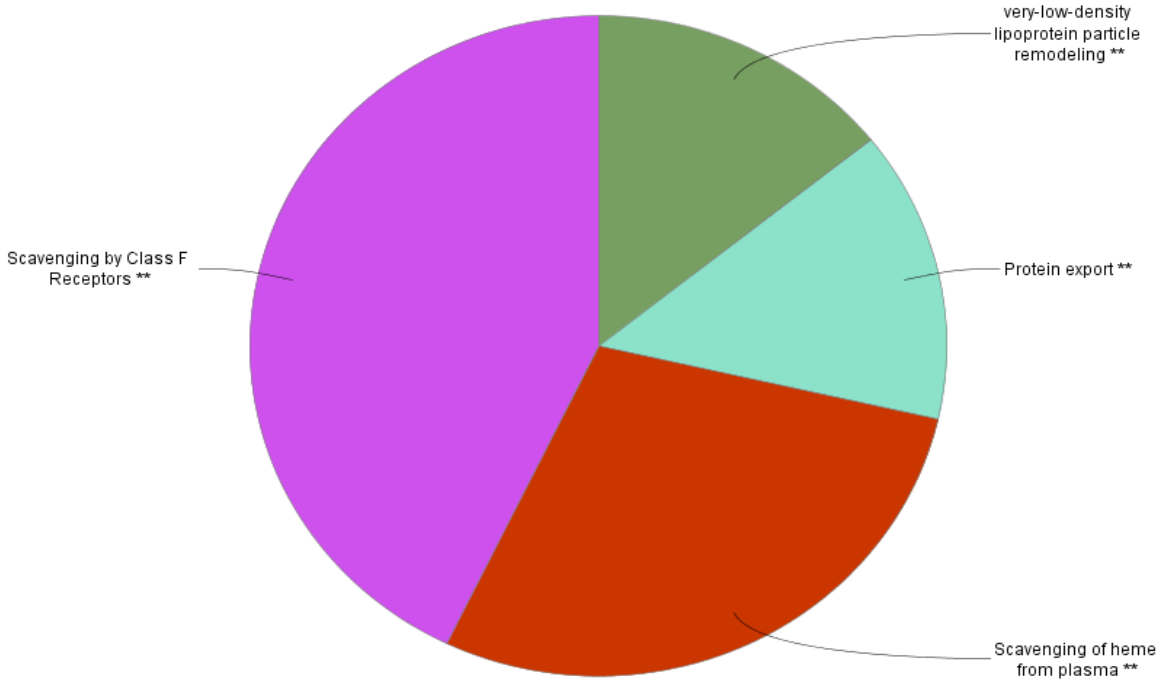

Figure 40. ClueGO analysis of hepatic expression upregulated DEGs in the Second comparison: The Figure shows an overview chart with functional groups including specific terms for upregulated genes.

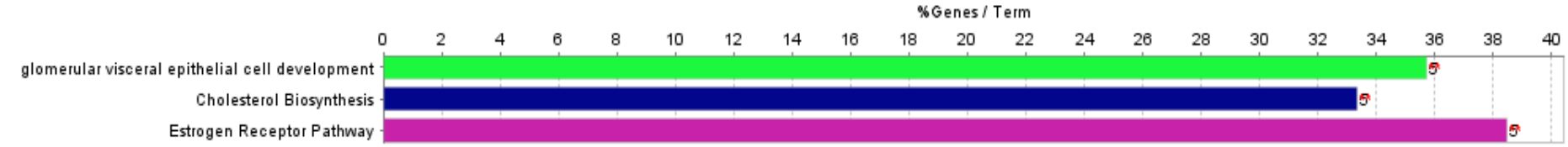

Figure 41. ClueGO analysis of hepatic expression of downregulated DEGs in the Second comparison: The Figure shows the GO/pathway terms specific for downregulated genes. The bars represent the number of genes associated with the terms. The percentage of genes per term is shown as a bar label.

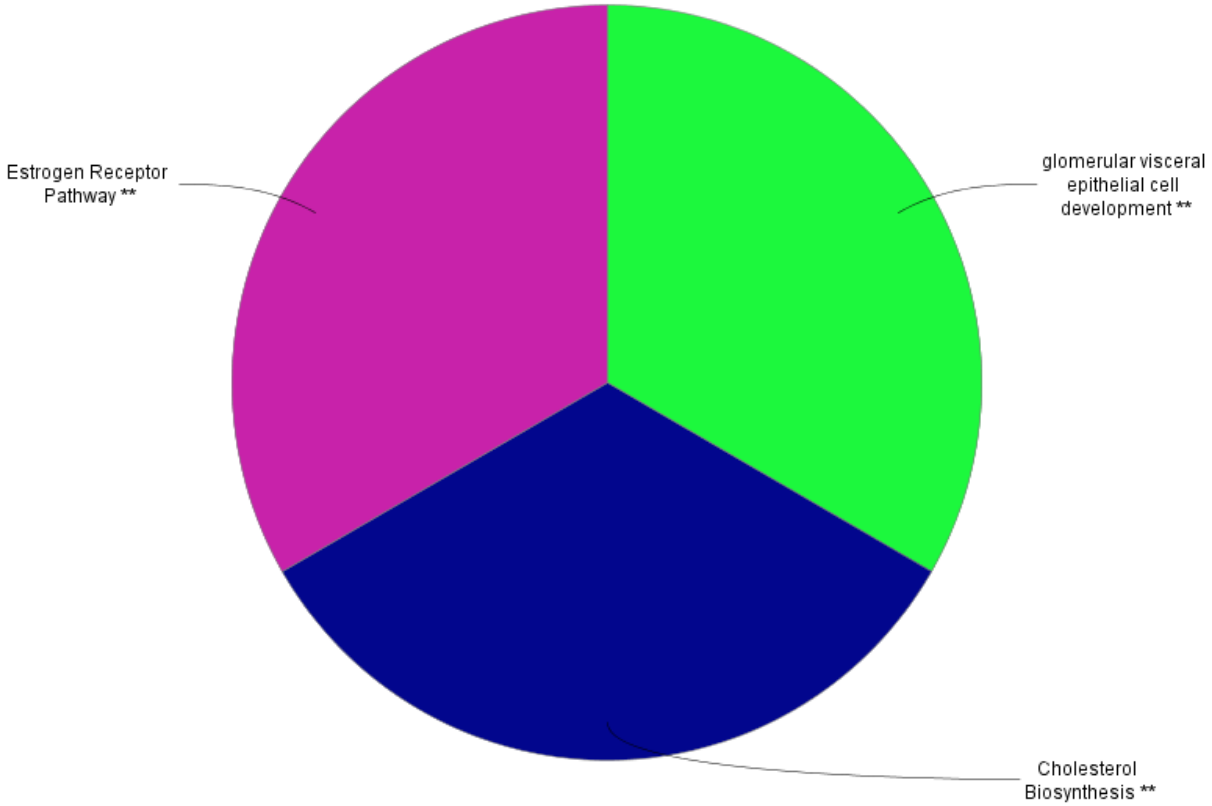

Figure 42. ClueGO analysis of hepatic expression downregulated DEGs in the Second comparison: The Figure shows an overview chart with functional groups, including specific terms for upregulated genes.

Identification of functional annotation of hepatic DEGs clusters: Functional annotation (GO, KEGG, BioCarta) of hepatic up and down-regulated genes were performed and visualized with ClueGO (kappa score: ≥0.3). For the hepatic upregulation, three upregulated gene networks namely: Very-low-density lipoprotein particle remodeling, Protein export, and Scavenging by Class F receptors, were identified. For the hepatic downregulation, three downregulation networks, namely: Glomerular visceral epithelial cell development, Cholesterol Biosynthesis and Estrogen Receptor pathway were identified. One network namely: Scavenging of heme from plasma with an equal proportion of two DEGs clusters was also identified (**FIGURE 43.**).

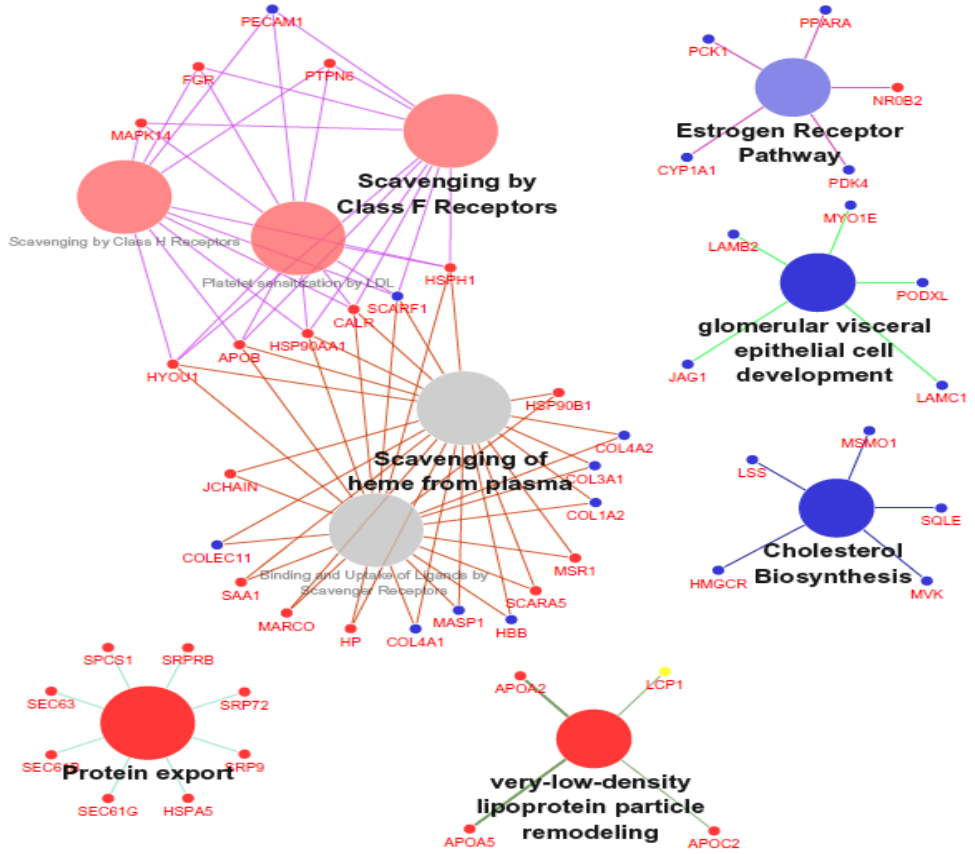

Figure 43. The distribution of two clusters (upregulated and downregulated DEGs) visualized on the network (Second comparison]). The Figure shows the functionally grouped network with terms as nodes (hubs) linked based on their kappa score level (≥0.3), where only the label of the most significant term per group is shown. The node size represents the term enrichment significance. Not grouped terms (equal proportions of the two clusters) are shown in gray color. Node color represents the functional groups; node size reflects the p-value, with the smaller the node size indicating the less significant p-values, while the larger node size represents the more significant p-values. The red hubs represent the up-regulated DEGs; the blue hubs represent the down-regulated DEGs; the lines represent the interactions between the genes.

4.4.3. Identification of biological gene networks and pathways analysis by comparing the Polish Landrace purebred *versus* Polish Landrace x Duroc crossbred pigs liver transcriptome after experimental feeding with standard (control) diet

Identification of GO/pathway terms: For upregulated hepatic genes ClueGO identified a total of 9 functional groups with 17 specific terms namely: Steroid biosynthesis, Protein export Cholesterol Biosynthesis, Complement Activation, Methylation, Aromatic amines can be N-hydroxylated or N-dealkylated by CYP1A2, Chylomicron-mediated lipid transport, ATF6 (ATF6-alpha) activates chaperones, Beta-oxidation of pristanoyl-CoA, Peroxisomal lipid metabolism, Activation of C3 and C5, Regulation of Complement cascade, Sulfide oxidation to sulfate, Degradation of cysteine and homocysteine, Sulfur amino acid metabolism, Cholesterol biosynthesis via desmosterol, and Cholesterol biosynthesis via lathosterol (**SUPPLEMENTARY TABLE S3** and **FIGURE 44**) were identified. Furthermore, a total of nine GO/pathway terms namely: Steroid biosynthesis, Valine, leucine and isoleucine degradation, Protein export, Cholesterol Biosynthesis, Complement Activation, Methylation, Chylomicron-mediated lipid transport, ATF6 (ATF6-alpha) activates chaperones, Beta-oxidation of pristanoyl-CoA, Activation of C3 and C5, Sulfide oxidation to sulfate, and Cholesterol biosynthesis (**SUPPLEMENTARY TABLE S3** and **FIGURE 45**) were identified.

Similarly, for downregulated hepatic genes, ClueGO identified a total of four functional groups with 6 specific terms namely: Acetyl-CoA biosynthetic process, Acetyl-CoA biosynthetic process from pyruvate, TCA Cycle, Citric acid cycle (TCA cycle), Tricarboxylic acid cycle, and Citrate metabolic process (**SUPPLEMENTARY TABLE S3** and **FIGURE 46).** Furthermore, a total of four GO/pathway terms namely: Acetyl-CoA biosynthetic process, Acetyl-CoA biosynthetic process from pyruvate, Citric acid cycle (TCA cycle), and Citrate metabolic process (**SUPPLEMENTARY TABLE S3** and **FIGURE 47**) were identified.

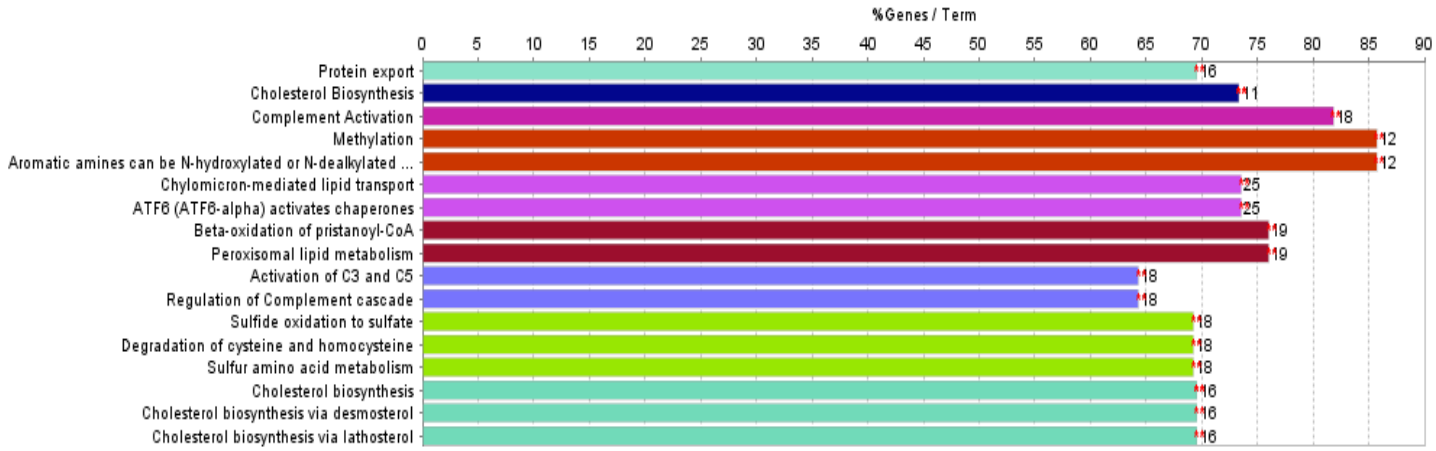

Figure 44. ClueGO analysis of hepatic expression of upregulated DEGs in the Third comparison: The Figure shows the GO/pathway terms specific for upregulated genes. The bars represent the number of genes associated with the terms. The percentage of genes per term is shown as a bar label.

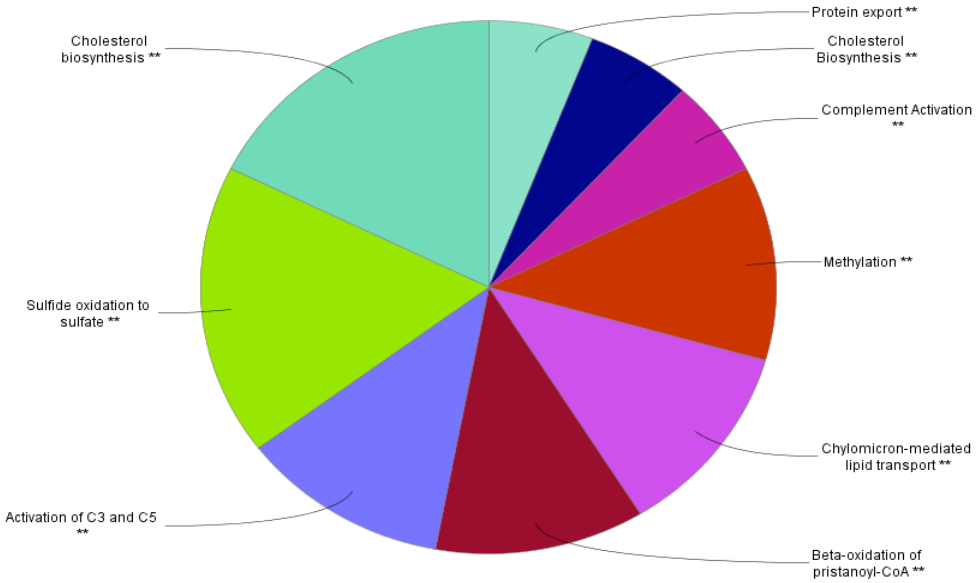

Figure 45. ClueGO analysis of hepatic expression upregulated DEGs in the Third comparison: Figure showing an overview chart with functional groups including specific terms for upregulated genes

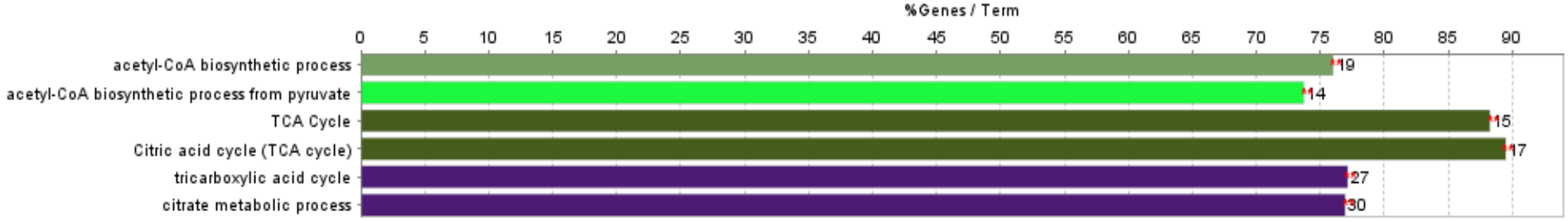

Figure 46. ClueGO analysis of hepatic expression of downregulated DEGs in the Third comparison: The Figure shows the GO/pathway terms specific for downregulated genes. The bars represent the number of genes associated with the terms. The percentage of genes per term is shown as a bar label.

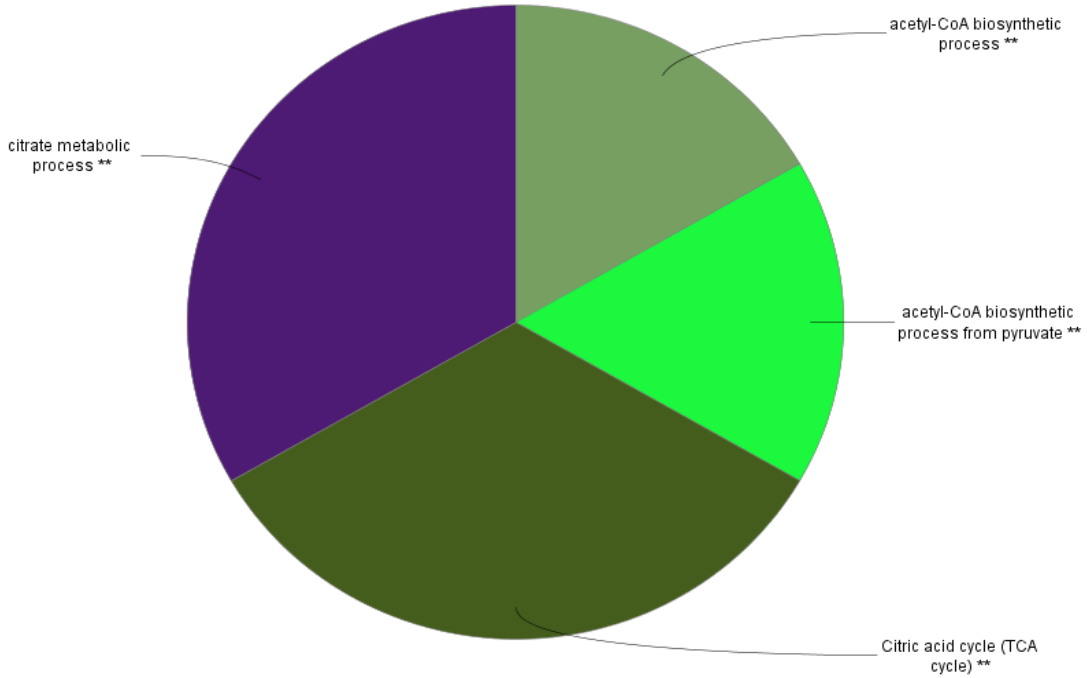

Figure 47. ClueGO analysis of hepatic expression of downregulated DEGs in the Third comparison: The Figure shows an overview chart with functional groups including specific terms for upregulated genes.

Identification of functional annotation of hepatic DEGs clusters: Functional annotation (GO, KEGG, BioCarta) of hepatic up and down-regulated genes were performed and visualized with ClueGO (kappa score: ≥ 0.3). For the hepatic upregulation, nine upregulated gene networks namely: Steroid biosynthesis, Valine, leucine and isoleucine degradation, Protein export, Cholesterol Biosynthesis, Complement Activation, Methylation, Chylomicron-mediated lipid transport, ATF6 (ATF6-alpha) activates chaperones, Beta-oxidation of pristanoyl-CoA, Activation of C3 and C5, Sulfide oxidation to sulfate, and Cholesterol biosynthesis were identified. However, For the hepatic downregulation, four downregulation networks namely: interaction between acetyl-CoA biosynthetic process and acetyl-CoA biosynthetic process from pyruvate, and interaction between Citric acid cycle (TCA cycle) and citrate metabolic process were identified **FIGURE 48**).

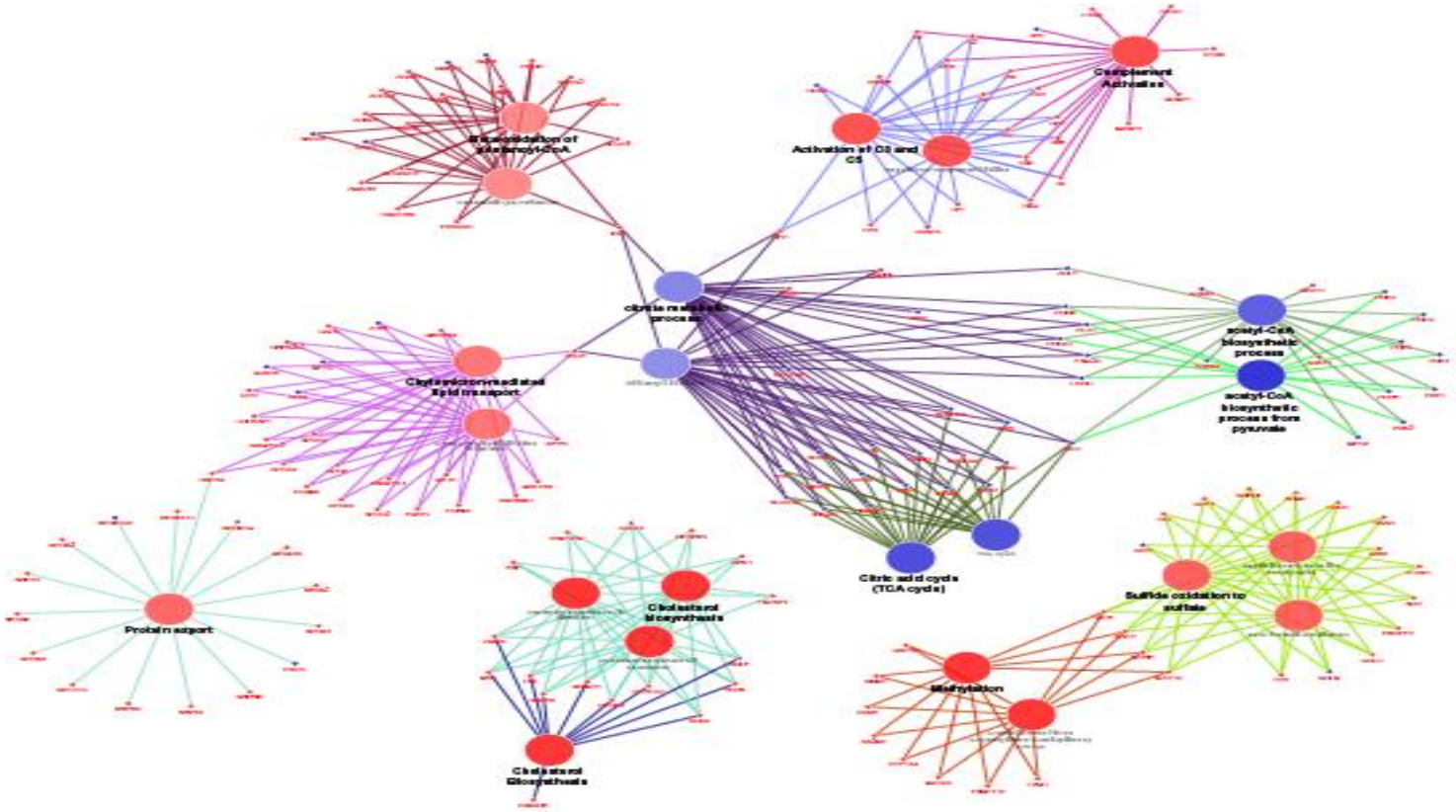

Figure 48. The distribution of two clusters (upregulated and downregulated DEGs) visualized on the network. (Third comparison). The Figure shows the functionally grouped network with terms as nodes (hubs) linked based on their kappa score level (≥0.3), where only the label of the most significant term per group is shown. The node size represents the term enrichment significance. Not grouped terms (Equal proportions of the two clusters) are shown in gray color. Node color represents the functional groups; node size reflects the p-value, with the smaller the node size indicating the less significant p-values, while the larger node size represents the more significant p-values. The red hubs represent the up-regulated DEGs; the blue hubs represent the down-regulated DEGs; the lines represent the interactions between the genes.

4.4.4. Identification of biological gene networks and pathways analysis by comparing the Polish Landrace purebred *versus* Polish Landrace x Duroc crossbred pigs liver transcriptome after experimental feeding with the diet enriched with omega-6 and omega-3 fatty acids (PUFAs)

Identification of GO/pathway terms: For upregulated hepatic genes ClueGO identified a total of five functional groups with 8 specific terms: namely: Complement Activation, Protein export, Cholesterol Biosynthesis, Methylation, Aromatic amines can be N-hydroxylated or N-dealkylated by CYP1A2, Cholesterol biosynthesis, Cholesterol biosynthesis via desmosterol, and Cholesterol biosynthesis via lathosterol (**SUPPLEMENTARY TABLE S4** and **FIGURE 49**). Furthermore, a total of five GO/pathway terms: namely: Complement Activation, Protein export, Cholesterol Biosynthesis, Methylation, and Cholesterol biosynthesis, (**SUPPLEMENTARY TABLE S4** and **FIGURE 50**) were identified.

Similarly, for downregulated hepatic genes, ClueGO identified a total of six functional groups with 8 specific terms namely: Acetyl-CoA biosynthetic process, N-terminal protein amino acid acetylation, Regulation of acetyl-CoA biosynthetic process from pyruvate, N-terminal protein amino acid modification, TCA Cycle, Citric acid cycle (TCA cycle), Tricarboxylic acid cycle, and Citrate metabolic process (**SUPPLEMENTARY TABLE S4** and **FIGURE 51**). Furthermore, a total of six GO/pathway terms: namely: acetyl-CoA biosynthetic process, N-terminal protein amino acid acetylation, regulation of acetyl-CoA biosynthetic process from pyruvate, N-terminal protein amino acid modification, Citric acid cycle (TCA cycle), and citrate metabolic process (**SUPPLEMENTARY TABLE S4** and **FIGURE 52**) were identified.

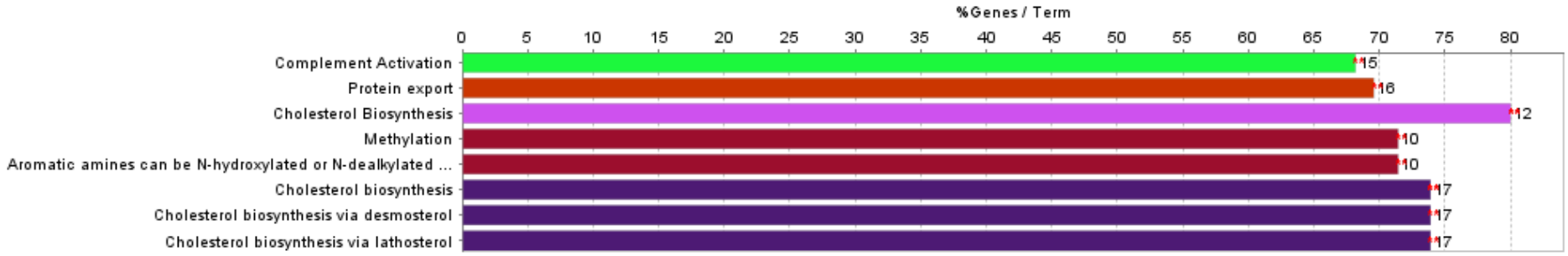

Figure 49. ClueGO analysis of hepatic expression of upregulated DEGs in the Fourth comparison: The Figure shows the GO/pathway terms specific for upregulated genes. The bars represent the number of genes associated with the terms. The percentage of genes per term is shown as a bar label.

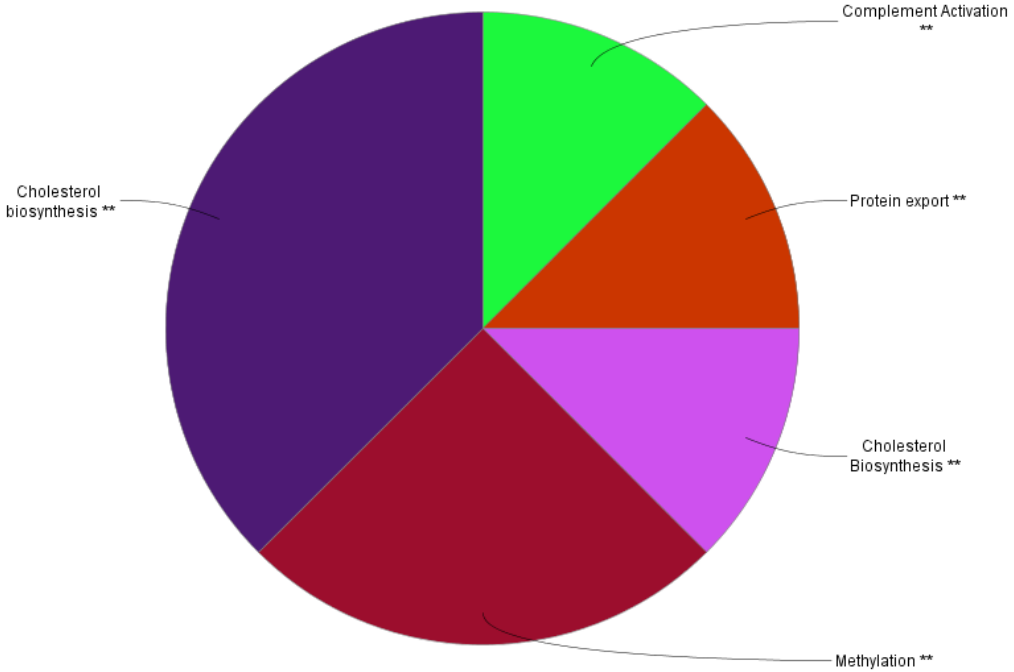

Figure 50. ClueGO analysis of hepatic expression of upregulated DEGs in the Fourth comparison: The Figure shows an overview chart with functional groups including specific terms for upregulated genes.

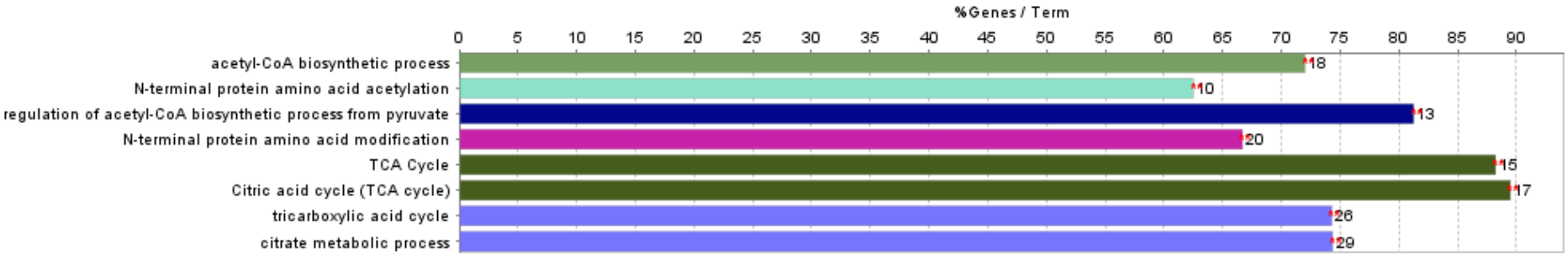

Figure 51. ClueGO analysis of hepatic expression of downregulated DEGs in the Fourth comparison: The Figure shows the GO/pathway terms specific for downregulated genes. The bars represent the number of genes associated with the terms. The percentage of genes per term is shown as a bar label.

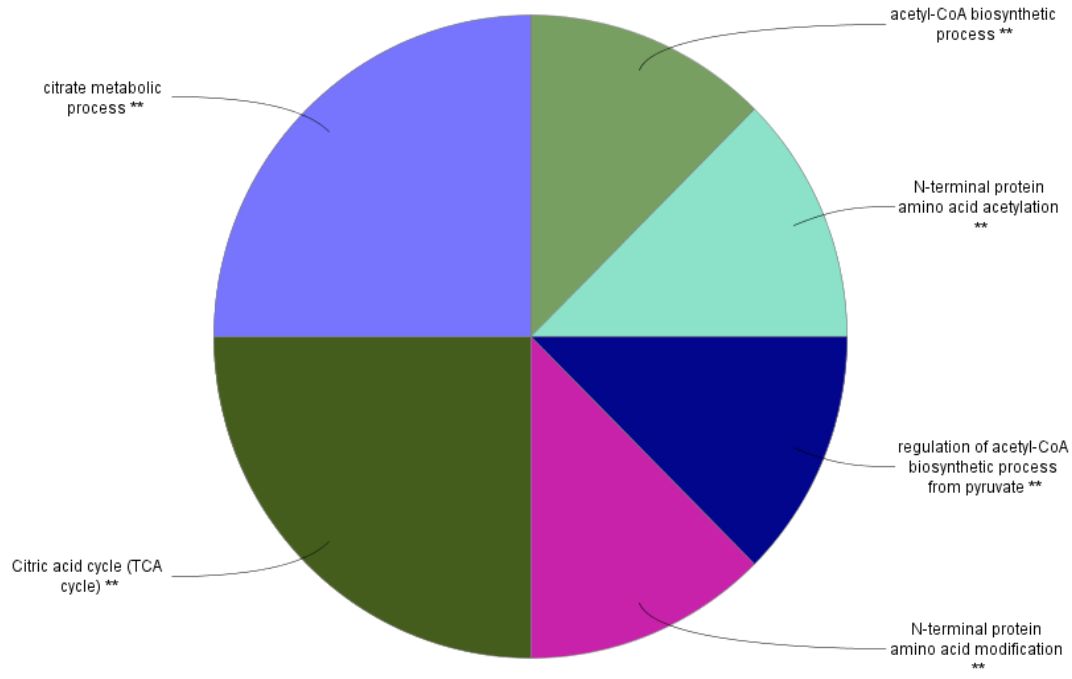

Figure 52. ClueGO analysis of hepatic expression downregulated DEGs in the Fourth comparison: The Figure shows an overview chart with functional groups including specific terms for upregulated genes.

Identification of functional annotation of hepatic DEGs clusters: Functional annotation (GO, KEGG, BioCarta) of hepatic up and downregulated genes were performed and visualized with ClueGO (kappa score ≥0.3). For the hepatic upregulated DEGs, five upregulated gene networks namely: Complement Activation, Protein export, Cholesterol Biosynthesis, Methylation, and Cholesterol biosynthesis) were identified. For the hepatic downregulated DEGs, six downregulation networks namely: Acetyl-CoA biosynthetic process, N-terminal protein amino acid acetylation, Regulation of acetyl-CoA biosynthetic process from pyruvate, N-terminal protein amino acid modification, Citric acid cycle (TCA cycle), and citrate metabolic process were identified (**FIGURE 53**).

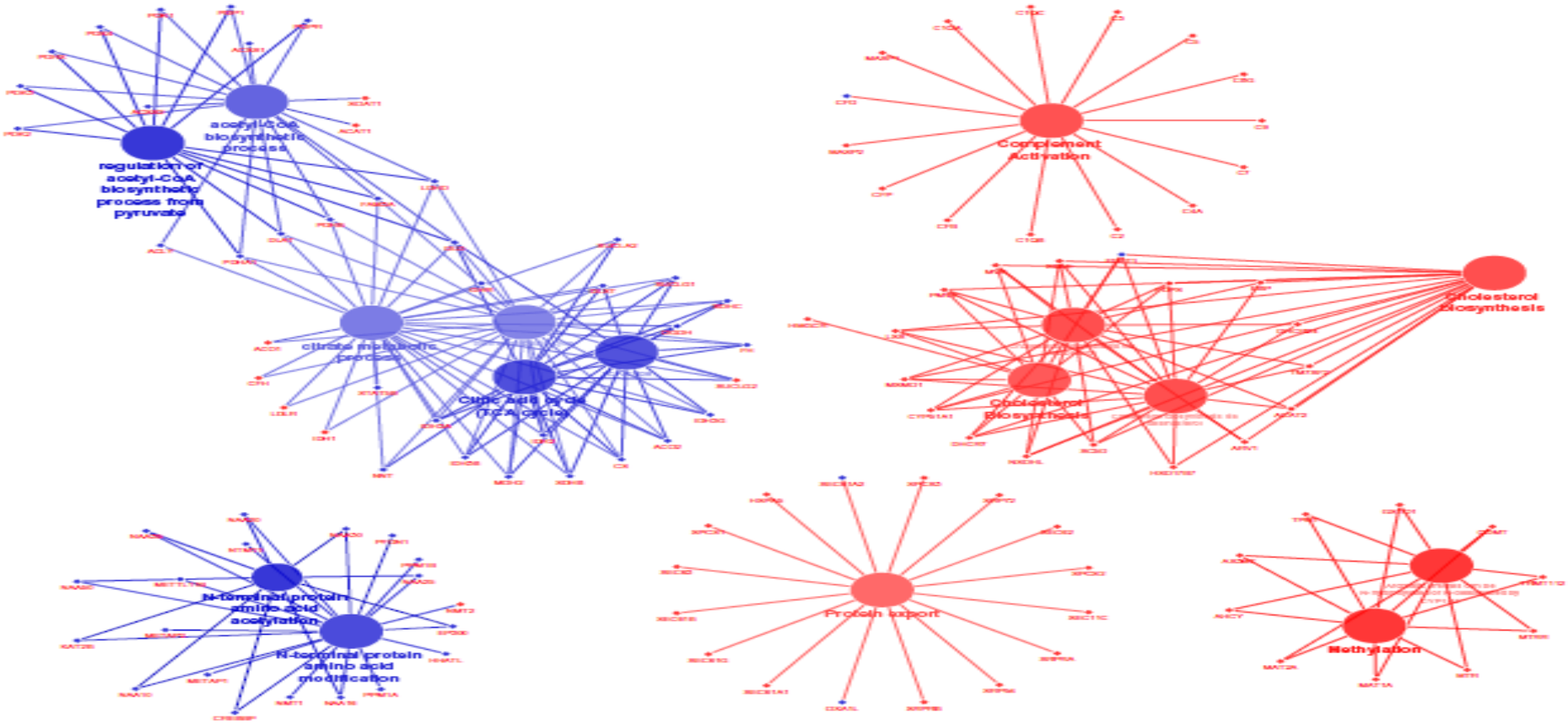

Figure 53. The distribution of two clusters (upregulated and downregulated DEGs) visualized on the network (Fourth comparison). The Figure shows the functionally grouped network with terms as nodes (hubs) linked based on their kappa score level (≥0.3), where only the label of the most significant term per group is shown. The node size represents the term enrichment significance. Not grouped terms (equal proportions of the two clusters) are shown in gray color. Node color represents the functional groups; node size reflects the p-value, with the smaller the node size indicating the less significant p-values, while the larger node size represents the more significant p-values. The red hubs represent the up-regulated DEGs; the blue hubs represent the down-regulated DEGs; the lines represent the interactions between the genes.

4.5. Validation of RNA-Seq data by quantitative real-time PCR

The validation of the RNA-Seq for confirmation of data reliability was made by measurement of relative mRNA expression using qRT-PCR. The samples of mRNA extracted from the liver of PL purebred (n=30) and PL x Duroc crossbred (n=20) pigs in the experimental feeding with control (standard) diet *versus* diet enriched with omega-6 and omega-3 fatty acids (PUFAs) were compared. qRT-PCR was performed for 12 selected DEGs, most of which were involved in lipid metabolism, namely fatty acyl-CoA biosynthesis (FASN, ACSL1, ELOVL6, ACACA, FADS1, FADS2), ALA and LA metabolism (ACSL1, FADS1, FADS2), lipid signaling and chylomicron mediated lipid transport (APOA4, APOA5), triacylglycerol biosynthesis (DGAT2, ACSL1, ELOVL6), lipid metabolism regulation by PPARα (ACSL1, APOA5, FADS1, DGAT2, ELOVL6), and cholesterol biosynthesis regulation by SREBP (ELOVL6, ACACA).

The effect of PUFAs enriched diet compared to the standard (control) diet for PL purebred was evaluated in 11 DEGs, while for PL x Duroc for 9 DEGs. Most genes showed similar changes in expression levels between the two methods, RNA-Seq and qRT PCR, indicating that the RNA-Seq data were reliable, except for EXTL1 and FASN, which had opposite results in a PL purebreed comparison groups, and for EXTL1 and DGAT2, with opposite results in PL x Duroc crossbreed comparison groups.

The expression changes measured by qRT-PCR in PL purebreed comprarison groups are shown in **FIGURE 54**, and were statistically significant for the following genes: **ACSL1** p-value=0.000004, **APOA4** p-value=0.00004, **APOA5** p-value=0.0000003 , **DGAT2** p-value=0.0175, **EXTL1** p-value=0.0023, **FADS1** p-value=0.0043, **ELOVL6** p-value=0.000009, **MMP2** p-value=0.0002, , **COL1A1** p-value=0.0181, except for **FASN** p-value=0.6117 and , **FADS2** p-value=0.2732.

Significance values for relative mRNA expression measured in PL x Duroc crossbreed comparisons groups are shown in **FIGURE 55**, and were as follows: **ACSL1** p-value=0.0128, **APOA4** p-value=0.0113, **APOA5** p-value=0.7399, **DGAT2** p-value=0.0113, **EXTL1** p-value=0.1142), **FADS1** p-value=0.1142, **FADS2** p-value=0.1142, **ACACA** p-value=0.0002, **ELOVL6** p-value=0.4051.

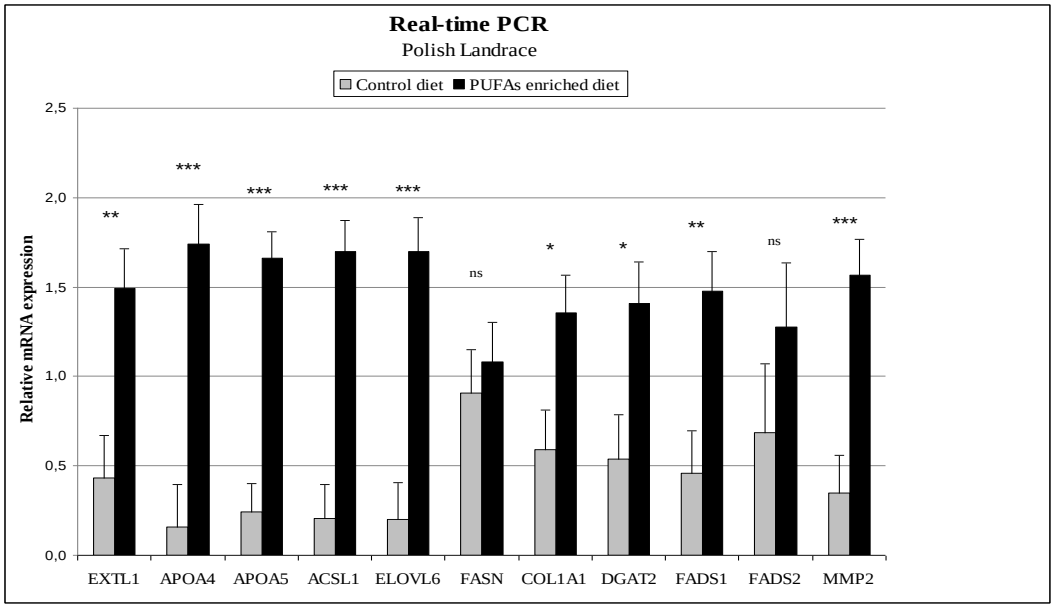

Figure 54. Relative mRNA abundance in the liver of Polish Landrace purebred pigs. The relative expression of mRNA in the liver of pigs fed control (standard) diet (light bars, n=15) or PUFAs enriched diet (dark bars, n=15). Data are expressed in arbitrary units relative to the TOP2B gene expression and normalized to the levels in the control diet group. Data are presented as mean + SD and analyzed by Student *t*-test, **p*-value < 0.05, ** *p*-value < 0.01.

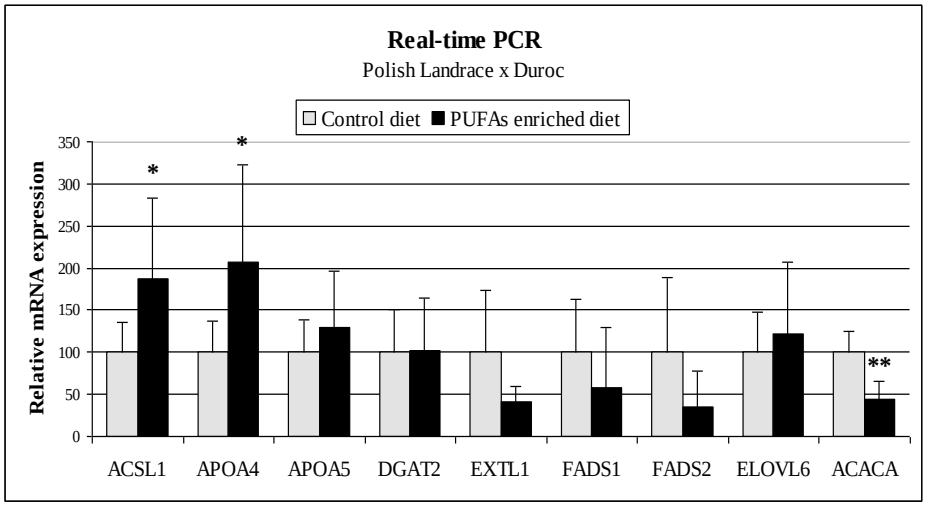

Figure 55. Relative mRNA abundance in the liver of Polish Landrace x Duroc crossbred pigs. The relative expression of mRNA in the liver of pigs fed control (standard) diet (light bars, n=8) or PUFAs enriched diet (dark bars, n=12). Data are expressed in arbitrary units relative to the RPS18 + GSR gene expression and normalized to the levels of the pigs fed the control diet. Data are presented as mean + SD and analyzed by Student *t*-test, **p*-value < 0.05, ** *p*-value < 0.01.

5. Discussion

Research progress on the biological effets of PUFAs, and in particular omega-3 and omega-6 fatty acids have been growing substantially in the past few years **(Shrestha et al., 2020, Lin et al., 2019, Zhang et al., 2019**). As an essential dietary constituent, omega-3 and omega 6 fatty acids play a wide range of vital roles in lipidomic and biophysical homeostasis, improving membrane fluidity to maintain cellular fitness (**Levental et al., 2020**). In critical illness omega-3 are precursors of anti-inflammatory derivatives (**Molfino et al., 2017, Zarate et al., 2017**). They are essential in fetal programming (**Shrestha et al., 2020**). Omega-3/6 ratio has a direct effect on the differentiation of the membrane phenotype in mesenchymal stem cells to potentiate osteogenesis (**Levental et al., 2017**), and it is suggested that it also have been associated with a direct connection to breast cancer (**Zanoaga et al., 2016**), or metabolic syndrome in adults (**Mirmiran et al., 2012**). Increased risk for obesity (**Simopoulos 2016**), disorders of lipids metabolism (**Jacometo et al. 2014**) and triglyceride metabolism in liver through disturbances in omega-6/omega-3 fatty acids ratio in western diet, are closely related to prevalence of obesity (**Simopoulos 2016**) or obesity related diseases like type II diabetes, and cardiovascular diseases (**Bowen et al., 2016**) or more and more common cases of nonalcoholic fatty liver disease (**Jump et al., 2018**). As outlined in this manuscript, omega-3 fatty acids play significant roles in at least four areas of liver physiology: by removing of cholesterol excess from hepatocytes, protection from excessive release of free free fatty acids acids from triglycerides, enhancement of catabolic processes in β-oxidation or counteraction of liver steatosis presumably through pathways pointed out in this study (**Terracciano et al., 2018**).

In this dissertation, the investigations of differences in hepatic gene expression of PL purebred and PL x Duroc crossbred pigs were conducted in order to reveal the specific effect of dietary fatty acids on hepatic gene expression depending on the breed of pigs, which are characterized by distinct fatness traits. The functional gene expression analysis was performed on the basis of the identified DEGs and gene network analysis in investigated purebred and crossbred pigs. In pig breeding in Poland, both purebred and crossbred pigs are commonly used in commercial farms for meat production. PL breed is the most commonly occurring pig breed in Poland. In Poland, PL is used as a maternal line and Duroc as a paternal line in a commercial crossbreeding. Duroc is often used as an additional genetic component, because of high intramuscular fat (IMF), which is responsible for improving the quality of meat and higher

technological meat quality value for production characteristics, and sensory value for consumers. The major difference between the two selected breeds concerns fatness traits. The crossbred PL x Duroc is characterized by the higher content of MUFA in IMF and higher content of SFA in back-fat in comparison to PL, which is known as a relatively lean pig, characterized by less fatness. These characteristic differences between investigated purebred and crossbred pigs in fatness are an interesting subject to investigate because of their different metabolism. Therefore we can investigate not only major mechanisms influenced by omega fatty acids on metabolism but additionally indicate the breed-specific differences in pigs fed with PUFAs diets. Moreover, this study is also relevant as an animal model for human studies to explain the different predisposition factors to obesity or the ability to lipid storage. In humans, despite the same diet and lifestyle, some people are more prone to obesity than others because of (genetically) different metabolism in the global human population. The goal of this doctoral dissertation was to study hepatic fatty acid metabolism.

5.1. Discussion on feeding experiment

Results finding on **the feeding experiment** revealed that linseed and rapeseed oils supplementation in appropriate contents of 2% and 1% in fodder, respectively, changed hepatic fatty acids profiles in both PL purebred and PL x Duroc crossbred. The results of the study underline the physiological effect of the increased dietary supply of unsaturated fatty acid. The mixture of two oils provided into the diet, contained the main precursors for both omega-6 as well as omega-3 fatty acids, namely LA and ALA, respectively, which quantity in the fodder was increased two fold compared to the control (standard) diet. Differences in the percentage content of particular fatty acids in whole hepatic profile under used PUFAs diet compared with standard (control diet) showed that the omega-3 fatty acids conversion pathway was preferentially affected by the supplementation over omega-6 fatty acids. Feeding experiment results showed increased percentage content of fatty acids being a product of ALA, the precursor of omega-3 fatty acids pathways, which can be supplied only exogenously. In the present work, despite doubled administration of both omega-3 ALA and omega-6 LA, absorption of omega-3 fatty acids was presumably predominant, what is shown by the substantial increase of hepatic long-chain omega-3 EPA and DHA for PL purebred and EPA for PL x Duroc crossbred pigs, which are produced by elongation and desaturation of omega-3 ALA. Additionally, the percentage content of omega-6 AA has not been changed for PL purebred and was even decreased for PL x Duroc crossbred. Disproportions in the hepatic

content of omega-6 and omega-3 fatty acids resulted in a decreased ratio of omega-6/omega-3 fatty acids, both for PL purebred and PL x Duroc crossbred.

Our results are consistent with a previous report (**Skiba et al., 2015**), which concern different absorption of omega-6 and omega-3 fatty acids. Omega-3 fatty acids are better absorbed in the porcine intestine than omega-6, substantially lowering the hepatic omega-6/omega-3 ratio. The efficiency of omega-3 fatty acids conversion and storage in the body is higher than for omega-6 fatty acids in pigs (**Skiba et al., 2015**). Nevertheless, omega-6 and omega-3 conversion pathways utilize the same enzymes responsible for elongation of the carboxylic chain by adding carbon atoms and desaturation steps resulting in additional double bonds. Competition for the same enzymes between these two pathways exists, however elongases and desaturases act preferentially in the omega-3 pathway. However, the mechanism responsible for directing the enzymes for one of the pathways remains unresolved.

The implications of increased omega-3 conversion and a significant decrease in omega-6/omega-3 ratio lay in the principle of the health benefits further achieved by these positive alterations in the liver **(Wang et al., 2020**). They are visible determinants of dietary fatty acids impact on liver components in terms of both particular fatty acids composition and possible enzymes coding by lipogenic genes. Starting with lipidomic data analysis changes in fatty acids profiles clearly showed modulated omega-3 PUFAs conversion pathway. Therefore, it can be assumed that processes revealed in functional analysis in our study are mainly related to the omega-3 fatty acids action in the liver.

5.2. Discussion on NGS experiment

Results findings on the **NGS experiment** revealed the effect of dietary fatty acids on gene expression alterations in liver independent on purebred and crossbred pigs. The results of functional gene expression analysis showed the general influence of dietary omega-3 fatty acids on gene expression. The biological processes affected by PUFAs supply independent on the breed of pigs were investigated using a large group of common genes for purebred and crossbred pigs.

The differentially expressed genes between PUFAs groups and standard diet belong to the pathways mostly related to lipid homeostasis as was shown by functional and GO term

enrichment analysis. The upregulated genes were enriched in processes with GO term named as lipid catabolic process, cholesterol homeostasis, Golgi apparatus transport and oxidation-reduction, while downregulated genes were identified as pre-autophagosomal structure membrane.

Another result found in **the NGS analysis** revealed that omega-3 PUFAs increased the lipid catabolic process and improved cholesterol metabolism. PUFAs supply influenced the relative abundances of the mRNAs involved in lipogenesis *de novo* (ACACA), synthesis of long-chain fatty acids (ACSL1), and fatty acids transport (APOA4). Intrahepatic ACACA mRNA level decreased substantially under PUFAs supply. ACACA is associated with lipogenesis. *De novo* lipogenesis is presumably suppressed after PUFAs supply. ACSL1 is associated with the synthesis of long-chain fatty acids from their precursors ALA or LA, and its expression is increased after PUFAs supply. APOA4 is associated with fatty acids transport, and its expression is increased. The enhancement of β-oxidation, which occurs in mitochondria and peroxisomes under PUFAs supply, results in degradation of fatty acids and their utilization as a source of ATP for energy production. In this experiment, upregulation of PPARα in both PL purebred and PL x Duroc crossbred pigs liver suggest that increased content of dietary fatty acids (LA and ALA) might sustain the rates of mitochondrial fatty acids β-oxidation for ATP production instead of fatty acids accumulation as triglycerides (**Gormaz et al., 2010**). The liver-specific transcription factor PPARα participates in hepatic lipid metabolism processes such as fatty acids uptake through membranes, fatty acids activation, intracellular fatty acid trafficking, fatty acid oxidation and ketogenesis, triglyceride storage, and lipolysis. PPARα also governs every enzymatic step within the fatty acid oxidation process. Increased cellular uptake of fatty acids via PPARα in hepatocytes induces genes responsible for fatty acids transport through mitochondria such as CPT1 localized on the outer membrane or CPT2 on the inner membrane. Other fatty acids membrane transporters, including SLC25A20 and SLC22A5, are also involved in PPARα mediated cellular transport. PPARα targets the major enzymes within the β-oxidation pathway, such as acyl-CoA dehydrogenases (ACAD, such as ACADL and ACAD11), as it was shown in our study mitochondrial trifunctional enzyme Hydroxyacyl-CoA Dehydrogenase (HADH) and β-oxidation of UFA (DCI, DECR). The PPARα not only induce fatty acids oxidation but additionally regulates hepatic lipogenesis by targeting genes such as FADS2, MOD1, LPIN2, SCD1, what is an indirect mechanism in *de novo* fatty acid synthesis. In our study after omega-3 and omega-6 supplementation, LPIN3 level was slightly decreased. This data suggest that *de novo* lipogenesis is suppressed due to

the exogenic fatty acid supply. Omega-3 fatty acids stimulate hepatic lipid catabolism by induction of the PPARα pathway, which further induces expression of its target genes. ACOX1 is the rate-limiting enzyme in peroxisomal fatty acid β-oxidation and target gene for PPARα. It is also a well documented the effect of dietary fatty acids on the up-regulation of PPARα, CPT1, and ACOX (oxidation in peroxisomes) and enhancement of fatty acids β-oxidation pathway. Although we showed in our analysis of upregulated genes, which are under the control of PPARα transcriptional factor, the direction of changes in crossbred pigs was opposite to purebred.

Results finding on **NGS analysis** also revealed that the DEGs between PUFAs enriched diet group and control (standard) diet group were involved in cholesterol metabolism pathways such as Proprotein convertase subtilisin/kexin type 9 (PCSK9). In our NGS studies, the Pcsk9 was identified among down-regulated genes in PUFAs enriched diet group compared to the control (standard) diet group. PCSK9 is expressed mainly in the liver, where it plays an important role as a cholesterol regulator (**Seidah et al., 2003**). The inhibition of PCSK9 increases the number of LDL receptors (LDLR) on the surface of hepatocytes. LDL cholesterol binds to LDLR, after which it is removed from the plasma and degraded in the liver (**Abifadel et al., 2005**). PCSK9 is a target for treating hypercholesterolemia, and nowadays, two novel inhibitors of PCSK9 are clinically available. In 2015, the Food and Drug Administration approved two monoclonal antibodies as medications to lower LDL cholesterol, which is a causative agent for atherosclerotic cardiovascular disease and familial hypercholesterolemia. Inhibitors of PCSK9 reduce plasma LDL cholesterol by 50-60% (**Chaudhary et al., 2017**). Our results of RNA-Seq demonstrated that PCSK9 level was decreased under omega-3 PUFAs action both in PL purebred and PL x Duroc crossbred. Cytoscape biological networks showed this gene in biological processes such as cholesterol homeostasis, regulation of receptor-mediated endocytosis and cholesterol metabolic process, and as one cellular component of the coated vesicle. To our knowledge, this is the first report showing that plant oils supplementation rich in PUFAs (e.g., ALA and LA) can lower PCSK9 mRNA expression in the liver of pigs, although this finding requires further confirmation. There are only a few studies showing the possible link between omega-3 PUFAs and PCSK9. **Graversen et al. (2015)** reported that marine omega-3 PUFAs reduced the level of plasma PCSK9 enzyme by 11.4% and 9.8% in pre- and postmenopausal woman, respectively. Marine n-3 PUFAs (38.5% EPA, 25.9%, DHA, and 6.0% DPA) were consumed for 12 weeks of 2.2 g (medium) daily dose. Although omega-3 fatty acids reduced the level of the cholesterol

regulator, LDL cholesterol in this study was unaffected. **Sorokin et al. (2016)** also indicated an inhibitory effect of fish oil on PCSK9 expression. ApoE gene knockout female mice were treated for 13 weeks with different diets deficient in omega-3 PUFAs, enriched with omega-3 PUFAs in the dose of 1.8 g omega-3 PUFAs/kg diet per day, or in combination with acetylsalicylic acid (aspirin). They reported decreased PCSK9 mRNA level, 70% lower protein levels of circulating PCSK9, and 40% less plasma cholesterol in VLDL and LDL fraction in mice fed omega-3 enriched diets compared to the control group. Additionally, they found the synergistic effect of omega-3 and acetylsalicylic acid in lowering the plasma PCSK9 level. Similarly, **Yuan et al. (2016)** used the RNA-Seq approach to show that omega-3 fatty acids in male rats reduce the expression of PCSK9 mRNA in the liver. Animals in the study were fed for 16 weeks (long term administration) with marine omega-3 PUFAs. Reduction of hepatic Pcsk9 expression was associated with lower LDL cholesterol in plasma (84% reduction) compared with high-fat dietary groups supplemented with 10% of fish oil and without supplementation. Additionally, genes regulated by omega-3 fatty acids identified in the transcriptomic study were also revealed in our RNA-Seq analysis, including ACADL, ABCG5, and ABCG8.

In our study, the pathway under the GO term 'cholesterol homeostasis' was revealed as another process affected by omega-3 fatty acids derived from a diet. Among the genes showed in Cytoscape analysis which were up-regulated for two pig breeds and grouped in the "cholesterol homeostasis" process were ABCG5 and ABCG8, 1.9 and 1.2 fold changed respectively. The transcription of ABCG5 and ABCG8 is mainly under the control of one transcription factor, which is PPARα. As omega-3 fatty acids are natural agonists of PPARα, its expression should be increased in PUFAs enriched diet groups. In our studies we observed such a result in PL but not in PL x Duroc.

Nevertheless, both ABCG5 and ABCG8 genes were increased in two breeds. The ABCG5 and ABCG8 are genes coding for the proteins responsible for cholesterol uptake and cholesterol transport outside the cell. Enhanced cholesterol efflux from hepatocytes is the outcome of replacing cholesterol in the cell membranes by unsaturated fatty acids (UFA). This process affects the fluidity and permeability of cell membranes and further signaling. In our studies cholesterol molecules in cell membranes are probably replaced by omega-3 fatty acids. The results of fatty acids profiles showed increased content of omega-3 derived fatty acids in comparison to omega-6 derivatives, which hints on enhanced conversion in the

omega-3 pathway. Thus, the molecules, replacing cholesterol from cell membranes likely belong to the omega-3 family.

Additionally, we found in our studies the increased expression of LIPG (FC=1,5 up-regulated). The gene coding for LIPG is another crucial indicator of cholesterol efflux from the hepatic cell to circulating healthy HDL. The functional analysis in clueGO showed the GO term oxidation-reduction pathway as the most enriched pathway in differentially expressed genes under PUFAs supply. The dietary unsaturated fatty acids improve lipids homeostasis by influence on the expression of genes involved in lipid catabolic processes and cholesterol homeostasis.

Results finding on **NGS analysis** further revealed that the down-regulation of genes involved in the autophagy process. In our NGS studies, we identified the down-regulation of the pre-autophagosomal structure membrane pathway as a result of dietary fatty acids supplementation and most probably omega-3 fatty acids action. Autophagy is a process for disposing of excessive or defective components of the cell through lysosomes activity. Autophagosomes as double-membrane vesicles enclose lipid droplets or defective organelles and fuse with lysosomes for degradation of the content. Subsequently, lipid droplets after degradation are utilized to generate energy and materials for cell recycling (Mizuschima **et al., 1998; Singh and Cuervo, 2012**). Among DEGs assigned to the autophagy process in Cytoscape analysis were the Atg2, ULK1, and WIPI1 genes. They were down-regulated in both breeds under PUFAs supply compared to the control diet. The ATG2, ULK1, and WIPI1 genes are essential during autophagosome formation. The action of autophagy-related protein 2 (ATG2) is required for complete autophagosome formation as a closed double-membrane vesicle and regulates the distribution and size of lipid droplets in mammalian cells (**Velikkakath et al., 2012**). The ATG2 interacts with other autophagy-related proteins creating the Atg9–Atg2–Atg18 complex responsible for autophagosome biogenesis (**Gómez-Sánchez et al., 2018**). Mammalian ULK1 kinase is a principal component of the ULK1–Atg13–FIP200 complex that is essential during autophagy initiation. mTORC1 regulates autophagy through binding and phosphorylation of ULK1 (**Hosokawa et al., 2009**). ULK1 activity depends on intracellular energy and nutrient levels. During mTOR inhibition or amino acid starvation, ULK1 phosphorylates Beclin-1 (**Russel et al., 2013**).

WIPI1 is an important indicator of autophagy (**Tsuyuki et al., 2014**). An increase or decrease in the mRNA abundance of WIPI1 is associated with autophagy dysregulation and can be used as a method of detecting autophagosome formation. Among 37 examined ATG genes in *in vitro* studies, WIPI1 was identified as the most significantly upregulated gene induced by autophagy (**Tsuyuki et al., 2014**). Diminished autophagy is accompanied by suppression of *de novo* lipogenesis and decreased expression of its markers (**Ma et al., 2013**) such as ATP-citrate lyase (*Acly*), acetyl-CoA carboxylase (*Acaca*), *Fasn* and stearoyl-CoA desaturase-1 (Scd1). According to this, we observed in our studies the reduced expression of *Acaca* and *Fasn* mRNA in PUFAs enriched group comparing to the control group, where autophagy-related genes were downregulated. The reduced level of *Acaca* expression was additionally confirmed by qRT-PCR. Recently, it has been shown that autophagy plays an essential role in the regulation of lipid metabolism, causing degradation of lipid droplets (**Singh et al., 2009**). This specific autophagy, primarily described in hepatocytes, was called 'lipophagy' (**Singh et al., 2009; Weidberg et al., 2009; Singh and Cuervo, 2012; Carmona-Gutierriez et al., 2016**). Lipophagy depends on the nutritional status of cells. Changes in intracellular free fatty acids content influence levels of lipophagy (**Liu and Czaja 2013**). Low levels of free fatty acids and excess accumulation of lipids stored in the form of triglycerides increase autophagy in the liver in order to enhance lipid degradation.

Conversely, a high level of free fatty acids in cells causes inhibition of autophagy (**Singh et al., 2009; Yang et al., 2010**). PUFAs are mostly utilized in the β-oxidation process producing free fatty acids instead of being accumulated in the form of triglycerides. The alternative way of lipid degradation is lipolysis by the action of cytosolic lipases. Initially, lipases and hydrolytic enzymes were thought to be exclusively responsible for the breakdown of triglycerides from lipid droplets before the recognition of lipophagy (**Singh and Cuervo, 2012; Liu and Czaja 2013**). Lipolysis by lipases is probably a sufficient way for lipid degradation in PUFAs enriched diet group. Protective action of lipophagy against lipid accumulation, in this case, is not necessary. Omega-3 fatty acids likely counteract excessive lipid storage through the catabolic process of β-oxidation, maintaining lipid homeostasis in the liver.

Our data suggest that omega-3 PUFAs might suppress lipophagy (autophagy of lipids). However, there are contradictory reports concerning the effect of different kinds of fatty acids on the autophagy process. Obesity, both genetic (ob/ob) and dietary-induced (HFD),

characterized by a high level of SFAs, are related to loss of autophagy in mice compared to lean controls (**Yang et al., 2010**). On the other hand, **Mei et al. (2011)** reported that HFD induced autophagy in mice liver while in HepG2 cells, SFAs (palmitic acid) did not activate autophagy. Recent studies reported that omega-3 fatty acids enhance autophagy during the pathological state in the liver, such as hepatitis (**Li et al., 2016**) and *in vitro* steatosis model (**Chen et al., 2015**). **Li et al. (2016)**, for instance, demonstrated that endogenous omega-3 PUFAs (mostly DHA) in the liver of fat-1 mice impair hepatitis by reduction of pro-inflammatory cytokines (e.g., TNF-α, IL-6, IFN-γ), inhibition of NF-κβ signaling and activation of autophagy. Increased autophagy was assessed based on western blotting for autophagy-associated protein LC3. Fat-1 mice were used to study omega-3 PUFAs function as they have a unique feature to convert omega-6 to omega-3 type in all tissues. These transgenic animals have an increased level of EPA and DHA in the liver and other tissues, and the omega-6/omega-3 ratio is 1/1 (**Kang et al., 2004**). Our RNA-Seq results indicated on downregulation of mRNA expression of autophagy-related genes under omega-3 action. However, in studies of **Johannsson et al. (2015),** silencing of one of the autophagy-related proteins, Atg5, was not associated with inhibition of the autophagy process in cells. Whether the autophagy process in our studies was suppressed or unchanged, require further analysis, despite downregulation of autophagy-related genes.

Results finding on the **NGS experiment** further revealed that different effect of dietary fatty acids on gene expression alterations in liver depended on the pig breed. The investigation of differences in gene expression for PL purebred and PL x Duroc crossbred pigs were conducted in order to reveal the specific effect of dietary fatty acids on hepatic gene expression depending on the genotype of pigs. The functional analysis was performed separately for DEGs, and the direction of expression changes was contradictory for two breeds. The following processes were distinguished as a breed-specific effect of omega-3 fatty acids action on genes transcription: blood vessel development (angiogenesis), proteolysis, mitochondrial processes, cell migration, Golgi apparatus, immune response and response to nutrients.

Results finding on the **NGS analysis** also revealed that Omega-3 PUFAs influence angiogenesis. The liver is one of the most vascularized organs in the body. However, sometimes the development of new vessels (angiogenesis) is associated with pathological changes in the liver leading to fibrosis, cirrhosis, and liver cancer (**Fernández et al., 2009;**

Elpek, 2015). In our study, the expression of genes involved in angiogenesis was changed under PUFAs supply. Functional analysis in ClueGO showed GO term named vasculature development as an up-regulated process in PL and blood vessel development as down-regulated in PL x Duroc. Dietary fatty acids probably stimulate new blood vessels development in PL and inhibit in PL x Duroc. Among differentially expressed genes assigned to the blood vessels development process in the Cytoscape analysis is Adiponectin receptor 2 (AdipoR2), involved both in angiogenesis and lipid metabolism pathways. Adiponectin receptor 2 (AdipoR2) is mainly expressed in the liver and acts as a receptor for hormone adiponectin (**Parker-Duffen et al., 2014**). AdipoR2 is necessary for adiponectin action to promote angiogenesis (**Parker-Duffen et al., 2014**) and enhances lipid catabolism by increased action of PPARα ligands (**Yamauchi et al., 2003**). AdipoR2 mediates AMP kinase activation and is associated with increased fatty acid oxidation process and glucose uptake by adiponectin (**Yamauchi et al., 2003; Parker-Duffen et al., 2014**). Together with vasculature development assigned as up-regulated processes in PL, ClueGO analysis has also shown response to nutrients (GO:0007584) and sterol metabolism (GO:) with the same direction of changes and the hormone stimulus-response pathway down-regulated in PL x Duroc. However, our obtained results do not explain the roles of particular genes and require further confirmation as other genes associated with angiogenesis suggest inhibition of vascularization in both breeds. For instance, vascular endothelial growth factor (VEGF) is the most critical growth factor required during this process. Previous studies have shown that omega-3 EPA and DHA inhibit angiogenesis in cell culture through reduced mRNA and protein level of VEGF in the endothelium (**Zhuang et al., 2013**).

Results finding on **NGS analysis** further revealed that Omega-3 fatty acids improve metabolism in PL x Duroc pig. Other processes regulated in opposite directions for both purebred and crossbred pigs were cell migration, signal transduction, membrane composition, and Golgi apparatus activity. The genes assigned to all these processes were up-regulated for PL and down-regulated for PL x Duroc breed. The pathways listed above reflect the significant functions of fatty acids in cells since they regulate the intracellular signaling and membranes structure and function. Moreover, the Golgi apparatus is responsible for posttranslational protein and lipid modifications necessary for membrane recycling. Additional pathways regulated in opposite directions of gene expression changes for two breeds were mitochondrial processes, ER and proteolysis, and pathways related to transcription (mRNA processing) and translation, ribosomes. The genes assigned to these

pathways were down-regulated for PL. These are processes generally related to metabolism and probably hints on the decreased rate of metabolism for PL. Conversely, metabolism for PL x Duroc is enhanced. The up-regulated pathways 'ER/protein synthesis' and 'proteolysis' hints on increased protein turnover, causes by dietary fatty acids. The opposite outcomes of omega-3 fatty acids revealed for two breeds are possibly the consequences of differences in metabolism, which is more intensive in the liver of PL x Duroc. The phenotypes of pigs chosen for analysis are characterized by distinct fatness traits. The carcass of PL x Duroc has a different composition of fatty acids and contains more SFA and MUFA than PL, which, on the contrary, contains more PUFA. Therefore, the conversion of fatty acids for PL x Duroc from the beginning necessitates more intensive metabolism. The changes caused by dietary PUFA are more substantial for PL x Duroc then for the pure breed of Polish Landrace, since PUFA extensively replaces SFA in the cell membranes. The administration of a diet enriched with the source of PUFA, caused likely more intensive transport of fatty acids to peripheral tissues, increased degradation of damaged and unnecessary proteins through proteolysis and synthesis of new proteins and wide-ranging remodeling of membrane structures. Polish Landrace may contain more PUFAs in cells per se and an additional exogenous source of PUFAs can be utilized for different purposes than disposal of 'unhealthy' lipids such as SFAs from the cells. Hence, angiogenesis, response to nutrients, and processes like signaling are enhanced for this breed. Additionally, the differences in metabolism for two breeds are reflected in the number of identified DEGs, which was 3,584 for Polish Landrace versus 4,502 for PL x Duroc.

Results finding on **NGS analysis** further revealed that Omega-3 fatty acids increase immune response in PL x Duroc pig. Furthermore, changes caused by omega-3 fatty acids increased gene expression involved in the 'immune response' pathway for PL x Duroc. The mechanism of health-promoting action of n-6 and n-3 PUFAs is perhaps mediated by down-regulation of SREBP-1 and FAS (FAS showed in Cytoscape not confirmed by real-time PCR, ACC1 – fatty acids *de novo* synthesis down-regulated in Cytoscape, confirmed by real-time PCR) and suppression of *de novo* fatty acid synthesis. Recently, the immune-modulatory effect of omega-3 EPA and DHA in the wide-scale analysis have been shown in humans (**Schmidt et al., 2012**). Studies on extensive genome expression studies using microarrays revealed a particular influence on pathways such as immune response and lipid metabolism. Moreover, the effect was more prominent (more genes were regulated) in dyslipidemic humans than normolipidemic. The above-mentioned studies on human dyslipidemia revealed anti-

inflammatory responses of the immune and lipid metabolism pathways after the administration of fish oil, which is consistent with our results in pigs.

6. Conclusions

1) Among three tested diets, PUFAs enriched diet in the content of 2% of linseed oil and 1% of rapeseed oil in the fodder mixture effectively changed hepatic fatty acid profile and decreases omega-6/omega-3 ratio in the liver for both analyzed pig genotypes.
2) Differences in the percentage content of particular fatty acids in the full hepatic profile after feeding a PUFAs enriched diet compared with standard (control diet) showed that the omega-3 fatty acids conversion pathway was preferentially affected by the supplementation over omega-6 fatty acids.
3) Besides improved fatty acids profiles in the liver, PUFA supplemented died changed gene expression at large scale transcriptomic level for both genotypes.
4) Endogenous omega-3 fatty acids affect physiological pathways associated mainly with processes involved in decreased cellular lipid accumulation (triglycerides content as lipid droplets): 1) elevated fatty acid oxidation, 2) enhanced cholesterol transport outside the hepatocytes, 3) decreased autophagy (lipophagy).
5) Affected pathways support the antisteatotic function of endogenous omega-3 fatty acids in the liver.
6) We found indications that omega-3 fatty acids can probably act against lipid accumulation in the liver through the improvement of the hepatic fatty acids profile.
7) The manner of conversion showed that PUFA enriched diet hint mainly on the omega-3 pathway.
8) Our results confirm the essential role of omega-6 and omega-3 fatty acids in homeostasis through markedly improved fatty acids profile (decreased omega-6/omega-3 ratio in the liver) and as a consequence regulation of expression of many genes involved in lipid metabolism, signal transduction and pathways related to the inflammatory response.

7. References

1. Simopoulos AP. Evolutionary aspects of diet and essential fatty acids. *World Rev Nutr Diet*. 2001;88:18-27.
2. El-Badry AM, Graf R, Clavien PA. Omega 3 - Omega 6: What is right for the liver?. *J Hepatol*. 2007;47(5):718-725.
3. Simopoulos AP. An Increase in the Omega-6/Omega-3 Fatty Acid Ratio Increases the Risk for Obesity. *Nutrients*. 2016;8(3):128. Published 2016 Mar 2.
4. Guixà-González R, Javanainen M, Gómez-Soler M, et al. Membrane omega-3 fatty acids modulate the oligomerisation kinetics of adenosine A2A and dopamine D2 receptors. *Sci Rep*. 2016;6:19839. Published 2016 Jan 22.
5. Storch J, Schachter D. Dietary induction of acyl chain desaturases alters the lipid composition and fluidity of rat hepatocyte plasma membranes. *Biochemistry*. 1984;23(6):1165-1170.
6. Turk HF, Chapkin RS. Membrane lipid raft organization is uniquely modified by n-3 polyunsaturated fatty acids. *Prostaglandins Leukot Essent Fatty Acids*. 2013;88(1):43-47.
7. Shaikh SR. Biophysical and biochemical mechanisms by which dietary N-3 polyunsaturated fatty acids from fish oil disrupt membrane lipid rafts. *J Nutr Biochem*. 2012;23(2):101-105.
8. Williams JA, Batten SE, Harris M, et al. Docosahexaenoic and eicosapentaenoic acids segregate differently between raft and nonraft domains. *Biophys J*. 2012;103(2):228-237.
9. Levental KR, Lorent JH, Lin X, et al. Polyunsaturated Lipids Regulate Membrane Domain Stability by Tuning Membrane Order. *Biophys J*. 2016;110(8):1800-1810.
10. Levental KR, Surma MA, Skinkle AD, et al. ω-3 polyunsaturated fatty acids direct differentiation of the membrane phenotype in mesenchymal stem cells to potentiate osteogenesis. *Sci Adv*. 2017;3(11):eaao1193. Published 2017 Nov 8.
11. Levental KR, Malmberg E, Symons JL, et al. Lipidomic and biophysical homeostasis of mammalian membranes counteracts dietary lipid perturbations to maintain cellular fitness. *Nat Commun*. 2020;11(1):1339. Published 2020 Mar 12.

12. Lamaziere A, Wolf C, Barbe U, Bausero P, Visioli F. Lipidomics of hepatic lipogenesis inhibition by omega 3 fatty acids. *Prostaglandins Leukot Essent Fatty Acids*. 2013;88(2):149-154.
13. Balogun KA, Albert CJ, Ford DA, Brown RJ, Cheema SK. Dietary omega-3 polyunsaturated fatty acids alter the fatty acid composition of hepatic and plasma bioactive lipids in C57BL/6 mice: a lipidomic approach. *PLoS One*. 2013;8(11):e82399.
14. Wymann MP, Schneiter R. Lipid signalling in disease. *Nat Rev Mol Cell Biol*. 2008;9(2):162-176.
15. Norris PC, Dennis EA. A lipidomic perspective on inflammatory macrophage eicosanoid signaling. *Adv Biol Regul*. 2014;54:99-110.
16. Dennis EA, Norris PC. Eicosanoid storm in infection and inflammation [published correction appears in Nat Rev Immunol. 2015 Nov;15(11):724]. *Nat Rev Immunol*. 2015;15(8):511-523.
17. Patterson E, Wall R, Fitzgerald GF, Ross RP, Stanton C. Health implications of high dietary omega-6 polyunsaturated Fatty acids. *J Nutr Metab*. 2012;2012:539426.
18. Molfino A, Amabile MI, Monti M, Muscaritoli M. Omega-3 Polyunsaturated Fatty Acids in Critical Illness: Anti-Inflammatory, Proresolving, or Both?. *Oxid Med Cell Longev*. 2017;2017:5987082.
19. Norris PC, Dennis EA. Omega-3 fatty acids cause dramatic changes in TLR4 and purinergic eicosanoid signaling. *Proc Natl Acad Sci U S A*. 2012;109(22):8517-8522.
20. Sessler AM, Ntambi JM. Polyunsaturated fatty acid regulation of gene expression. *J Nutr*. 1998;128(6):923-926. doi:10.1093/jn/128.6.923
21. Jump DB, Tripathy S, Depner CM. Fatty acid-regulated transcription factors in the liver. *Annu Rev Nutr*. 2013;33:249-269.
22. Oppi-Williams C, Suagee JK, Corl BA. Regulation of lipid synthesis by liver X receptor α and sterol regulatory element-binding protein 1 in mammary epithelial cells. *J Dairy Sci*. 2013;96(1):112-121.
23. Chamouton J, Latruffe N. PPARα/HNF4α interplay on diversified responsive elements. Relevance in the regulation of liver peroxisomal fatty acid catabolism. *Curr Drug Metab*. 2012;13(10):1436-1453.
24. Jiao Y, Lu Y, Li XY. Farnesoid X receptor: a master regulator of hepatic triglyceride and glucose homeostasis. *Acta Pharmacol Sin*. 2015;36(1):44-50.

25. Lu H. Crosstalk of HNF4*α* with extracellular and intracellular signaling pathways in the regulation of hepatic metabolism of drugs and lipids. *Acta Pharm Sin B*. 2016;6(5):393-408.
26. Preidis GA, Kim KH, Moore DD. Nutrient-sensing nuclear receptors PPARα and FXR control liver energy balance. *J Clin Invest*. 2017;127(4):1193-1201.
27. Gormaz JG, Rodrigo R, Videla LA, Beems M. Biosynthesis and bioavailability of long-chain polyunsaturated fatty acids in non-alcoholic fatty liver disease. *Prog Lipid Res*. 2010;49(4):407-419.
28. Murakami K, Ide T, Suzuki M, Mochizuki T, Kadowaki T. Evidence for direct binding of fatty acids and eicosanoids to human peroxisome proliferators-activated receptor alpha. *Biochem Biophys Res Commun*. 1999;260(3):609-613.
29. IJpenberg A, Jeannin E, Wahli W, Desvergne B. Polarity and specific sequence requirements of peroxisome proliferator-activated receptor (PPAR)/retinoid X receptor heterodimer binding to DNA. A functional analysis of the malic enzyme gene PPAR response element. *J Biol Chem*. 1997;272(32):20108-20117.
30. Chakravarthy MV, Pan Z, Zhu Y, et al. "New" hepatic fat activates PPARalpha to maintain glucose, lipid, and cholesterol homeostasis. *Cell Metab*. 2005;1(5):309-322.
31. Clarke SD. The multi-dimensional regulation of gene expression by fatty acids: polyunsaturated fats as nutrient sensors. *Curr Opin Lipidol*. 2004;15(1):13-18.
32. Rakhshandehroo M, Knoch B, Müller M, Kersten S. Peroxisome proliferator-activated receptor alpha target genes. *PPAR Res*. 2010;2010:612089.
33. Afman LA, Müller M. Human nutrigenomics of gene regulation by dietary fatty acids. *Prog Lipid Res*. 2012;51(1):63-70.
34. Tobin KA, Steineger HH, Alberti S, et al. Cross-talk between fatty acid and cholesterol metabolism mediated by liver X receptor-alpha. *Mol Endocrinol*. 2000;14(5):741-752.
35. Heckmann BL, Zhang X, Saarinen AM, et al. Liver X receptor **α** mediates hepatic triglyceride accumulation through upregulation of G0/G1 Switch Gene 2 expression. *JCI Insight*. 2017;2(4):e88735. Published 2017 Feb 23.
36. Clarke SD. Polyunsaturated fatty acid regulation of gene transcription: a molecular mechanism to improve the metabolic syndrome. *J Nutr*. 2001;131(4):1129-1132.
37. Ramírez M, Amate L, Gil A. Absorption and distribution of dietary fatty acids from different sources. *Early Hum Dev*. 2001;65 Suppl:S95-S101.

38. Kerr BJ, Kellner TA, Shurson GC. Characteristics of lipids and their feeding value in swine diets. *J Anim Sci Biotechnol*. 2015;6(1):30. Published 2015 Jul 1.
39. Nguyen P, Leray V, Diez M, et al. Liver lipid metabolism. *J Anim Physiol Anim Nutr (Berl)*. 2008;92(3):272-283.
40. Bergen WG, Mersmann HJ. Comparative aspects of lipid metabolism: impact on contemporary research and use of animal models. *J Nutr*. 2005;135(11):2499-2502.
41. Vallim T, Salter AM. Regulation of hepatic gene expression by saturated fatty acids. *Prostaglandins Leukot Essent Fatty Acids*. 2010;82(4-6):211-218.
42. Guillevic M, Kouba M, Mourot J. Effect of a linseed diet on lipid composition, lipid peroxidation and consumer evaluation of French fresh and cooked pork meats. *Meat Sci*. 2009;81(4):612-618.
43. Osada J. The use of transcriptomics to unveil the role of nutrients in Mammalian liver. *ISRN Nutr*. 2013;2013:403792. Published 2013 Aug 28.
44. Gabás-Rivera C, Martínez-Beamonte R, Ríos JL, et al. Dietary oleanolic acid mediates circadian clock gene expression in liver independently of diet and animal model but requires apolipoprotein A1. *J Nutr Biochem*. 2013;24(12):2100-2109.
45. Nojima K, Sugimoto K, Ueda H, Babaya N, Ikegami H, Rakugi H. Analysis of hepatic gene expression profile in a spontaneous mouse model of type 2 diabetes under a high sucrose diet. *Endocr J*. 2013;60(3):261-274.
46. Luo Y, Burrington CM, Graff EC, et al. Metabolic phenotype and adipose and liver features in a high-fat Western diet-induced mouse model of obesity-linked NAFLD. *Am J Physiol Endocrinol Metab*. 2016;310(6):E418-E439.
47. Siersbæk M, Varticovski L, Yang S, et al. High fat diet-induced changes of mouse hepatic transcription and enhancer activity can be reversed by subsequent weight loss. *Sci Rep*. 2017;7:40220. Published 2017 Jan 10.
48. Dong H, Czaja MJ. Regulation of lipid droplets by autophagy. *Trends Endocrinol Metab*. 2011;22(6):234-240.
49. Singh R, Cuervo AM. Lipophagy: connecting autophagy and lipid metabolism. *Int J Cell Biol*. 2012;2012:282041.
50. Liu K, Czaja MJ. Regulation of lipid stores and metabolism by lipophagy. *Cell Death Differ*. 2013;20(1):3-11.
51. Carmona-Gutierrez D, Zimmermann A, Madeo F. A molecular mechanism for lipophagy regulation in the liver. *Hepatology*. 2015;61(6):1781-1783.

52. Debeer LJ, Beynen AC, Mannaerts GP, Geelen MJ. Lipolysis of hepatic triacylglycerol stores. *FEBS Lett*. 1982;140(2):159-164.
53. Alves-Bezerra M, Cohen DE. Triglyceride Metabolism in the Liver. *Compr Physiol*. 2017;8(1):1-8. Published 2017 Dec 12.
54. Decsi T, Kennedy K. Sex-specific differences in essential fatty acid metabolism. *Am J Clin Nutr*. 2011;94(6 Suppl):1914S-1919S.
55. Lohner S, Fekete K, Marosvölgyi T, Decsi T. Gender differences in the long-chain polyunsaturated fatty acid status: systematic review of 51 publications. *Ann Nutr Metab*. 2013;62(2):98-112.
56. Howe PR, Buckley JD, Murphy KJ, Pettman T, Milte C, Coates AM. Relationship between erythrocyte omega-3 content and obesity is gender dependent. *Nutrients*. 2014;6(5):1850-1860. Published 2014 May 5.
57. De Groot RHM, Emmett R, Meyer BJ. Non-dietary factors associated with n-3 long-chain PUFA levels in humans - a systematic literature review. *Br J Nutr*. 2019;121(7):793-808.
58. Ghasemifard S, Hermon K, Turchini GM, Sinclair AJ. Metabolic fate (absorption, β-oxidation and deposition) of long-chain n-3 fatty acids is affected by sex and by the oil source (krill oil or fish oil) in the rat. *Br J Nutr*. 2015;114(5):684-692.
59. Extier A, Langelier B, Perruchot MH, et al. Gender affects liver desaturase expression in a rat model of n-3 fatty acid repletion. *J Nutr Biochem*. 2010;21(3):180-187.
60. Kitson AP, Smith TL, Marks KA, Stark KD. Tissue-specific sex differences in docosahexaenoic acid and Δ6-desaturase in rats fed a standard chow diet. *Appl Physiol Nutr Metab*. 2012;37(6):1200-1211.
61. Bowen KJ, Harris WS, Kris-Etherton PM. Omega-3 Fatty Acids and Cardiovascular Disease: Are There Benefits?. *Curr Treat Options Cardiovasc Med*. 2016;18(11):69.
62. Matsumoto M, Sata M, Fukuda D, et al. Orally administered eicosapentaenoic acid reduces and stabilizes atherosclerotic lesions in ApoE-deficient mice. *Atherosclerosis*. 2008;197(2):524-533.
63. Amminger GP, Schäfer MR, Schlögelhofer M, Klier CM, McGorry PD. Longer-term outcome in the prevention of psychotic disorders by the Vienna omega-3 study. *Nat Commun*. 2015;6:7934. Published 2015 Aug 11.
64. Pawełczyk T, Grancow M, Kotlicka-Antczak M, et al. Omega-3 fatty acids in first-episode schizophrenia - a randomized controlled study of efficacy and relapse

prevention (OFFER): rationale, design, and methods. *BMC Psychiatry*. 2015;15:97. Published 2015 May 2.

65. Guixà-González R, Javanainen M, Gómez-Soler M, et al. Membrane omega-3 fatty acids modulate the oligomerisation kinetics of adenosine A2A and dopamine D2 receptors. *Sci Rep*. 2016;6:19839. Published 2016 Jan 22.
66. Jump DB, Lytle KA, Depner CM, Tripathy S. Omega-3 polyunsaturated fatty acids as a treatment strategy for nonalcoholic fatty liver disease. *Pharmacol Ther*. 2018;181:108-125.
67. Perdomo CM, Frühbeck G, Escalada J. Impact of Nutritional Changes on Nonalcoholic Fatty Liver Disease. *Nutrients*. 2019;11(3):677. Published 2019 Mar 21.
68. Liebig M, Dannenberger D, Vollmar B, Abshagen K. n-3 PUFAs reduce tumor load and improve survival in a NASH-tumor mouse model. *Ther Adv Chronic Dis*. 2019;10:2040622319872118. Published 2019 Sep 5.
69. Li Y, Chen D. The optimal dose of omega-3 supplementation for non-alcoholic fatty liver disease. *J Hepatol*. 2012;57(2):468-470.
70. Bechmann LP, Hannivoort RA, Gerken G, Hotamisligil GS, Trauner M, Canbay A. The interaction of hepatic lipid and glucose metabolism in liver diseases. *J Hepatol*. 2012;56(4):952-964.
71. Gentile CL, Pagliassotti MJ. The role of fatty acids in the development and progression of nonalcoholic fatty liver disease. *J Nutr Biochem*. 2008;19(9):567-576.
72. Koopmans SJ, Dekker R, Ackermans MT, et al. Dietary saturated fat/cholesterol, but not unsaturated fat or starch, induces C-reactive protein associated early atherosclerosis and ectopic fat deposition in diabetic pigs. *Cardiovasc Diabetol*. 2011;10:64. Published 2011 Jul 14.
73. Litten-Brown JC, Corson AM, Clarke L. Porcine models for the metabolic syndrome, digestive and bone disorders: a general overview. *Animal*. 2010;4(6):899-920.
74. Koopmans SJ, Schuurman T. Considerations on pig models for appetite, metabolic syndrome and obese type 2 diabetes: From food intake to metabolic disease. *Eur J Pharmacol*. 2015;759:231-239.
75. Lunney JK. Advances in swine biomedical model genomics. *Int J Biol Sci*. 2007;3(3):179-184. Published 2007 Feb 10.
76. Bendixen E, Danielsen M, Larsen K, Bendixen C. Advances in porcine genomics and proteomics--a toolbox for developing the pig as a model organism for molecular biomedical research. *Brief Funct Genomics*. 2010;9(3):208-219.

77. Gutierrez K, Dicks N, Glanzner WG, Agellon LB, Bordignon V. Efficacy of the porcine species in biomedical research. *Front Genet*. 2015;6:293. Published 2015 Sep 16.
78. Neeb ZP, Edwards JM, Alloosh M, Long X, Mokelke EA, Sturek M. Metabolic syndrome and coronary artery disease in Ossabaw compared with Yucatan swine. *Comp Med*. 2010;60(4):300-315
79. Te Pas MF, Koopmans SJ, Kruijt L, Calus MP, Smits MA. Plasma proteome profiles associated with diet-induced metabolic syndrome and the early onset of metabolic syndrome in a pig model. *PLoS One*. 2013;8(9):e73087. Published 2013 Sep 23.
80. Newell-Fugate AE, Taibl JN, Clark SG, Alloosh M, Sturek M, Krisher RL. Effects of diet-induced obesity on metabolic parameters and reproductive function in female Ossabaw minipigs. *Comp Med*. 2014;64(1):44-49.
81. Zhang X, Lerman LO. Investigating the Metabolic Syndrome: Contributions of Swine Models. *Toxicol Pathol*. 2016;44(3):358-366.
82. Eirin A, Woollard JR, Ferguson CM, et al. The metabolic syndrome induces early changes in the swine renal medullary mitochondria. *Transl Res*. 2017;184:45-56.e9.
83. Te Pas MF, Koopmans SJ, Kruijt L, Boeren S, Smits MA. Changes in Plasma Protein Expression Indicative of Early Diet-induced Metabolic Disease in Male Pigs (*Sus scrofa*). *Comp Med*. 2018;68(4):286-293.
84. Ferguson LR. Nutrigenomics approaches to functional foods. *J Am Diet Assoc*. 2009;109(3):452-458.
85. Fenech M, El-Sohemy A, Cahill L, et al. Nutrigenetics and nutrigenomics: viewpoints on the current status and applications in nutrition research and practice. *J Nutrigenet Nutrigenomics*. 2011;4(2):69-89.
86. Ordovas JM, Ferguson LR, Tai ES, Mathers JC. Personalised nutrition and health. *BMJ*. 2018;361:bmj.k2173. Published 2018 Jun 13.
87. Mead MN. Nutrigenomics: the genome--food interface. *Environ Health Perspect*. 2007;115(12):A582-A589.
88. German JB, Zivkovic AM, Dallas DC, Smilowitz JT. Nutrigenomics and personalized diets: What will they mean for food?. *Annu Rev Food Sci Technol*. 2011;2:97-123.
89. Rana S, Kumar S, Rathore N, Padwad Y, Bhushana S. Nutrigenomics and its Impact on Life Style Associated Metabolic Diseases. *Curr Genomics*. 2016;17(3):261-278.
90. Depner CM, Philbrick KA, Jump DB. Docosahexaenoic acid attenuates hepatic inflammation, oxidative stress, and fibrosis without decreasing hepatosteatosis in a

Ldlr(-/-) mouse model of western diet-induced nonalcoholic steatohepatitis. *J Nutr*. 2013;143(3):315-323.

91. Gladine C, Newman JW, Durand T, et al. Lipid profiling following intake of the omega 3 fatty acid DHA identifies the peroxidized metabolites F4-neuroprostanes as the best predictors of atherosclerosis prevention. *PLoS One*. 2014;9(2):e89393. Published 2014 Feb 18.
92. Manousopoulou A, Scorletti E, Smith DE, et al. Marine omega-3 fatty acid supplementation in non-alcoholic fatty liver disease: Plasma proteomics in the randomized WELCOME* trial. *Clin Nutr*. 2019;38(4):1952-1955.
93. Szostak A, Ogłuszka M, Te Pas MF, Poławska E, Urbański P, Juszczuk-Kubiak E, Blicharski T, Pareek CS, Dunkelberger JR, Horbańczuk JO, Pierzchała M. Effect of a diet enriched with omega-6 and omega-3 fatty acids on the pig liver transcriptome. *Genes Nutr*. 2016 Mar 17;11:9.
94. Ogłuszka M, Szostak A, Te Pas MFW, Poławska E, Urbański P, Blicharski T, Pareek CS, Juszczuk-Kubiak E, Dunkelberger JR, Horbańczuk JO, Pierzchała M. A porcine gluteus medius muscle genome-wide transcriptome analysis: dietary effects of omega-6 and omega-3 fatty acids on biological mechanisms. *Genes Nutr*. 2017 Jan 31;12:4.
95. Vitali M, Dimauro C, Sirri R, et al. Effect of dietary polyunsaturated fatty acid and antioxidant supplementation on the transcriptional level of genes involved in lipid and energy metabolism in swine. *PLoS One*. 2018;13(10):e0204869. Published 2018 Oct 4.
96. Zhang H, Xu P, Jiang Y, et al. Genomic, Transcriptomic, and Epigenomic Features Differentiate Genes That Are Relevant for Muscular Polyunsaturated Fatty Acids in the Common Carp. *Front Genet*. 2019;10:217. Published 2019 Mar 15.
97. Xue X, Hall JR, Caballero-Solares A, et al. Liver Transcriptome Profiling Reveals That Dietary DHA and EPA Levels Influence Suites of Genes Involved in Metabolism, Redox Homeostasis, and Immune Function in Atlantic Salmon (Salmo salar). *Mar Biotechnol (NY)*. 2020;22(2):263-284.
98. Yang K, Han X. Lipidomics: Techniques, Applications, and Outcomes Related to Biomedical Sciences. *Trends Biochem Sci*. 2016;41(11):954-969.
99. Zárate R, El Jaber-Vazdekis N, Tejera N, Pérez JA, Rodríguez C. Significance of long chain polyunsaturated fatty acids in human health. *Clin Transl Med*. 2017;6(1):25.
100. Folch J, Lees M, Sloane Stanley GH. A simple method for the isolation and purification of total lipides from animal tissues. *J Biol Chem*. 1957;226(1):497-509.

101. Polawska E, Horbanczuk JO, Pierzchala M, Strzalkowska N, Jozwik A, Wojcik A, Pomianowski J, Gutkowska K, Wierzbicka A, Hoffman LC. Effect of dietary linseed and rapeseed supplementation on fatty acid profiles in the ostrich. Part 1. Muscles. *Anim Sci Pap Rep*.2013; 31:239–248
102. Bolger AM, Lohse M, Usadel B. Trimmomatic: a flexible trimmer for Illumina sequence data. *Bioinformatics*. 2014;30(15):2114-2120.
103. Andrews S. (2010). FastQC: a quality control tool for high throughput sequence data. Available online at: http://www.bioinformatics.babraham.ac.uk/projects/fastqc
104. Mortazavi A, Williams BA, McCue K, Schaeffer L, Wold B. Mapping and quantifying mammalian transcriptomes by RNA-Seq. *Nat Methods*. 2008;5(7):621-628.
105. Chepelev I, Wei G, Tang Q, Zhao K. Detection of single nucleotide variations in expressed exons of the human genome using RNA-Seq. *Nucleic Acids Res*. 2009;37(16):e106.
106. Anders S, Huber W. Differential expression analysis for sequence count data. *Genome Biol*. 2010;11(10):R106.
107. Barrett T, Wilhite SE, Ledoux P, et al. NCBI GEO: archive for functional genomics data sets--update. *Nucleic Acids Res*. 2013;41(Database issue):D991-D995.
108. Saito R, Smoot ME, Ono K, et al. A travel guide to Cytoscape plugins. *Nat Methods*. 2012;9(11):1069-1076.
109. Andersen CL, Jensen JL, Ørntoft TF. Normalization of real-time quantitative reverse transcription-PCR data: a model-based variance estimation approach to identify genes suited for normalization, applied to bladder and colon cancer data sets. *Cancer Res*. 2004;64(15):5245-5250.
110. Koressaar T, Remm M. Enhancements and modifications of primer design program Primer3. *Bioinformatics*. 2007;23(10):1289-1291.
111. Untergasser A, Cutcutache I, Koressaar T, et al. Primer3--new capabilities and interfaces. *Nucleic Acids Res*. 2012;40(15):e115.
112. Ye J, Coulouris G, Zaretskaya I, Cutcutache I, Rozen S, Madden TL. Primer-BLAST: a tool to design target-specific primers for polymerase chain reaction. *BMC Bioinformatics*. 2012;13:134. Published 2012 Jun 18.
113. Chomczynski P, Sacchi N. Single-step method of RNA isolation by acid guanidinium thiocyanate-phenol-chloroform extraction. *Anal Biochem*. 1987;162(1):156-159.

114. Chomczynski P, Sacchi N. The single-step method of RNA isolation by acid guanidinium thiocyanate-phenol-chloroform extraction: twenty-something years on. *Nat Protoc*. 2006;1(2):581-585.
115. Huggett JF, Foy CA, Benes V, et al. The digital MIQE guidelines: Minimum Information for Publication of Quantitative Digital PCR Experiments. *Clin Chem*. 2013;59(6):892-902.
116. Bustin SA, Benes V, Garson J, et al. The need for transparency and good practices in the qPCR literature. *Nat Methods*. 2013;10(11):1063-1067.
117. Pfaffl MW. A new mathematical model for relative quantification in real-time RT-PCR. *Nucleic Acids Res*. 2001;29(9):e45.
118. Shrestha N, Sleep SL, Cuffe JSM, Holland OJ, Perkins AV, Yau SY, McAinch AJ, Hryciw DH. Role of omega-6 and omega-3 fatty acids in fetal programming. Clin Exp Pharmacol Physiol. 2020 May;47(5):907-915.
119. Lin G, Thevasagayam NM, Wan ZY, Ye BQ, Yue GH. Transcriptome Analysis Identified Genes for Growth and Omega-3/-6 Ratio in Saline Tilapia. Front Genet. 2019 Mar 20;10:244.
120. Zhang H, Xu P, Jiang Y, Zhao Z, Feng J, Tai R, Dong C, Xu J. Genomic, Transcriptomic, and Epigenomic Features Differentiate Genes That Are Relevant for Muscular Polyunsaturated Fatty Acids in the Common Carp. Front Genet. 2019 Mar 15;10:217
121. Levental KR, Malmberg E, Symons JL, et al. Lipidomic and biophysical homeostasis of mammalian membranes counteracts dietary lipid perturbations to maintain cellular fitness. *Nat Commun*. 2020;11(1):1339. Published 2020 Mar 12.
122. Molfino A, Amabile MI, Monti M, Muscaritoli M. Omega-3 Polyunsaturated Fatty Acids in Critical Illness: Anti-Inflammatory, Proresolving, or Both?. *Oxid Med Cell Longev*. 2017;2017:5987082.
123. Zárate R, El Jaber-Vazdekis N, Tejera N, Pérez JA, Rodríguez C. Significance of long chain polyunsaturated fatty acids in human health. *Clin Transl Med*. 2017;6(1):25.
124. Levental KR, Surma MA, Skinkle AD, et al. ω-3 polyunsaturated fatty acids direct differentiation of the membrane phenotype in mesenchymal stem cells to potentiate osteogenesis. *Sci Adv*. 2017;3(11):eaao1193. Published 2017 Nov 8.
125. Zanoaga O, Jurj A, Raduly L, Cojocneanu-Petric R, Fuentes-Mattei E, Wu O, Braicu C, Gherman CD, Berindan-Neagoe I. Implications of dietary ω-3 and ω-6

polyunsaturated fatty acids in breast cancer. *Exp Ther Med*. 2018 Feb;15(2):1167-1176.

126. Mirmiran P, Hosseinpour-Niazi S, Naderi Z, Bahadoran Z, Sadeghi M, Azizi F. Association between interaction and ratio of ω-3 and ω-6 polyunsaturated fatty acid and the metabolic syndrome in adults. *Nutrition*. 2012 Sep;28(9):856-63.
127. Simopoulos AP. An Increase in the Omega-6/Omega-3 Fatty Acid Ratio Increases the Risk for Obesity. *Nutrients*. 2016;8(3):128. Published 2016 Mar 2.
128. Jacometo CB, Schmitt E, Pfeifer LF, Schneider A, Bado F, da Rosa FT, Halfen S, Del Pino FA, Loor JJ, Corrêa MN, Dionello NJ. Linoleic and α-linolenic fatty acid consumption over three generations exert cumulative regulation of hepatic expression of genes related to lipid metabolism. *Genes Nutr*. 2014 Jul;9(4):405.
129. Bowen KJ, Harris WS, Kris-Etherton PM. Omega-3 Fatty Acids and Cardiovascular Disease: Are There Benefits?. *Curr Treat Options Cardiovasc Med*. 2016;18(11):69.
130. Jump DB, Lytle KA, Depner CM, Tripathy S. Omega-3 polyunsaturated fatty acids as a treatment strategy for nonalcoholic fatty liver disease. *Pharmacol Ther*. 2018;181:108-125.
131. Terracciano A, Stephan Y, Sutin AR. Omega-3 fatty acid: A promising pathway linking personality and health. *J Psychosom Res*. 2018 Aug;111:50-51
132. Skiba G, Poławska E, Sobol M, Raj S, Weremko D. Omega-6 and omega-3 fatty acids metabolism pathways in the body of pigs fed diets with different sources of fatty acids. *Arch Anim Nutr*. 2015;69(1):1-16.
133. Wang Y, Zhang W, Wu X, Wu C, Qian L, Wang L, Zhang X, Yang M, Li D, Ding J, Wang C, Yin Z, Ding Y. Transcriptomic comparison of liver tissue between Anqing six-end-white pigs and Yorkshire pigs based on RNA sequencing. **Genome**. 2020 Apr;63(4):203-214.
134. Seidah NG, Benjannet S, Wickham L, et al. The secretory proprotein convertase neural apoptosis-regulated convertase 1 (NARC-1): liver regeneration and neuronal differentiation. *Proc Natl Acad Sci U S A*. 2003;100(3):928-933.
135. Abifadel M, Varret M, Rabès JP, et al. Mutations in PCSK9 cause autosomal dominant hypercholesterolemia. *Nat Genet*. 2003;34(2):154-156.
136. Chaudhary R, Garg J, Shah N, Sumner A. PCSK9 inhibitors: A new era of lipid lowering therapy. *World J Cardiol*. 2017;9(2):76-91.
137. Graversen CB, Lundbye-Christensen S, Thomsen B, Christensen JH, Schmidt EB. Marine n-3 polyunsaturated fatty acids lower plasma proprotein convertase subtilisin

kexin type 9 levels in pre- and postmenopausal women: A randomised study. *Vascul Pharmacol*. 2016;76:37-41.

138. Sorokin AV, Yang ZH, Vaisman BL, et al. Addition of aspirin to a fish oil-rich diet decreases inflammation and atherosclerosis in ApoE-null mice. *J Nutr Biochem*. 2016;35:58-65.
139. Yuan F, Wang H, Tian Y, et al. Fish oil alleviated high-fat diet-induced non-alcoholic fatty liver disease via regulating hepatic lipids metabolism and metaflammation: a transcriptomic study. *Lipids Health Dis*. 2016;15:20. Published 2016 Feb 1.
140. Mizushima N, Noda T, Yoshimori T, et al. A protein conjugation system essential for autophagy. *Nature*. 1998;395(6700):395-398.
141. Singh R, Cuervo AM. Lipophagy: connecting autophagy and lipid metabolism. *Int J Cell Biol*. 2012;2012:282041.
142. Velikkakath AK, Nishimura T, Oita E, Ishihara N, Mizushima N. Mammalian Atg2 proteins are essential for autophagosome formation and important for regulation of size and distribution of lipid droplets. *Mol Biol Cell*. 2012;23(5):896-909.
143. Gómez-Sánchez R, Rose J, Guimarães R, et al. Atg9 establishes Atg2-dependent contact sites between the endoplasmic reticulum and phagophores. *J Cell Biol*. 2018;217(8):2743-2763.
144. Hosokawa N, Hara T, Kaizuka T, et al. Nutrient-dependent mTORC1 association with the ULK1-Atg13-FIP200 complex required for autophagy. *Mol Biol Cell*. 2009;20(7):1981-1991.
145. Russell RC, Yuan HX, Guan KL. Autophagy regulation by nutrient signaling. *Cell Res*. 2014;24(1):42-57.
146. Tsuyuki S, Takabayashi M, Kawazu M, et al. Detection of WIPI1 mRNA as an indicator of autophagosome formation. *Autophagy*. 2014;10(3):497-513.
147. Ma Y, Galluzzi L, Zitvogel L, Kroemer G. Autophagy and cellular immune responses. *Immunity*. 2013;39(2):211-227.
148. Singh R, Kaushik S, Wang Y, et al. Autophagy regulates lipid metabolism. *Nature*. 2009;458(7242):1131-1135.
149. Weidberg H, Shvets E, Elazar Z. Lipophagy: selective catabolism designed for lipids. *Dev Cell*. 2009;16(5):628-630.
150. Mei S, Ni HM, Manley S, et al. Differential roles of unsaturated and saturated fatty acids on autophagy and apoptosis in hepatocytes. *J Pharmacol Exp Ther*. 2011;339(2):487-498.

151. Li M, Gao P, Zhang J. Crosstalk between Autophagy and Apoptosis: Potential and Emerging Therapeutic Targets for Cardiac Diseases. *Int J Mol Sci*. 2016;17(3):332. Published 2016 Mar 3.
152. Chen Y, Xu C, Yan T, Yu C, Li Y. ω-3 Fatty acids reverse lipotoxity through induction of autophagy in nonalcoholic fatty liver disease. *Nutrition*. 2015;31(11-12):1423-1429.e2.
153. Kang JX, Wang J, Wu L, Kang ZB. Transgenic mice: fat-1 mice convert n-6 to n-3 fatty acids [published correction appears in Nature. 2004 Feb 19;427(6976):698]. *Nature*. 2004;427(6974):504.
154. Johansson I, Monsen VT, Pettersen K, et al. The marine n-3 PUFA DHA evokes cytoprotection against oxidative stress and protein misfolding by inducing autophagy and NFE2L2 in human retinal pigment epithelial cells. *Autophagy*. 2015;11(9):1636-1651.
155. Fernández M, Semela D, Bruix J, Colle I, Pinzani M, Bosch J. Angiogenesis in liver disease. *J Hepatol*. 2009;50(3):604-620.
156. Elpek GÖ. Angiogenesis and liver fibrosis. *World J Hepatol*. 2015;7(3):377-391.
157. Parker-Duffen JL, Nakamura K, Silver M, et al. Divergent roles for adiponectin receptor 1 (AdipoR1) and AdipoR2 in mediating revascularization and metabolic dysfunction in vivo. *J Biol Chem*. 2014;289(23):16200-16213.
158. Yamauchi T, Kamon J, Ito Y, et al. Cloning of adiponectin receptors that mediate antidiabetic metabolic effects [published correction appears in Nature. 2004 Oct 28;431(7012):1123]. *Nature*. 2003;423(6941):762-769.
159. Zhuang W, Wang G, Li L, Lin G, Deng Z. Omega-3 polyunsaturated fatty acids reduce vascular endothelial growth factor production and suppress endothelial wound repair. *J Cardiovasc Transl Res*. 2013;6(2):287-293.
160. Schmidt S, Stahl F, Mutz KO, Scheper T, Hahn A, Schuchardt JP. Different gene expression profiles in normo- and dyslipidemic men after fish oil supplementation: results from a randomized controlled trial. *Lipids Health Dis*. 2012;11:105. Published 2012 Aug 29.